

Copyright Warning & Restrictions

The copyright law of the United States (Title 17, United States Code) governs the making of photocopies or other reproductions of copyrighted material.

Under certain conditions specified in the law, libraries and archives are authorized to furnish a photocopy or other reproduction. One of these specified conditions is that the photocopy or reproduction is not to be “used for any purpose other than private study, scholarship, or research.” If a user makes a request for, or later uses, a photocopy or reproduction for purposes in excess of “fair use” that user may be liable for copyright infringement,

This institution reserves the right to refuse to accept a copying order if, in its judgment, fulfillment of the order would involve violation of copyright law.

Please Note: The author retains the copyright while the New Jersey Institute of Technology reserves the right to distribute this thesis or dissertation

Printing note: If you do not wish to print this page, then select “Pages from: first page # to: last page #” on the print dialog screen

The Van Houten library has removed some of the personal information and all signatures from the approval page and biographical sketches of theses and dissertations in order to protect the identity of NJIT graduates and faculty.

ABSTRACT

DYNAMIC MULTI-RAMP METERING CONTROL WITH SIMULTANEOUS PERTURBATION STOCHASTIC APPROXIMATION (SPSA)

by
Jiangtao Luo

Ramp metering was proven to be a viable form of freeway traffic control strategy, which could eliminate, or at least reduce, freeway congestion. In this study, the development of ramp metering control strategies, models, and constraints (e.g., meter locations, ramp storage capacities, lower and upper bounds of ramp metering rates) are discussed in detail. The pre-timed and demand/capacity metering control strategies were first evaluated, while the potential metered ramps were determined. A Simultaneous Perturbation Stochastic Approximation (SPSA) algorithm is proposed to dynamically optimize multiple-ramp metering control by maximizing the total throughput subject to a number of constraints. The ramp metering rates subject to dynamic traffic conditions and capacity constraints are considered as decision variables in the SPSA algorithm. Based on the collected geometric and traffic data, a CORSIM model was developed to simulate traffic operation for the study site. The potential benefit of the dynamic multi-ramp metering control model under time varying traffic condition was simulated and evaluated. The increased total throughput and reduced total delay were observed, while the traffic conditions suitable for implementing ramp metering control were suggested. The developed dynamic multi-ramp metering control with SPSA algorithm has demonstrated its effectiveness to improve freeway operation.

**DYNAMIC MULTI-RAMP METERING CONTROL WITH SIMULTANEOUS
PERTURBATION STOCHASTIC APPROXIMATION (SPSA)**

by

Jiangtao Luo

**A Dissertation
Submitted to the Faculty of
New Jersey Institute of Technology
In Partial Fulfillment of the Requirements for the Degree of
Doctor of Philosophy in Transportation**

Interdisciplinary Program in Transportation

May 2003

APPROVAL PAGE

DYNAMIC MULTI-RAMP METERING CONTROL WITH SIMULTANEOUS PERTURBATION STOCHASTIC APPROXIMATION (SPSA)

Jiangtao Luo

Dr. Steven I-Jy Chien, Dissertation Advisor Date
Associate Professor of Department of Civil and Environmental Engineering, NJIT

Dr. Athanassios K. Bladikas, Committee Member Date
Associate Professor of Industrial and Manufacturing Engineering, NJIT

Dr. Lazar Spasovic, Committee Member Date
Professor of School of Management, NJIT

Dr. Janice R. Daniel, Committee Member Date
Assistant Professor of Department of Civil and Environmental Engineering, NJIT

Dr. Kyriacos C. Mouskos, Committee Member Date
Research Professor of Department of Civil Engineering, CUNY

BIOGRAPHICAL SKETCH

Author: Jiangtao Luo
Degree: Doctor of Philosophy
Date: May 2003

Undergraduate and Graduate Education:

- Doctor of Philosophy in Transportation,
New Jersey Institute of Technology, Newark, NJ, 2003
- Master of Science in Highway Engineering,
Beijing Polytechnic University, Beijing, China, 1994
- Bachelor of Science in Civil Engineering,
Hebei Institute of Technology, Tianjin, China, 1988

Major: Transportation Engineering

Presentations and Publications:

J. Luo, F. Ren, and X. Liu

"The Gray Evaluation of Road Traffic Safety", China Journal of Highway and Transportation, Vol.8, No.4, 1995, Page 78-83.

J. Luo, F. Ren, and X. Liu

"Traffic Safety Analysis and Evaluation of Beijing Area", China Journal of Highway and Transportation, Vol.8, Sup.No.1, 1995, Page 137-142.

J. Luo and S. Chien

"Optimal Multi-ramp Metering Control with Simultaneous Perturbation Stochastic Approximation (SPSA)", Submitted to Computer-Aided in Civil and Infrastructure Engineering, 2003.

S. Chien, J. Luo, and C. Ting

"Optimization of Dynamic Ramp Metering Control with Simultaneous Perturbation Stochastic Approximation", Submitted to Journal of Transportation Engineering, ASCE, 2002.

Copyright © 2003 by Jiangtao Luo

ALL RIGHTS RESERVED

To my beloved family

ACKNOWLEDGMENT

I would like to express my deepest appreciation to Dr. Steven Chien, who not only served as my research supervisor, providing valuable and countless resources, insight, and intuition, but also constantly gave me support, encouragement, and reassurance. Special thanks are given to Dr. Athanassios Bladikas, Dr. Lazar Spasovic, Dr. Janice Daniel and Dr. Kyriacos C. Mouskos for actively participating in my committee.

My fellow graduate students, Mr. Xiaobo Liu, Mr. Changqian Guan, Mr. Rajat Rajbhandari, and Mr. Chuck Tsai, are deserving of recognition for their support.

I also appreciate supports from the New Jersey Department of Transportation, National Center for Transportation and Industrial Productivity, and New Jersey Institute of Technology on the research project “Evaluation of the Potential for Using Ramp Metering in the ATMS of the I-80 Showcase Corridor”.

TABLE OF CONTENTS

Chapter	Page
1 INTRODUCTION	1
1.1 Background	1
1.2 Problem Statement	5
1.3 Objectives and Scope of Work	6
1.4 Organization	7
2 LITERATURE REVIEW	8
2.1 General Requirements	9
2.1.1 Metering Alternatives.....	9
2.1.2 Feasible Range of Metering Rates.....	10
2.1.3 Signals and Signs.....	11
2.1.4 Ramp Geometric Conditions.....	11
2.2 Technical Requirements	12
2.2.1 Freeway Surveillance Systems.....	12
2.2.2 Ramp Metering Controllers.....	16
2.2.3 Constraints for Ramp Metering Control Systems	17
2.3 Ramp Metering Control Strategies.....	20
2.3.1 Pre-timed Control	20
2.3.2 Local Traffic Responsive Control	21
2.3.3 System-wide Control	22
2.3.4 Integrated System Control.....	22

TABLE OF CONTENTS
(Continued)

Chapter	Page
2.4 Ramp Metering Control Models.....	23
2.4.1 Pre-Timed Linear Programming (LP) Models	23
2.4.2 Local Traffic Responsive Models	24
2.4.3 System-wide Non-linear Quadratic Programming Models	27
2.4.4 Emerging Large-Scale Heuristic Models	29
2.5 Research Algorithms	31
2.5.1 Artificial Neural Network (ANN)	32
2.5.2 Fuzzy Theory	33
2.5.3 Simultaneous Perturbation Stochastic Approximation (SPSA)	34
2.6 Simulation Models	35
2.7 Summary	37
3 METHODOLOGY	38
3.1 Development of Ramp Metering Control Model	38
3.2 Development of the SPSA Algorithm	43
3.3 Dynamic Multi-ramp Metering Control with SPSA	49
3.4 Summary	51
4 CASE STUDY	52
4.1 Site Identification	52
4.2 Site Visit	53
4.3 Data	53
4.4 Simulation	57

TABLE OF CONTENTS
(Continued)

Chapter	Page
4.5 Network Modeling	59
4.6 Calibration and Validation	60
4.6.1 Data Collection and Processing	61
4.6.2 Model Calibration	62
4.6.3 Model Validation	68
4.7 Summary	70
5 SYSTEM EVALUATION	71
5.1 Evaluation of Ramp Metering Control	71
5.1.1 Constraints	71
5.1.2 Simulation Analysis and Evaluation	75
5.1.3 Summary	82
5.2 Model Testing.....	82
5.2.1 Constraints.....	83
5.2.2 Testing Cases.....	83
5.2.3 Data Collection.....	85
5.2.4 Analysis and Evaluation.....	86
5.3 Individual Ramp Control.....	89
5.4 Dynamic Multi-ramp Metering Control	92
5.5 Road User Cost.....	95
5.6 Fuel Consumption and Emissions	96
5.7 Sensitive Analysis	97

TABLE OF CONTENTS
(Continued)

Chapter	Page
5.7.1 Short Ramp.....	97
5.7.2 Control at Different Groups of Metered Ramps.....	99
5.7.3 Optimal Simulation	100
5.8 Summary	103
6 CONCLUSIONS AND FUTURE RESEARCH.....	105
6.1 Conclusions and Recommendations.....	105
6.2 Future Research.....	109
APPENDIX A FIGURES	112
APPENDIX B CORSIM INPUT FILES	125
APPENDIX C THEORY ANALYSIS	176
REFERENCES	183

LIST OF TABLES

Table	Page
1.1 Existing Ramp Metering Sites.....	2
2.1 Summary of Traffic Detectors.....	14
2.2 Characteristics of Detectors for Metering Control.....	16
2.3 Objectives of Ramp Metering Strategies	20
4.1 Geometric Data	55
4.2 Traffic Data	56
4.3 O/D Demand Distribution (%).....	56
4.4 Required Data for CORSIM Simulation Model.....	59
4.5 Links and Nodes of the Simulation Network.....	60
4.6 Volume & Speed Data (Link 302-303, MP 30.2, 7:00 am-8:00 am).....	61
4.7 Volume Data (8:00 am-9:00 am, May 26, 1999).....	61
4.8 Car-Following Sensitivity Factor.....	62
4.9 Other Calibrated Parameters	63
5.1 Length of the Auxiliary Lane on the Freeway	73
5.2 Distance from Meter Location to the On-ramp Gore.....	73
5.3 Storage Capacity of On-ramps	75
5.4 Pre-timed Metering Headways.....	76
5.5 MOEs under Pre-timed Metering Control and No Control Situations.....	77
5.6 Metering Headway for Demand/Capacity Control	80
5.7 MOEs under Demand/Capacity Control and No Control Situations	81
5.8 Benefits of Demand/Capacity Control (Reduced Delay).....	81

LIST OF TABLES
(Continued)

Table	Page
5.9 Benefits of Demand/Capacity Control (Increased Throughput)	81
5.10 Traffic Demand Distribution for the Three Test Cases.....	84
5.11 Optimal Metering Rates for Various Test Cases.....	85
5.12 Traffic Demand Distribution.....	90
5.13 Optimal Metering Rates (vph) for Individual Ramps	90
5.14 Network-wide Total Throughput for Individual Ramp Control.....	91
5.15 Network-wide Total Delay for Individual Ramp Control	91
5.16 Suggested Entry Flows of Mainline for the Proposed Control Model.....	92
5.17 Optimal Metering Rates and Headways for Multi-ramp Control	93
5.18 Results of Multi-ramp Control	93
5.19 Road User Costs and Benefits for Multi-ramp Control.....	96
5.20 Fuel Consumption and Emissions Analysis for Joint Ramp Control.....	97
5.21 Network-wide Total Throughput for Multiple Ramps Control.....	99
5.22 Network-wide Total Delay for Multiple Ramps Control	100
5.23 Simulation Results after Optimal Metering Control at Node 356.....	101
5.24 Change of the Throughput and Delay with Adjusted Optimal Rates.....	103

LIST OF FIGURES

Figure	Page
2.1 Configuration of a typical metering ramp	15
2.2 Configuration of a ramp junction	18
3.1 General freeway configuration.....	39
3.2 The configuration of the SPSA algorithm.....	46
3.3 The configuration of proposed dynamic metering control model.....	50
4.1 Map of the study site	52
4.2 Traffic volumes on different links for various car following sensitivity factors (CFF).....	63
4.3 Traffic volumes on different links for various collision avoidance time periods (PFCA)	64
4.4 Traffic volumes on different links for various courtesy factors (CF).....	64
4.5 Field Data vs. Simulated Data (Mainline).....	67
4.6 Field Data vs. Simulated Data (On-Ramps).....	67
4.7 MAPE of volumes on the mainline	69
4.8 RMSE of volumes on the mainline	69
5.1 Configuration of the study site at node 307	83
5.2 Total delay and total throughput over time (Case 1).....	87
5.3 Total delay and total throughput over time (Case 2).....	88
5.4 Total delay and total throughput over time (Case 3).....	88
5.5 Total throughput over time (multi-ramp control).....	94
5.6 Total delay over time (multi-ramp control).....	94
5.7 Optimal metering rate with SPSA vs. ramp storage area (node 307)	98

**LIST OF FIGURES
(Continued)**

Figure	Page
5.8 The benefits of total delay and total throughput (node 307)	98
5.9 Metering rate change vs. queue reduction (node 356)	102
A.1 Mainline I-80 (Route 513/Hibernia Avenue)	113
A.2 Ramp 1 on I-80 (Route 513/Hibernia Avenue).....	113
A.3 Ramp 2 on I-80 (Route 513/Hibernia Avenue).....	114
A.4 Ramp on I-80 (Route 661/Mount Hope).....	114
A.5 Ramp 1 on I-80 (Route 615/Howard Boulevard).....	115
A.6 Ramp 2 on I-80 (Route 615/Howard Boulevard).....	115
A.7 Geometric diagram of eastbound I-80 mileposts	116
A.8 Link – Node diagram converted from Figure A.7.....	116
A.9 Average delay and total throughput vs. metering headway (Pre-timed Metering Control at Node 306)	117
A.10 Total delay and veh-mile vs. metering headway (Pre-timed metering vontrol at node 306).....	117
A.11 Average felay and total throughput vs. metering headway (Pre-timed metering control at node 307)	118
A.12 Total delay and veh-mile vs. metering headway (Pre-timed Metering Control at Node 307).....	118
A.13 Average delay and total throughput vs. metering headway (Pre-timed Metering Control at Node 376).....	119
A.14 Total delay and veh-mile vs. metering headway (Pre-timed Metering Control at Node 376).....	119
A.15 Average delay and total throughput vs. metering headway (Pre-timed Metering Control at Node 395).....	120

LIST OF FIGURES
(Continued)

Figure	Page
A.16 Total delay and veh-mile vs. metering headway (Pre-timed Metering Control at Node 395).....	120
A.17 Average delay and total throughput vs. metering headway (Pre-timed Metering Control at Node 306).....	121
A.18 Total delay and veh-mile vs. metering headway (Pre-timed Metering Control at Node 306).....	121
A.19 Average delay and total throughput vs. metering headway (Demand/Capacity Control at Node 307).....	122
A.20 Total delay and veh-mile vs. metering headway (Demand/Capacity Control at Node 307).....	122
A.21 Average delay and total throughput vs. metering headway (Demand/Capacity Control at Node 376).....	123
A.22 Total delay and veh-mile vs. metering headway (Demand/Capacity Control at Node 376).....	123
A.23 Average delay and total throughput vs. metering headway (Demand/Capacity Control at Node 395).....	124
A.24 Total delay and veh-mile vs. metering headway (Demand/Capacity Control at Node 395).....	124

NOTATION

SPSA	Simultaneous Perturbation Stochastic Approximation;
MOEs	Measures of Effectiveness;
TSM	Transportation Systems Management;
O/D	Origin/Destination;
MP	Milepost;
MAPE	Mean Absolute Percent Error;
RMSE	Root Mean Square Error;
<i>TTT</i>	Total Traffic Throughput;
<i>n</i>	the sample size;
S_i	the observation i of simulation output;
O_i	the observation i of field measurement;
d	the travel distance;
a	the vehicle acceleration rate;
V_t	the average speed of vehicles on the mainline at time t ;
V_0	the initial speed of a vehicle released by a ramp meter;
t	the acceleration time from the ramp meter to the on-ramp gore;
m	the mean arrival rate (vehicles per hour);
L_q	the queue length (number of vehicles);
τ	the ratio of vehicle arrival rate m and ramp service rate $R_r(k)$;
$L(\lambda)$	the objective function for minimization with the vector λ ;
$g(\lambda)$	the gradient of $L(\lambda)$;

$\mathbf{y}(\boldsymbol{\lambda})$	the measurement of $\mathbf{L}(\boldsymbol{\lambda})$;
$\hat{\boldsymbol{\lambda}}_0$	the initial guess of the optimal $\boldsymbol{\lambda}$;
$\boldsymbol{\lambda}_h^*$	the optimal solution of $\boldsymbol{\lambda}$ (at iteration h);
$\hat{\boldsymbol{\lambda}}_{h+1}$	the $(h+1)^{\text{th}}$ estimate of $\boldsymbol{\lambda}$;
h	the index of iteration;
\mathbf{a}	non-negative coefficient in SPSA;
\mathbf{c}	non-negative coefficient in SPSA;
β	non-negative coefficient in SPSA;
γ	non-negative coefficient in SPSA;
\mathbf{a}_h	the parameter in the h^{th} iteration;
\mathbf{c}_h	the parameter in the h^{th} iteration;
$\hat{g}(\hat{\boldsymbol{\lambda}}_h)$	the approximation of $g(\hat{\boldsymbol{\lambda}}_h)$;
Δ_h	random simultaneous perturbation vector in iteration h ;
Δ_{hi}	the i^{th} component of vector Δ_h ;
N	number of segments on a freeway;
$\rho_i(k)$	the density of link i in interval k ;
$q_i(k)$	the flow rate entering link $i+1$ from link i in interval k ;
$R_i(k)$	the metering rate for an on ramp of link i in interval k ;
$Q_i(k)$	the mean flow rate of link i in interval k ;
δ_i^{on}	the on-ramp parameter (= 1 if an on-ramp of link i exists, otherwise = 0);
δ_i^{off}	the off-ramp parameter (= 1 if an off-ramp of link i exists, otherwise = 0);
$\theta_i(k)$	the turning percentage to the off ramp of link i in interval k ;

T	the duration of a time interval;
L_i	the length of link i ;
l_i	the number of through lanes of link i .
$a_i(k)$	the weight parameter representing the interaction between flows of links i and $i+1$ in interval k ;
$S_i(k)$	the mean speed of link i in interval k ;
Z	a large positive number;
$R_i^{\min}(k)$	the minimum metering rate of on-ramp i in interval k ;
$R_i^{\max}(k)$	the maximum metering rate of on-ramp i in interval k ;
D	the total delay;
V_C	the value of time for cars;
V_T	the value of time for trucks;
I_C	the idling cost rate for cars;
I_T	the idling cost rate for trucks;
P_C	the percentage of cars in the traffic flow;
P_T	the percentage of trucks in the traffic flow.

CHAPTER 1

INTRODUCTION

1.1 Background

Motorists traveling on urban freeways often experience heavy congestion in peak periods, during which demand and delay increases, and the level of service deteriorates. Congestion delay on freeways is a serious problem because of not only the inconvenience experienced by travelers but also the increased sideswipe and rear-end accidents associated with the disturbed traffic flow. The need to implement effective traffic control has long been recognized by transportation professionals. Starting from the early 1960s, a variety of congestion control strategies have been proposed (Wattleworth 1967; Masher et al., 1975; Chang et al., 1994). Ramp metering control is regarded as one of the most effective freeway traffic management strategies for alleviating congestion.

Ramp metering provides a mechanism to control the rate of traffic entering the freeway. By releasing traffic from entering ramps to the freeway mainline in measured or regulated amounts, a single vehicle or a small platoon of vehicles can smoothly merge into the mainline traffic stream. Thus, the turbulence in the mainline traffic stream caused by the merging flow can be reduced. Metering control can be pre-timed, allowing vehicles to enter the freeway every few seconds, or traffic responsive, based on the real-time traffic information (e.g., gaps, speeds, occupancies and queues) collected from the freeway and ramps.

In 1963, the first ramp metering facility was installed in Chicago. Since then, over 2,100 meters were deployed on over 2,000 miles of freeways in the USA (Piotrowicz, et al., 1995). Many new or reconstructed roadways were designed to use ramp meters as a

component of their traffic management systems. A list of existing ramp metering sites and the corresponding measures of effectiveness (MOEs) in the evaluation are summarized in Table 1.1 (Piotrowicz, et al., 1995). Various MOEs were used to evaluate the benefit of ramp metering in freeway systems. Among them, speed, traffic volume, travel time, accident rate, and density were most widely used (e.g., the freeways in Denver, CO; Detroit, MI; Long Island, NY; Los Angeles, CA; Minneapolis, MN; Portland, OR; San Diego, CA; and Seattle, WA).

Table 1.1 Existing Ramp Metering Sites

Location	Freeway System	Miles Covered	No. of Meters	MOEs for Evaluation
Arlington, VA	I-95, I-66	32	26	NA
Chicago, IL	I-90, I-94, I-290, I-57	136	109	NA
Denver, CO	I-25, I-70, I-270, I-225, US-6	NA	28	Average speed, volume, travel time, accident rate
Detroit, MI	I-94	32	49	Average speed, volume, density
Long Island, NY	Long Island Expressway	35	75	Average speed, travel time, throughout, accident rate
Los Angeles, CA	I-5, I-105, I-110	700	808	Delay, accident rate
Milwaukee, WI	I-94, I-43, I-894, I-794, US-45	32	43	NA
Minneapolis, MN	I-35, I-94, I-394, I-494, I-694, SR- 169, SR-62	160	367	Average speed, volume, accident rate, fuel consumption
Phoenix, AR	I-10, I-17, US-60	200	93	NA
Portland, OR	I-5	6	58	Average speed, fuel consumption, accident rate
San Diego, CA	I-8	126	134	Average speed, volume
Seattle, WA	I-5, I-90, SR-520	NA	54	Volume, travel time

According to the practice discussed in previous studies (Wattleworth, 1967, CALTRANS, 1979, ITE, 1989, Minnesota DOT, 1994, Piotrowicz, et al., 1995, Chien, 1998), appropriate implementation of ramp metering control significantly improved traffic operations, particularly in preventing stop-and-go and erratic traffic conditions and balancing demand distributions on the mainline. Such improvements were achieved by

allowing ramp traffic to take advantage of gaps in the mainline traffic stream instead of merging with platoons and interrupting the congested traffic flow. The benefit of metering control was classified into various categories listed below: (1) maintaining freeway capacity, (2) maximizing throughput, (3) increasing travel speed, (4) decreasing travel time, and (5) reducing auto emissions and accidents due to a smoother mainline traffic flow (CALTRANS, 1979; Piotrowicz, et al., 1995; Chien, 1998).

As discussed in a report developed by Minnesota DOT (1994), ramp metering operations in several metropolitan areas (e.g., Minneapolis, MN; San Diego, CA; Seattle, WA; and Denver, CO) demonstrated that the freeway throughput of the metered sections during peak period increased by 17% to 25%, while the throughput of the entire highway systems increased by 5% to 6%. In a survey conducted by Piotrowicz et al. (1995), it was found that the mainline speed increased by 16% to 62%, while the number of accidents was reduced by 24% to 50%. In general, the average speed increased by 29% after performing ramp metering control. Even considering ramp delays, the average speed was found to increase by 20%.

Ramp metering control has been considered as one of the most effective methods to improve freeway operations. It may, however, alter the volume of traffic flow entering metered ramps. Due to the delays experienced by travelers waiting at metering sites, a portion of ramp flow might shift to other freeway entries, or adjacent arterials and surface streets. According to previous studies (Wattleworth, et al., 1967; Masher, et al., 1975; Chang, et al., 1994), the majority of the diverted trips were short trips (e.g., traveling only one or two freeway interchanges) since their waiting times spent at metered ramps were proportionally greater than that of long trips. Some attention has been paid on whether

the ramp metering control might favor freeway operations at the expense of increased congestion in adjacent streets.

Extensive evaluation of existing metering systems was conducted, and the impact of potential diversion of freeway trips was also analyzed by Piotrowicz, et al. (1995). Criteria used in the evaluation included travel distance and time, queue length, and delay at metering sites while considering the availability of alternate routes. It was found that there was no significant traffic diversion from freeways to adjacent alternate routes (e.g., Portland, OR; Los Angeles, CA; Seattle, WA; Detroit, MI; Denver, CO; Chicago, IL; and San Jose, CA) where ramp meters were operated. Also, freeway systems with access control at ramps seldom broke down even if traffic volume exceeded 2,000 passenger cars per hour per lane (pcphpl). In addition, it was found that diverting short trips from congested ramps to other under-utilized ramps or alternate routes might be desirable to alleviate congestion in both freeways and parallel arterials/streets. Several states, as mentioned above, have had the implementation experience of ramp metering control on freeways, while the state of New Jersey has considered the potential and benefits of implementing dynamic ramp metering control on freeways.

As an effective freeway traffic management method, ramp metering control has been discussed for more than four decades. Many control strategies varying from the simplest pre-timed metering to traffic responsive metering have been developed and examined. A lot of work has been done on optimizing metering rates for individual and/or a set of ramps. However, little research has been done on developing dynamic optimization metering control models and quantifying their benefits, while considering the impact of short ramps on local streets, arterials and freeways. Therefore, developing a dynamic ramp metering

control model that can efficiently optimize ramp metering rates subject to limited storage on the ramp and developing a sound approach to quantify its benefits are the major objectives of this study.

1.2 Problem Statement

In many studies, the purpose of utilizing ramp meters was the avoidance of flow breakdown on the freeway. To meet this goal, the capacity and demand of each freeway segment were estimated, and then metering rates were imposed such that the freeway could operate with less congestion. This process was rather straightforward and was described elsewhere in the literature (Jacobson, 1989). However, the job of optimizing metering rates is complex due to geometric conditions and dynamic traffic conditions. Thus, the process of quantifying the benefit of ramp metering control becomes difficult. It is necessary to study whether an effective algorithm can be utilized for simplifying the complexity of the dynamic optimization issue, and whether a suitable approach can be developed to quantify and evaluate the potential effectiveness of dynamic ramp metering control systems.

Delay reduction is often viewed as the primary benefit of implementing ramp metering control. Nevertheless, the increased total throughput and decreased fuel consumption and emissions may also be consequent benefits. In this study, the resulting throughput and delay after implementing various types of ramp metering control strategies are analyzed.

1.3 Objectives and Scope of Work

The goal of this study is to develop a dynamic metering control model and evaluate the potential of its implementation in a transportation corridor. To achieve this goal, the following objectives are identified:

1. Develop a dynamic multiple-ramp metering control system.

A dynamic metering control system will be developed to capture the dynamic traffic characteristics. An effective solution algorithm will be developed for the control system to determine optimal metering rates in real-time. The algorithm will focus on dynamically optimizing a set of on-ramp metering rates rather than the coordination with local surface traffic control systems.

2. Evaluate MOEs of freeways with and without ramp metering control.

A simulation approach, rather than actual field studies, will be applied in the evaluation. Simulation can generate various MOEs (e.g., total travel time and queuing delays) and experiments for testing different metering control strategies.

3. Evaluate the effects of “short ramps” to determining feasible metering rates.

Short ramps do not purely refer to those ramps short of physical storage area but depend on both storage area and the queue incurred by the entering flow.

4. Quantify benefits of ramp metering control.

The benefits of metering control under recurrent congestion during the peak period on a daily basis will be quantified in this study.

1.4 Organization

The remainder of the dissertation is organized into five chapters. Chapter 2 summarizes findings from previous studies. A number of ramp metering control strategies and models are reviewed, while the requirements and guidelines for implementing ramp metering control on freeway and ramps are discussed. The potential solution algorithms and tools that might be used to solve a dynamic multi-variant optimization problem are also investigated in this chapter. In Chapter 3, the development of a Simultaneous Perturbation Stochastic Approximation (SPSA) algorithm and dynamic ramp metering control model is discussed. Chapter 4 identifies a study site and illustrates various data that will be used for analyses. It also emphasizes the importance of the simulation approach and models the study network with CORSIM. In Chapter 5, the proposed dynamic metering control model is evaluated. The model developed in Chapter 3 is implemented at studied ramps, while analyses are performed on the ramp meter location, ramp storage capacity and various benefits under ramp metering control strategies. Finally, conclusions, recommendations, and suggestions for future study are presented in Chapter 6.

CHAPTER 2

LITERATURE REVIEW

There is a great deal of skepticism as to whether the control of metered ramps can be successfully implemented on a freeway network. Previous studies (Blumentritt, et al., 1981; Masher, et al., 1975; Piotrowicz, et al., 1995) addressed the success of metering control systems applied in various locations. However, very broad guidelines with limited recommended practices were discussed and no national standards were developed. The major reason was that control decisions were location and time dependent.

The Manual on Uniform Traffic Control Devices (MUTCD, 4H.01, 2000) states that the installation of ramp meters might be justified when the average delay of a subject freeway corridor was expected to be reduced. MUTCD also suggested that a thorough analysis of the geometric and traffic conditions of the freeway corridor should be conducted to determine whether ramp metering control was feasible. It was generally agreed among various highway authorities that the potential metering sites were those having poor traffic conditions (e.g., low speeds of 30-48 mph, low volumes of 1200-1500 vphpl) or higher rates of merging accidents (Masher et al., 1975). In a ramp meter design guideline (CALTRANS, 1991), typical design practices for new or modified ramp meters were described. In 1996, system operating strategies and user guidelines for the coordinated operation of ramp metering and adjacent traffic signal control system were developed (USDOT, 1996). In a study conducted by Taylor and Meldrum (2000), it was stated that the metering control should be implemented at places where flow breakdown could be prevented. Besides, special consideration should be given to the feasible range of metering rates (e.g., the upper and lower bounds), locations of signals and signs, and

ramp geometric condition. Requirements for developing a ramp metering control system are discussed in Sections 2.1 and 2.2 of this chapter. A review of ramp metering control strategies and models developed in previous studies has been systematically conducted and discussed in Sections 2.3 and 2.4. In addition, the review of solution algorithms and tools are discussed in Sections 2.5 and 2.6. A summary is contained in Section 2.7.

2.1 General Requirements

In this section, the general requirements of metering alternatives, feasible range of metering rates, signs and signals, and ramp geometric conditions are discussed.

2.1.1 Metering Alternatives

According to the way vehicles are released, two metering control alternatives were generally discussed: one-by-one metering and platoon metering control (Masher et al., 1975). One-by-one metering control only allows releasing a single vehicle per lane per cycle. Since the merging of one vehicle is smoother than the merging of a platoon of vehicles, one-by-one metering control can greatly reduce the interference of merging traffic and the associated accidents. Thus, one-by-one metering control was preferred in many places, where especially a bottleneck was in the vicinity of an on-ramp gore. One-by-one metering control is used in this study also.

Platoon metering control allows releasing two or more vehicles per cycle. This can be achieved by increasing the green time at the metered ramps. Platoon metering control is designed to handle higher ramp metering rates. Based on the operational experience on two-lane ramps, platoon metering control worked well and was preferred by practitioners. For single-lane ramps, however, platoon metering required a longer

cycle that may induce uncertainty in driver behavior and thus increase the probability of interrupted mainline traffic. Thus, platoon metering control should be applied with caution.

2.1.2 Feasible Range of Metering Rates

A very general rule for choosing the feasible range of metering rates was recommended by traffic agencies and practitioners (CALTRANS, 1975; Minnesota DOT, 1994). Usually, it might take several weeks or even months of data to calibrate the feasible range of metering rates for a specific metering system based on local traffic operations and geometric conditions.

Poitrowicz, et al. (1995) found that drivers would lose patience if they wait for more than 15 seconds before a ramp signal. Beyond 15 seconds, the number of violations increased significantly. Considering an acceptable queue length on a ramp, the feasible metering rates should be determined subject to the ramp storage constraint. The minimum metering rate was determined based on the maximum acceptable queue length.

Considering short ramps, Masher, et al. (1975) developed a method to estimate the minimum metering rate subject to the constraint of the storage capacity and the traffic demand entering the ramp. Practically, the minimum metering rate was about 240 vphpl (equal to 15 seconds/veh), and the maximum metering rate for one-by-one metering varied from 600 - 900 vphpl (CALTRANS, 1991). The metering rate of 900 vphpl was based on a cycle length of 4 seconds (2 seconds each for green and red intervals, respectively). For platoon metering control, the maximum metering rate could be increased to 1200 vphpl.

2.1.3 Signals and Signs

Ramp meters should meet all design specifications for control signals. Signal heads of a ramp meter can be either two-colored (red/green) or three-colored (red/green/amber), which was discussed by MUTCD (2000). A two-head signal is suggested because it provides a backup in case of malfunction or damage. The signal can be located on the left-hand side only or on both sides of a ramp for best visibility. Highway authorities should choose signal types according to local design regulations, and ensure consistency throughout the entire system.

Even if the public is well informed, drivers may not expect to stop before ramp signals. Therefore, advance-warning signs downstream of ramp meters are required to alert drivers. Many states have their own standard for the design of warning signs. For example, CALTRANS suggested using strobe lights with a red lens to reduce accidents at metered ramps. The locations of advance-warning signs usually depends on ramp geometry and sight distance. Moreover, supplementary signs with the legend “**STOP HERE ON RED**” or “**WAIT HERE FOR GREEN**” are commonly used to inform drivers of the existence of a ramp meter.

2.1.4 Ramp Geometric Conditions

The ramp geometric conditions (e.g., adequate sight distance, acceleration distance, and availability of storage space) should be carefully investigated before implementing ramp metering control. To prevent vehicles on the metered ramps from spilling back onto the adjacent local streets, adequate ramp storage is required. Otherwise, a better traffic diversion plan should be applied for relieving local traffic congestion. CALTRANS (1979) used an arrival-discharge chart, while Minnesota DOT (1994) used a rule-of-

thumb for estimating queue length that was 5-10% of the pre-metered peak hour volume. The estimated queue length could then be used for designing enough storage spaces on metered ramps.

A commonly used technique to increase the size of ramp storage is to increase the number of lanes on ramps. Minnesota DOT (1994) required all metered ramps to have at least two lanes before the ramp signal. In San Diego, a portion of the surface street was used to store vehicles, and then appropriate lane channelization and signal timing adjustments were required. Occasionally, the queue might exceed the storage capacity because of stochastic or unexpected vehicles arrivals. To avoid this situation, an alarm would be triggered when a long queue is detected before spillback can occur over the ramp entrance. The metering rate can then be increased to discharge more vehicles. In addition to the criteria mentioned above, the issues of public acceptance, enforcement requirements/regulation and availability of suitable alternate surface routes should be considered before implementing ramp metering control (Masher, et al., 1975; MUTCD, 2000; Poitrowicz, et al., 1995).

2.2 Technical Requirements

Freeway surveillance systems and their elements, ramp metering controller and constraints for ramp metering control are discussed in this section.

2.2.1 Freeway Surveillance Systems

While applying ramp metering control on a freeway network, various types of data (e.g., volume, speed and occupancy) are required for determining appropriate metering rates. Most freeway surveillance systems can provide such information through the connection

between detectors installed on freeways/ramps and communication devices (e.g., data transmission and processing devices). Considering the rapid growth in solid-state electronics and computer communication technologies, freeway surveillance systems nowadays have demonstrated desirable performance. A good surveillance system should be reliable and easily maintained.

As a primary component of a surveillance system, detectors play an important role in collecting traffic data. The commonly used detectors in freeway surveillance systems are classified into two types: the embedded detector and the non-intrusive detector as shown in Table 2.1 (FHWA, 1997).

According to the functions for the use of ramp metering control, detectors can be classified into (1) mainline, (2) merge, (3) passage, (4) demand, and (5) queue detectors, as shown in Figure 2.1. Note that all detectors in the figure are shown to be loop detectors, while functional equivalent detectors, such as magnetometers, sonic or other detectors can be applied to collect more accurate information (e.g., speed, occupancy, volume, and queue status).

(1) Mainline Detectors

Mainline detectors installed on the freeway mainline are usually located either prior to or after the merge area as shown in Figure 2.1. Information collected from the detectors includes flow rates, speeds and occupancies. Sometimes two sets of detectors are jointly used for estimating the number of vehicles within the merging area.

Table 2.1 Summary of Traffic Detectors

Detector Type	Description	Advantages	Disadvantages
Embedded Inductive Loop	Coil of cables embedded in pavement surface, which recognize the presence of vehicles through minute changes in electrical voltage caused by passing of vehicles.	Flexible Design. Wide range of application. Provides basic traffic parameters (e.g., vehicle counts and occupancy).	Requires pavement cuts to install. Subject to stress of traffic. Frequent maintenance requires lane closure.
Magneto-meter	Small-cylinders contain sensor coils that operate similar to inductive loops. Developed as alternative to loop detector in special situations.	Used in situations where loops are not feasible. (e.g. bridge decks) Less susceptible than loops to stress of traffic	Small detection zone. Typically used to provide only vehicle counts and occupancy.
Non-Intrusive Microwave Radar	Transmits electromagnetic wave to vehicles on roadway. Calculate traffic parameters by measuring the feedback signal frequency.	Generally insensitive to weather conditions. Provides day and night operation.	May lock on to the strongest signal (e.g., large truck.)
Infrared	Active infrared detectors transmit thermal radiation, while passive infrared detectors only measure the changes in thermal radiation that vehicles emit.	Active detectors emit narrow beam allowing for accurate determination of vehicle position. Provides most basic traffic parameters during day and night operation.	Operation affected by precipitation (e.g., snow and fog). Difficult in maintaining alignment on vibrating structures.
Ultrasonic	Transmits sound waves at frequency ranging 20 and 200 kHz. Detects vehicles by measuring return waves.	Provides most basic traffic parameters.	Weather conditions (e.g., temperature, humidity, air turbulence) can affect performance.
Acoustic	Uses microphones and signal processing technology to detect sounds associated with vehicles.	Generally insensitive to weather conditions. Provides day and night operation.	Relatively new technology for traffic surveillance.
Video Image processing	Video image processors receive information from video cameras and use algorithms to process the video image input.	Provides basic traffic parameters. Provides wide-area detection.	Performance may be negatively affected by harsh weather, shadows, and dim lighting. High installation and maintenance cost.

Note: The information of this table is derived from Federal Highway Administration “Freeway Management Handbook”, 1997.

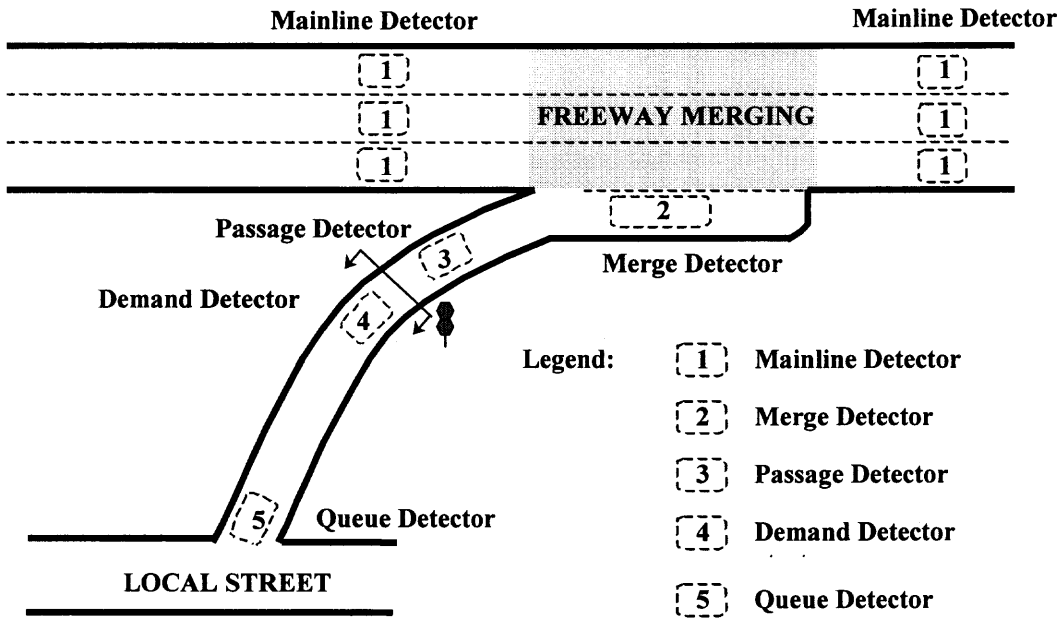


Figure 2.1 Configuration of a typical metering ramp.

(2) Merge Detectors

Merge detectors are installed after the on-ramp gore to detect the number of vehicles merging into the mainline traffic stream and whether the status of the merging area is jammed. When a jam occurs, the controller may hold the ramp signal in red to avoid stacking on the merging area.

(3) Passage Detectors

Passage detectors are installed just beyond the stop bar of the metering signal (e.g., 8 ft), which can register released vehicles during each green interval. As soon as the anticipated number of vehicles passing the stop bar is sensed, the green signal shifts to red. Sometimes passage detectors serve both as passage and merge detectors, but with less accuracy (Masher, et al., 1975).

(4) Demand Detectors

Demand detectors are installed at a sufficient distance before the stop bar of the metering signal (e.g., 18 ft), and their function is to register the presence of vehicles waiting for passage.

(5) Queue Detectors

Queue detectors are usually installed at the entrance of an on-ramp, or sometimes at the adjacent local street. The main function of queue detectors is to detect the queue length that may spillback onto the local street and report this information to the controller. Thus, adequate control actions can be taken to avoid queuing vehicles blocking the local street.

Note that the determination of detector locations is highly dependent on the type of metering control (e.g., pre-timed, traffic responsive) and the geometric condition of the study site (e.g., length of auxiliary lane, storage capacity, weaving length, etc.). Characteristics of various types of detectors are summarized in Table 2.2.

Table 2.2 Characteristics of Detectors for Metering Control

Type of Metering Detector	Approximate Dimensions (ft)	Traffic Parameters Measured
Mainline	6×6	Speed, Occupancy, Vehicle Counts
Merge	40×6	Occupancy
Passage	6×6	Vehicle Counts
Demand	Two 6×6 loops or one 15×6 loop	Occupancy
Queue	6×6	Occupancy

Note: The information of this table is derived from Federal Highway Administration “Traffic Control Handbook”, 1996.

2.2.2 Ramp Metering Controllers

The ramp metering controller is responsible for determining metering rates/cycles by implementing control strategies and tactics. For pre-timed controllers (e.g., dial-and-stepped-cam controller, digital controller), metering rates or intervals of red, yellow and green lights can

be set up either with a time clock or by remote control. The duration of each metering interval determined by such a controller corresponds only to recurrent traffic conditions. Therefore, the major disadvantage of the pre-timed controller is its limited ability to respond to non-recurrent traffic conditions and significant traffic variations during a time period. For centralized controllers, the timing and control operations can be determined by computer software that optimizes metering rates based on extensive traffic information collected from detectors. The centralized controller can be supplemented by a backup pre-timed controller that initializes pre-specified metering rates in case of computer failure during metering periods. The centralized controller can dynamically change signal timings to adapt to the change of traffic conditions.

The advantages of using a centralized controller are universally agreed as being flexibility, reliability and capability to adapt to dynamic changes in traffic demand (Masher, et al., 1975; Piotrowicz, et al., 1995). However, a pre-timed controller may also be used in some systems if detectors are not available at the control site.

2.2.3 Constraints for Ramp Metering Control Systems

Several constraints are usually considered in the application of ramp metering control to ensure that the solution metering rates are feasible or workable at individual ramps. These constraints include: (1) the upper and lower bounds of metering rates allowed for the metered ramp, (2) the demand-capacity restriction at the vicinity of the metered ramp, and (3) the storage capacities of the metered ramps, which are described below.

(1) Upper and Lower Bounds of Metering Rates

According to the literature review conducted in Section 2.1.2, traffic engineers determined the highest and lowest metering rates based on practical considerations. For example, for one-by-one metering control, the minimum metering rate was about 240 vehicles

per hour per lane (vphpl), since a rate lower than that might cause high violation rates. On the other hand, since drivers needed at least four seconds to stop, respond to the ramp signal, and prepare to merge into the mainline, the maximum metering rate for one-by-one metering control was generally 900 vphpl (Masher, et al., 1975; Piotrowicz, et al., 1995,).

The appropriate metering rates were suggested to be within the range between the upper and lower bounds of 240 and 900 vphpl, respectively. Assume that a general freeway segment has N links, numbered from 1 through N from the upstream end to the downstream end of the freeway. The metering rate $R_j(t)$ for the metered ramp located on the j^{th} link at time t (see Figure 2.2) should be greater than the minimum allowable metering rate F_j and less than the maximum allowable metering rate U_j , as formulated in Equation 2.1. If $R_j(t)$ is greater than U_j , $R_j(t)$ is set in default and equal to U_j . Similarly, if $R_j(t)$ is less than F_j , $R_j(t)$ is set in default and equal to F_j .

$$F_j \leq R_j(t) \leq U_j \quad (j=1, \dots, N) \quad (2.1)$$

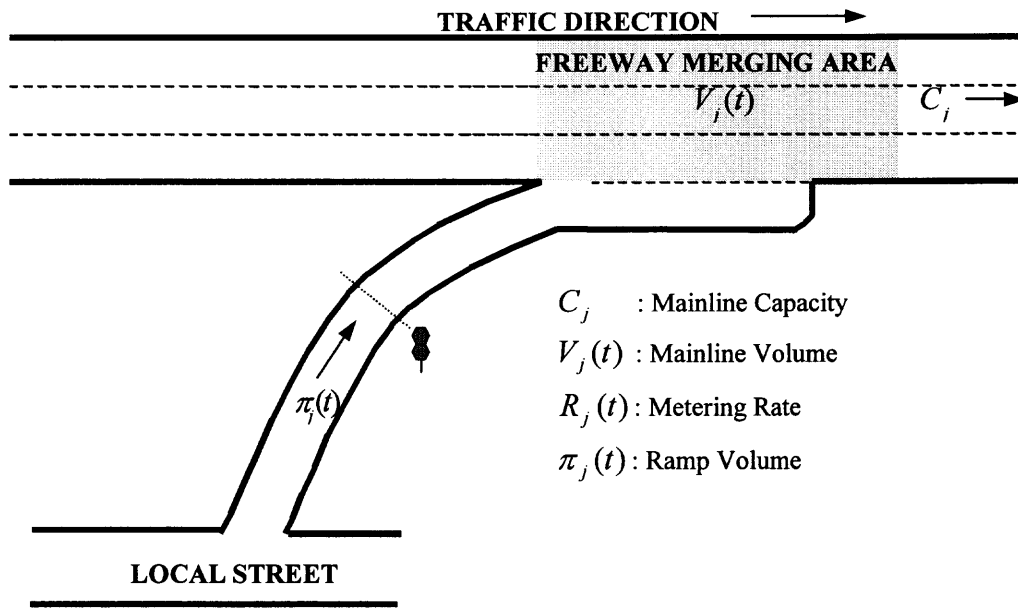


Figure 2.2 Configuration of a ramp junction.

(2) Capacity Constraints

The capacity constraints discussed here are used to determine metering rates if the freeway capacity C_j and the entering volume $V_j(t)$ at time t can be estimated. The metering rate $R_j(t)$ should be less than or equal to the difference between C_j and $V_j(t)$. Thus,

$$R_j(t) \leq C_j - V_j(t) \quad (j=1, \dots, N) \quad (2.2)$$

In Equation 2.2, if $V_j(t)$ approaches C_j , the metering rate decreases and congestion may occur in the ramp junction. In such a situation, the metering rate should be the minimum metering rate (i.e., 240 vphpl) to secure that the traffic flow is always less than the mainline capacity.

(3) Queue Constraints

Queue constraints are used to prevent the congestion caused by queuing vehicles spilling back from the metered ramp to the local street. Usually, short ramps have limited storage areas because of physical restrictions or large entry demand. Therefore, the metering rate should be optimized subject to the relationship between the ramp storage and the entry flow into the ramp.

The function of the queue detector installed at the entrance of the on-ramp is to monitor the queue length and the duration that the detector has been occupied. If the duration is greater than a pre-specified threshold duration, the metering rate will be increased to quickly discharge the queue (Masher, et al., 1975; Poitrowicz, et al., 1995). In practice, several threshold durations are specified to invoke different metering rates. A solid-green state will be given when a long queue occurs.

2.3 Ramp Metering Control Strategies

Over the past four decades, various ramp metering control strategies have been studied. These strategies were used to determine the optimal metering rates and achieve certain objectives shown in Table 2.3. In this table, the objectives vary from minimizing travel time, delay, and number of diversion vehicles to maximizing entry volume and throughput. Despite of the diversity of these objectives, they can be grouped into two categories: (1) maximizing total input and (2) maximizing total output (capacity utilization). The theoretical proof of the equivalence for the objectives under the same category can be found in previous studies conducted by Wattleworth, et al. (1965 and 1967) and Masher, et al. (1975).

Table 2.3 Objectives of Ramp Metering Strategies

Category	Objectives	Unit(s)
Maximize total input	Minimize total travel time	Vehicle-hour, person-hour
	Minimize overall queuing delay	Vehicle-hour, person-hour
	Maximize total input volume	Vehicle, person
	Minimize total diversion	Vehicle, person
Maximize total output	Maximize total mainline volume given a level of service	Vehicle, person
	Maximize total throughput	Vehicle-mile, person-mile

In general, ramp metering control strategies can be classified into four categories: (1) Pre-timed, (2) Local Traffic Responsive, (3) System-wide and (4) Integrated System Control, which are discussed in the following sections.

2.3.1 Pre-timed Control

One of the pioneer ramp metering control strategies is pre-timed control. The metering rate is determined by analyzing historical volume-capacity conditions during a specific time period for the target ramp. The pre-timed control provides the basic function of

breaking up platoons by setting an upper flow rate at the metered ramp. Although such a strategy can not effectively respond to variations in traffic conditions over time (only historical average volumes for the mainline and on-ramp are considered), it can often be implemented as an initial operating strategy until individual ramps can be incorporated into a traffic responsive system. Pre-timed control can be implemented on a number of ramps to reduce accidents (Pooran, et al, 1996) and travel times (Kang, et al., 1999).

2.3.2 Local Traffic Responsive Control

A local traffic responsive control strategy determines metering rates for a single or a set of ramps. The metered ramps are considered independent rather than interconnected. Unlike pre-timed control, local traffic responsive control determines metering rates based on measured traffic conditions collected from traffic surveillance devices (e.g., detectors on the ramp and mainline). The commonly used local traffic responsive strategies are demand-capacity, occupancy, gap acceptance and speed control (Drew, 1967; Wiener, et al., 1970; Papageorgiou, et al., 1991, and Hadj-Salam, et al., 1995). Among those, demand-capacity and occupancy-based strategies are operated similarly. In both, the metering rates are based on the difference between the mainline capacity (or the volume for a desired service level) immediately downstream of the ramp and the upstream traffic volume. However, occupancy-based control estimates traffic volume based on detected occupancy instead of measuring the volume directly. For gap-acceptance and speed-control, the gap at the merging area and the upstream speed are detected respectively and applied to determine the proper metering rates.

Although local traffic-responsive control strategies do respond to actual traffic conditions, they cannot perform very well especially for the upstream metered ramps of a bottleneck. It is because that the downstream congestion cannot be detected until the

shock wave reaches back to the metered ramp. The existing practices are ALINEA (to be discussed later) in Paris, France (Papageogiou, et al, 1991) and in Austin, Texas (Poitrowicz, et al., 1995).

2.3.3 System-wide Control

System-wide control strategies refer to dynamic control on a series of on-ramps. The major feature of system-wide control is that all metered ramps are considered to be interconnected. Therefore, the metering rate at a ramp is influenced by traffic conditions at other metered locations. System-wide control determines metering rates from both overall system and local capacity constraints, and real-time traffic measurements. The strategy usually leads to non-linear optimization programming governed under centralized computer systems. Existing practices are METALINE (to be discussed later) implemented in Paris, France (Papageogiou, et al., 1990), Seattle, Washington, and Denver, Colorado (Poitrowicz, et al., 1995; Taylor, et al., 2000).

2.3.4 Integrated System Control

Recently, the concept of integrated system control has attracted considerable interest (Chang, et al., 1994b). Integrated system control coordinates not only the freeways and ramps, but also the arterials and local streets to achieve desirable corridor wide performances (e.g., total travel time and delay). The ramp meters and arterial traffic signals/signs can be jointly optimized in response of real-time traffic conditions. The potential advantage of integrated system control is that the corridor wide surveillance and control can benefit travelers on both freeways and arterials. Projects toward developing and implementing such integrated control are underway in Seattle, Washington (Jacobson, 1989 and 1994).

2.4 Ramp Metering Control Models

Various models have been developed and tested in real-world freeways or in a simulated environment. According to the optimization method used for the development of ramp metering control models, the models can be grouped in four categories: (1) Pre-timed Linear Programming Models, (2) Local Traffic Responsive Models, (3) System-wide Non-linear Programming Models, and (4) Emerging Large-scale Heuristic Models.

2.4.1 Pre-timed Linear Programming (LP) Models

Pre-timed linear programming models are static models that search for the optimal combination of metering rates for a single or a set of ramps. Such models aim at sending as many vehicles as possible onto the freeway subject to the demand and capacity constraints on each freeway segment. Because the availability of LP software packages and only historical data are needed, the LP models are fairly simple to use and implement (Marshner, et al., 1975). However, such models with pre-specified metering rates could not respond to significant variation in the traffic stream over a time period.

Wattleworth and Berry (1965) analyzed the theoretical considerations of ramp metering control during peak periods. In that study, the objective functions (i.e., total travel time and system output) of the metering control were developed, while the traffic measurements as well as the locations of the detectors needed for control were discussed. A LP model was formulated. The pre-timed metering rates were optimized by maximizing the system output (total exiting volume via the mainline exit and off ramps). Two linear constraints were considered in the model: the bottleneck capacity constraint and the upper bound of metering rate constraint. A segment of Congress Street Expressway in Chicago was analyzed. The optimal ramp metering rates were determined

based on assumed O/D demand information. However, the queue constraints on the metered ramps were not considered.

A similar LP model was developed by Wattleworth (1967). The total input to the freeway system (including mainline and on-ramps) was maximized for a pre-timed metering system, while the constraints of bottleneck capacity, the upper bound metering rate, and the queue length were considered. He found that metering control would be one of the most effective ways to maintain a stable traffic flow condition on a congested freeway network. Moreover, he concluded that adequate ramp storage area should be designed to keep adjacent streets from being adversely impacted. Later, Papageorgiou (1980) further enhanced Wattleworth's LP model, considering time-varying traffic fluctuations on the mainline. However, the mainline volume could only change at a pre-specified frequency (e.g., twice during the peak period), which was still incapable to respond to situations with significant traffic variations.

Chen, et al. (1974) developed a metering control model that maximized average freeway throughput when peak demand exceeded freeway capacity. In that model, the ramp metering rates were optimized subject to the upper bound metering rate and density constraints. Greenshield's model was applied to define the speed and density of the studied freeway.

2.4.2 Local Traffic Responsive Models

With local traffic responsive models, ramp metering rates are optimized based on real-time traffic conditions. The pioneer research on local traffic responsive models was conducted by Drew (1967) and Wiener, et al. (1970). Statistical gap-acceptance models were used to analyze vehicle movements in a merging area. Their models could be

applied to a traffic responsive controller to break up vehicle platoons into single or a smaller group of vehicles merging into the mainline traffic stream according to the sizes of detected gaps.

Drew (1967) studied the merging behavior on Gulf Freeway in Houston, Texas. Factors affecting the critical gap (acceptable gap by half of the drivers when merging with the mainline) were identified, while the critical gaps were found to follow a gamma distribution. The vehicle merging delays and the average queue length were formulated by assuming that the vehicle headways on the mainline followed Erlang distributions. In that study, the ramp metering rate was optimized based on the queue length and pre-specified critical gap of the metered ramps.

In a later study conducted by Wiener, et al. (1970), gap-acceptance models were developed to optimize the critical gap by minimizing the expected queue length and wait time for a ramp. The stochastic process of queue reduction and regeneration on the ramps of Gulf Freeway in Houston was studied. The gap-acceptance models for stationary queue length and wait time were formulated as a function of critical gaps by assuming that vehicle arrivals at ramps followed a Poisson distribution. The optimal metering rates could be adjusted based on detected queue length.

Stephanedes, et al. (1993) evaluated a traffic responsive control model for I-35w developed by Minnesota DOT. For each metered ramp, a rate table was developed according to the volume-occupancy thresholds and the corresponding metering rates derived from historical data of the ramp. In real-time operations, the upstream volume and downstream occupancy of the ramp were compared with the thresholds in the rate table, and then the proper metering rate could be identified. The MOEs used for

evaluation included the total entry volume and the total delay experienced by vehicles traveling under 45 mph. The results suggested that the rate table should consider the trade-off between increased capacity and increased delay.

ALINEA, developed by Papageorgiou, et al., (1991, 1995), is a local occupancy-based metering control strategy designed through the application of classical feedback control law. Only two measurements, occupancies on the ramp and immediately downstream of the ramp, were used to dynamically adjust the metering rates. ALINEA was tested on the Peripherique Corridor in Paris (Salem and Papageorgiou, 1995), while three MOEs (i.e., total travel distance, total travel time and mean speed) were used to assess the efficiency of the control. Although the results were encouraging, the excessive queue length on ramps frequently caused the control to be overridden with the maximum metering rates to discharge the queues.

Banks (1991) analyzed ALINEA and found that the linear controller was more effective for regulating non-congested traffic when nonlinearities in traffic behavior were not presented. He developed a local traffic responsive model, within which the metering rate was determined by the difference between the upstream and downstream mainline volumes, while the difference between the actual released volume and metered volume was used to adjust the metering rate dynamically. The model was tested on WB I-8 and WB SR-94 in San Francisco, and the results showed that the model was more applicable when the analyzed freeway had sufficient capacity (i.e., un-congested traffic conditions).

2.4.3 System-wide Non-linear Quadratic Programming Models

In view of the deficiencies of local traffic responsive model (e.g., ramps are considered isolated rather than connected), several system-wide metering control models were developed (Papageorgiou, 1983; Papageorgiou, et al., 1989 and 1990; Banks, 1990; Stephanedes, et al., 1993; Chang, et al., 1993 and 1994). The system-wide models could handle a series of ramps in a traffic responsive scheme, while considering the interconnections of traffic conditions between consecutive ramps in real-time. The system-wide models often led to hierarchical non-linear optimization programming carried by centralized computer systems, which processed traffic data, optimized metering rates, and executed the control rules through ramp meters in real-time.

System-wide non-linear models were first developed by Yuan, et al. (1971). The equivalent traffic demand was formulated as the sum of traffic and queue demand in order to balance the queues on all metered ramps and prevent vehicle spillback onto local streets. A quadratic programming problem was formulated to determine the desirable metering rate by penalizing the deviation from the equivalent traffic demand. In the optimization, three constraints were used: the vehicle conservation constraint, the Greenshields' speed-density constraint, and the upper bound metering rate constraint. The model was tested on a hypothetical freeway with only one on-ramp. The results showed that the optimal metering rate could shorten the queue length on the ramp without a significant reduction on freeway throughput.

Stephanedes, et al. (1993) presented a non-linear metering control model to alleviate congestion during peak periods. In his study, the vehicle conservation and Greenshields' speed-density models were used to describe the traffic flow in a freeway

corridor, while the total vehicle travel time was used as the objective function to optimize the metering rates. The optimal ramp metering rates were determined by minimizing the quadratic objective function using a conjugate gradient search method. The model was tested on a hypothetical freeway segment with one on-ramp. The results showed that due to the limitation of the network size, the total travel time was not reduced significantly.

In a real-time traffic control system, the short-term prediction of traffic information (e.g., speed, volume, density, and occupancy) became a necessity to respond to traffic variation effectively (Smith and Demetsky, 1995). Thus, prediction was proposed as a very important component in system-wide metering control models. Papageorgiou (1983) developed a hierarchical decomposition algorithm that could deal with large-scale nonlinear problems including optimization, prediction and control. This algorithm consisted of three functional layers: adaptation layer, optimization layer and direct control layer. The adaptation layer predicted exogenous parameters to the control model, including traffic speed, volume, and occupancy. With the predicted parameters, the optimization layer determined the optimal metering rates for a set of ramps by minimizing the total vehicle travel time. The direct control layer then implemented a local feedback control law to maintain the optimal metering rates for individual ramps despite various disturbances such as traffic incidents in real-time. The model was tested on a hypothetical freeway network with six on-ramps and six off-ramps.

Later, Papageorgiou, et al. (1989) developed three dynamic traffic flow models (vehicle conservation, volume-density and speed-density models) while considering the impact of weaving movements at ramp junctions. The three nonlinear models were tested using real traffic data collected from the Boulevard Peripherique in Paris. After

thorough investigation of the mathematical structure, parameter calibration, and sensitivity analysis, the models were integrated with a system-wide ramp metering control model and simulated in Paris (Papageorgious, et al., 1990). In that study, a metering control model METALINE was developed, within which a Linear-Quadratic (LQ) control law was implemented. The simulation results showed that METALINE could be activated earlier before congestion formed at the ramp junction and thus dissolve congestion more effectively than pre-timed control or local control systems, such as ALINEA.

2.4.4 Emerging Large-scale Heuristic Models

Because the system-wide ramp metering models usually involve rather complex nonlinear optimization techniques, which require considerable computation efforts for obtaining optimal solutions, these models are too time-consuming for real-time implementation. Besides, these models might result in oscillatory metering rates because of the difficulty to describe non-linear and time-varying freeway systems, especially when traffic data are frequently corrupted with noise or transmission errors. Some heuristic ramp metering models are developed to achieve sub-optimal solutions for large-scale freeway systems (Goldstein, et al., 1982; Chen, et al., 1990; McDonnell, et al., 1995; Taylor, et al., 1998), which could quickly respond to dynamic traffic conditions in freeway operations and efficiently release ramp vehicles.

Goldstein and Kumar (1982) developed a decentralized metering control model to obtain the sub-optimal metering rates for large-scale freeway systems. They argued that the widely used centralized control model might require manipulation on large size matrices, which is fairly time-consuming. In their study, metered ramps were divided

into overlapping groups (e.g., ramps 1, 2, 3 as group 1, ramps 2, 3, 4 as group 2, and ramps 3, 4, 5 as group 3, etc.). The centralized model was transformed using a cascading technique such that a sub-controller could handle the ramps in each group. The decentralized control model needed less time because of the smaller matrix size, yet the traffic conditions in both upstream and downstream ramps were considered. The model was tested by simulating a freeway network in San Diego, California. The results showed that the model could respond to dynamic changes in local traffic conditions much more quickly than the centralized controller, while similar improvements in average speed and delays were achieved.

Chen, et al. (1990) developed an expert fuzzy controller for a ramp metering control system near the San Francisco-Oakland Bay Bridge. The objectives of the controller were maximizing system throughput and minimizing adverse impacts on local streets. Seven rules were designed based on expert knowledge from the bridge operators, in the form of IF “freeway condition” THEN “control action”. A look-up table was integrated with the seven rules to determine adjusted metering rates under various traffic conditions, ranging from heavily congested to extremely light flow in the rule base. Through fuzzy logic implication, the controller could infer to what degree the condition was true, thus determining metering rates. The simulation results showed that the possible saving percentage in person-hours with the expert fuzzy control was 40%.

McDonnell, et al. (1995) presented an evolutionary programming technique for freeway ramp metering control. The rule-based controller determined metering rates based on upstream, downstream, and adjacent freeway occupancy levels. Evolutionary

programming was demonstrated as a viable approach to integrate ramp metering control strategies to alleviate freeway congestion effectively.

Taylor, et al. (1998) developed a fuzzy logic model to control multiple ramps in a large-scale freeway network. Seventeen rules, including five rules for occupancy, four rules for speed coupled with occupancy, six rules for shock waves/acceptable gaps, and two rules for excessive queues, were developed and integrated with FRESIM, a microscopic freeway simulation model developed by FHWA. A simulation of northbound traffic on I-5 in Seattle was conducted, and three MOEs (total vehicle travel distance, total travel time, and average delay) were evaluated. The simulation results showed that the fuzzy logic control outperformed the Local Metering Model and the Bottleneck Model that were used in the freeway control system in Seattle. The testing results indicated that the fuzzy logic control algorithm could achieve lower mainline occupancy and higher throughput than the Local Algorithm (Taylor, et al., 2000).

2.5 Research Algorithms

In the area of ramp metering control, the key issue is to optimize the metering rate over space and time. Many traffic control theory and optimization algorithms have been proposed and implemented based on optimization techniques, automatic control, optimal control theory and artificial intelligence methods such as artificial neural networks, fuzzy systems, and expert systems (Chu, et al., 2002). Some of these algorithms are discussed in the following sections.

2.5.1 Artificial Neural Network (ANN)

Based on the findings in biological neural networks, Artificial Neural Networks (ANNs) try to mimic interconnected multiprocessor architecture and attain the power and flexibility. It consists of a multi-layer structure and multiple nodes (e.g., input nodes, output nodes and intermediate nodes in intermediate layers) that communicate through their connecting synapses. Each node is linked to other nodes with varying coefficients of connectivity that represent the strengths of these connections. The network has learning ability by adjusting these strengths to produce appropriate output through training examples fed to the network. ANNs use precise inputs and outputs to train a generic model that has sufficient degrees of freedom to formulate a good approximation of the complex relationship between the inputs and the outputs variables (Tsoukalas, et al., 1996).

Over the past decade, ANNs as a class of learning algorithms have expanded enormously and applied successfully in transportation research. In ramp metering control, ANNs are used to track error information, produce ramp metering rates, feed back them into the traffic system, compare the output (e.g., traffic density) with the target critical value, generate a new tracking error and complete a feedback cycle until the freeway system being controlled maintains a desired level of service (Zhang, 1997). ANNs have the advantage of being capable of modeling non-linear systems, handling a variety of variables (e. g., symbolic, nominal or categorical variables) and noisy data, and finding the solution automatically (Mohammadian, et al., 2002). These advantages make ANNs an attractive alternative to traditional modeling frameworks.

However, ANNs need substantial data that are representative and cover the entire range, while substantial time is needed to properly train an ANN (Tsoukalas, et al., 1996). ANNs having less transparency in processing data do not appear to offer explicit measures of sensitivity, which limits their ability to analyze alternative policies. Additionally, ANNs have difficulties to integrate different modeling structures into an integrated modeling system (Mohammadian, et al., 2002).

2.5.2 Fuzzy Theory

In fuzzy systems, the input and output variables are directly defined with fuzzy sets that can be expressed in linguistic terms, while their interrelationship takes the form of well-defined if/then rules. Fuzzy is a methodology for dealing with imprecision, approximate reasoning, rule-based systems, and computing with words (Tsoukalas, et al., 1996).

Fuzzy logic systems allow far greater flexibility in formulating system descriptions at the appropriate level of detail. Complex process behavior can be described in general terms without precisely defining the complex (usually nonlinear) phenomena involved (Tsoukalas, et al., 1996). Fuzzy logic control is suitable for ramp metering with complex traffic conditions because it can regulate nonlinear, stochastic, and time delay systems (Chen, 1990). Fuzzy logic can utilize incomplete or inaccurate data, balance conflicting objectives and handle nonlinear systems with unknown models. It does not require extensive system modeling and it is easy to fine tune (Taylor, et al., 2000).

Fuzzy logic is an extremely suitable concept to combine subjective knowledge (linguistic information) and objective knowledge (Bogenberger, et al., 2002). However, the rule base (the set of rules) has to incorporate human expertise. In expert systems, exhaustive rules and databases are required for accurate dynamic model control. When

this is not possible, special techniques have to be applied for compensation (Chen, 1990). Human behavior-like factors are involved in fuzzy logic control, which preprocesses raw data rather than calculates metering rates directly from raw data. These procedures diminish the attraction of fuzzy logic control to those practitioners who generally are more comfortable with the greater transparency of statistically-based methods (Mohammadian, et al., 2002).

2.5.3 Simultaneous Perturbation Stochastic Approximation (SPSA)

Recently, Simultaneous Perturbation Stochastic Approximation (SPSA) has attracted attention from transportation researchers. SPSA is a mathematical algorithm which searches for an optimization solution starting with an initial guess and then updating it with iterations until the desired result is approximated.

SPSA does not rely on direct measurements of the gradient (derivative) of the objective function being optimized. Instead, it relies on measurements of the objective function, avoiding the difficulties to obtain detailed modeling information describing the relationship between the parameters to be optimized and the objective function. SPSA is especially efficient in multivariate optimization problems of minimizing or maximizing an objective function dependent on multiple variables. Since there are fewer algorithm coefficients that need to be specified, SPSA will be easier to implement than other stochastic optimization methods (Spall, 1998). SPSA is a powerful method for optimization in challenging nonlinear problems. Theoretical and numerical studies generally show that SPSA has equal or greater efficiency in terms of the overall cost of the optimization process (Spall, et al., 1999; Spall, 2000). SPSA is quite promising and an easy-to-use optimization algorithm (Ting, et al., 1998; Kleinman, 1998).

In this study, SPSA algorithm is proposed to solve the optimization problem in ramp metering control. The detailed SPSA algorithm will be introduced in the next chapter.

2.6 Simulation Models

Traffic simulation models can be classified as being microscopic (CORSIM, TRANSIM, MITSIM, PARAMICS, VISSIM, AIMSUN2, etc.), mesoscopic (FREFLO, METANET, AUTOS, VISUM, etc.), macroscopic (DYNASMART, DYNAMIT, INTEGRATION, METROPOLIS, etc.) according to their representation of traffic flow or vehicle movement (Chu, 2002). In this study, vehicle movement will be analyzed under ramp metering control. A microscopic simulation mode is required to calculate and measure the state of individual vehicles (e.g., speed, travel time, delay, etc.). CORSIM is a popular and powerful simulator that can meet the study needs.

CORSIM, a microscopic corridor traffic simulator developed by Federal Highway Administration (FHWA), has been applied extensively to a wide variety of areas by both practitioners and researchers and it is one of the most widely used traffic simulation models. It can simulate stochastic individual traffic vehicle operations and control systems on integrated networks containing freeway and surface streets. The behavior of each vehicle is represented in the model through interaction with its surrounding environment including roadway geometry and adjacent vehicles in the traffic stream. CORSIM can also simulate fairly complex geometric conditions (e.g., curvature, super-elevation, lane add/drop, acceleration/deceleration lanes, grade section, and interchanges) and realistic driver behavior after the model is appropriately calibrated and validated

(Ven der Zijpp, et al., 2001). CORSIM is capable of simulating most freeway geometric, traffic, and surveillance and control conditions by different card types.

To execute the CORSIM traffic simulation model, the windows version of TSIS provides an integrated, user-friendly, interface and environment. Specifically, it is designed to support the CORSIM simulator and CORSIM output processor, TRAFVU (TRAF Visualization Utility). The user can extend TSIS functionality by adding other traffic engineering or analysis software tools that have been designed to conform to the TSIS traffic tool interface. The advantages of operating within the TSIS environment include an intuitive, user-friendly graphical interface; scrollable screen output; better memory management for CORSIM; and on-line context-sensitive help that encompasses the TSIS, TRAFVU, and CORSIM User's Guides. TSIS provides an efficient mechanism for communicating results from traffic analysis tools, such as simulation systems. TSIS is evolving into a common repository to support the data requirements of many traffic models and simulation systems.

The graphics processor TRAFVU deployed in FHWA's Traffic Research Laboratory (TREL), is a state-of-the-art, object-oriented, user-friendly graphics post-processor for CORSIM. TRAFVU displays traffic networks; animates simulated traffic, signals, and Measures of Effectiveness (MOEs). TRAFVU takes full advantage of the processing power and graphics capabilities of today's computers. The expanded capability of this product (the ability to animate in multiple windows and to simultaneously process multiple cases) over previously available graphics processors provides users with an easy-to-use, yet powerful tool for conducting traffic analyses.

2.7 Summary

In this chapter, the general requirements for various ramp metering control systems were discussed, including the freeway surveillance systems, metering controllers and constraints for previous metering control algorithms. The freeway surveillance systems were focused on discussing locations of detectors for metering control. Two types of metering controllers, pre-timed and computer-centralized controllers were described in detail. Three types of constraints associated with ramp metering control were investigated, the upper and lower bounds of metering rates, the capacity and the queue constraints. These constraints are widely used for both localized and system-wide systems and are critical for developing the real-time ramp metering control in this study.

This chapter discussed various ramp metering control strategies (e.g. pre-timed, local traffic responsive, system-wide and integrated system control strategies) developed in previous studies. Four metering control models (pre-timed linear programming, local traffic responsive, system-wide non-linear programming and emerging large-scale heuristic models) have been developed in the past and used in practice and through simulations.

Fuzzy theory, ANNs, and SPSA were discussed as the potential research algorithms. In this study, SPSA optimization will be implemented based on the advantages of its properties, while the microscopic simulator CORSIM will be used for modeling and evaluation proposes.

CHAPTER 3

METHODOLOGY

3.1 Development of Ramp Metering Control Model

The goal of ramp metering control is to alleviate freeway congestion and improve its operational performance. Several MOEs (e.g., total delay, total vehicle-miles, total traffic throughput, etc.) can be candidate objectives to be optimized (Chang, et al., 1994). The total traffic throughput is relatively more appealing than others, since the number of discharged vehicles from a freeway system can be easily detected in practice. The total throughput was thus selected as the objective to be maximized subject to constraints of link densities, capacities and the boundaries of metering rates in this study. Before formulating the dynamic metering control model, the following assumptions are made:

1. The traffic flow on the mainline is steady without serious incidents blocking the freeway, which can represent the steady relationship among flow, speed and density.
2. Each vehicle passes through a meter separately from other vehicles based on a first-come first-released discipline.
3. The average vehicle length is 20 feet. This assumption is used to approximate the storage capacity of the metered ramp.

To develop a ramp metering control model, a freeway including N small segments with multiple on-ramps and off-ramps was assumed and is shown in Figure 3.1. Each small segment contains at most one on-ramp and one off-ramp. The control time period is a series of equal intervals. Assuming an equilibrium flow-density relationship exists for each freeway link i , and the traffic status on a segment can be simply described by the mean link density, the dynamic equation of link density $\rho_i(k)$ (vehs/mi/ln) can be formulated as Equation 3.1 (Chang, et al., 1994).

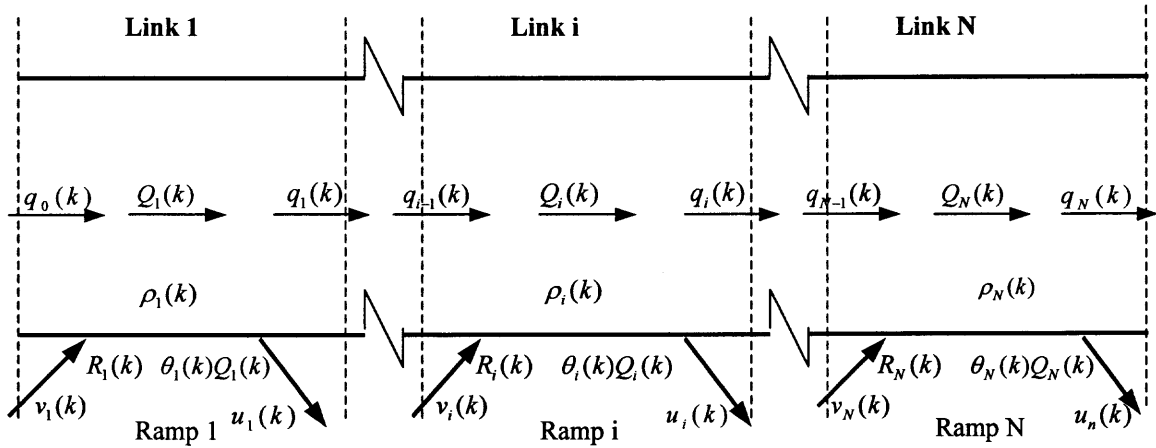


Figure 3.1 General freeway configuration.

$$\rho_i(k) = \rho_i(k-1) + [q_{i-1}(k) + \delta_i^{on} R_i(k) - \delta_i^{off} \theta_i(k) Q_i(k) - q_i(k)] \frac{T}{L_i l_i} \quad \forall i \quad (3.1)$$

where $q_i(k)$: the flow rate entering link $i+1$ from link i during interval k , (vph);

$R_i(k)$: the metering rate for an on-ramp of link i during interval k , (vph);

$Q_i(k)$: the mean flow rate of freeway link i during interval k , (vph);

δ_i^{on} : equal to 1 if an on-ramp of link i exists, otherwise equal to 0;

δ_i^{off} : equal to 1 if an off-ramp of link i exists, otherwise equal to 0;

$\theta_i(k)$: the turning percentage of traffic to the off ramp of link i during interval k ,

(%);

$v_i(k)$: the volume entering the on-ramp of link i during interval k , (vph);

$u_i(k)$: the volume exiting the off-ramp of link i during interval k , (vph);

T : the duration of a time interval, (hours);

L_i : the physical length of link i , (miles);

l_i : the number of through lanes of link i .

In Equation 3.1, $\rho_i(k-1)$ is the link i mean density during interval $k-1$. The item $q_{i-1}(k) - q_i(k)$ reflects the change of the flow rate entering link i . $\delta_i^{on} R_i(k)$ and $\delta_i^{off} \theta_i(k) Q_i(k)$ express the expected flow rates entering and exiting link i through on-ramps and off-ramps, respectively. The item $\delta_i^{on} R_i(k) - \delta_i^{off} \theta_i(k) Q_i(k)$ indicates the change of the flow rate at link i as a result of the traffic fed from the on-ramp and released from the off-ramp. Thus, Equation 3.1 expresses the dynamic density relationship that the projected mean density $\rho_i(k)$ of time interval k as the sum of the mean density at time interval $k-1$ and the change of mean density at time interval k . The flow rate entering link i , $q_i(k)$ can be approximated with the weighted sum of two segment boundary flows: $[1 - \delta_i^{off} \theta_i(k)] Q_i(k)$ and $[Q_{i+1}(k) - \delta_{i+1}^{on} R_{i+1}(k)]$. Thus,

$$q_i(k) = \alpha_i(k) [1 - \delta_i^{off} \theta_i(k)] Q_i(k) + [1 - \alpha_i(k)] [Q_{i+1}(k) - \delta_{i+1}^{on} R_{i+1}(k)] \quad \forall i \quad (3.2)$$

where $\alpha_i(k)$ is the weighted factor representing the interaction between flows on links i and $i+1$ at interval k , which captures the interrelations between adjacent segment flows. The value of 0.5 set for $\alpha_i(k)$ can indicate the same influence to flows of links i and $i+1$. Note that $\alpha_N(k)$ is equal to 1 on the last link N .

Thus, by substituting Equation 3.2 into Equation 3.1, Equation 3.3 representing density functions for links from 1 to N can be derived.

$$\begin{aligned} \rho_i(k) = & \rho_i(k-1) + \frac{T}{L_i l_i} \alpha_{i-1}(k) [1 - \delta_{i-1}^{off} \theta_{i-1}(k)] Q_{i-1}(k) + \frac{T}{L_i l_i} \{1 - \alpha_{i-1}(k) \\ & - \alpha_i(k) - \delta_i^{off} [1 - \alpha_i(k)] \theta_i(k)\} Q_i(k) + \frac{T}{L_i l_i} [\alpha_i(k) - 1] Q_{i+1}(k) \\ & + \frac{T}{L_i l_i} \alpha_{i-1}(k) \delta_i^{on} R_i(k) + \frac{T}{L_i l_i} [1 - \alpha_i(k)] \delta_{i+1}^{on} R_{i+1}(k) \quad \forall i \quad (3.3) \end{aligned}$$

where $\alpha_0(k) = \alpha_N(k) = 1$; $Q_0(k) = q_0(k)$; $\delta_0^{off} = 0$; and $\theta_0(k) = 0$. Given the parameter value $\alpha_i(k)$, if $Q_i(k)$ is a non-linear function of $\rho_i(k)$. The density $\rho_i(k)$ calculated by Equation 3.3 represents a non-linear dynamic system varying with k .

Based on the basic principle of traffic flow theory, a nonlinear relationship between flow and density can be formulated as

$$Q_i(k) = \rho_i(k)S_i(k) \quad (3.4)$$

where $S_i(k)$ represents the mean speed of link i during interval k , which can be estimated by analyzing individual vehicle speeds collected by detectors.

The objective total traffic throughput (TTT) is defined as the total number of vehicles discharging from the freeway section over the control period and formulated as

$$TTT = \sum_{k=1}^K \left[\sum_{i=1}^{N-1} \delta_i^{off} \theta_i(k) Q_i(k) + Q_N(k) \right] T \quad (3.5)$$

where K is the last time interval of the control period. By substituting Equation 3.4 into Equation 3.5, TTT is

$$TTT = \sum_{k=1}^K \left[\sum_{i=1}^{N-1} \delta_i^{off} \theta_i(k) \rho_i(k) S_i(k) + \rho_N(k) S_N(k) \right] T \quad (3.6)$$

One of the objectives in this study is to maximize (TTT). However, the Simultaneous Perturbation Stochastic Approximation (SPSA) technique discussed in the next section, which will be used to optimize TTT , was designed to minimize an objective function. Thus, the objective function $L(\lambda)$ will be reformulated as a very large positive number Z minus TTT :

$$L(\lambda) = Z - \sum_{k=1}^K \left[\sum_{i=1}^{N-1} \delta_i^{off} \theta_i(k) \rho_i(k) S_i(k) + \rho_N(k) S_N(k) \right] T \quad (3.7)$$

where λ is a set of variables $R_i(k)$ and $Q_i(k)$ that are considered as optimization decision variables. Thus, $L(\lambda)$ can be minimized with SPSA. In Equations 3.3, 3.4 and 3.7, geometric parameters such as Z , N , δ_i^{on} , δ_i^{off} , $\alpha_i(k)$, T , L_i , and l_i can be collected from the study site, while $\theta_i(k)$, $\rho_i(k-1)$, $q_o(k)$ and $S_i(k)$ can be either detected from sensors or estimated from historical data.

Considering densities, capacities and boundaries to define the feasible range of metering rates, the objective function formulated in Equation 3.7 should be minimized subject to a set of constraints formulated in Equations 3.8, 3.9, and 3.10:

$$0 \leq \rho_i(k) \leq \rho^{\max} \quad \forall i, k \quad (3.8)$$

$$0 \leq Q_i(k) \leq Q_i^{\max} \quad \forall i, k \quad (3.9)$$

$$R_i^{\min} \leq R_i(k) \leq R_i^{\max} \quad \forall i, k \quad (3.10)$$

Equation 3.8 indicates that the density of link i at interval k should be positive and less than the maximum density ρ^{\max} . Similarly, the flow of link i at any interval k in Equation 3.9 must be positive and less than the link capacity Q_i^{\max} . The constraint in Equation 3.10 indicates that the range of feasible metering rates, where R_i^{\min} and R_i^{\max} represent the lower and upper boundaries of metering rates, respectively.

Assuming that vehicles approach a ramp meter with a mean arrival rate m , the relation between the queue length L_q (number of vehicles) and the metering rate $R_i(k)$ can be expressed by an M/M/1 queuing model as shown in Equation 3.11.

$$L_q = \frac{\tau m}{R_i(k) - m} \quad (3.11)$$

where τ is the ratio of vehicle arrival rate m and ramp rate $R_i(k)$. Assumptions for the queuing system and the derivation of the equation can be found in Appendix C.

The maximum storage capacity of a metered ramp can be determined by the total lane-miles of the ramp divided by the average vehicle length (e.g., 20 feet). The minimum metering rate R_i^{min} guarantees that the queue length L_q will not exceed the storage capacity. Thus, the queuing vehicles on the metered ramp will not spillback to the local street. R_i^{min} can be derived from Equation 3.11 (for derivation see Appendix C) as

$$R_i^{min} = \left(\frac{L_q + \tau}{L_q} \right) m \quad (3.12)$$

According to previous studies (Masher, et al., 1975, and Federal Highway Administration, 1996), the maximum metering rate R_i^{max} is suggested to be 900 vphpl (based on the minimum metering headway of 4.0 seconds/vehicle), which considers the driver's reaction and operation time and the time consumed for vehicle acceleration required by a single vehicle to proceed past the ramp. The feasible range of metering rates (R_i^{min} , R_i^{max}) for each metered ramp could thus be determined.

3.2 Development of the SPSA Algorithm

In the past, various ramp metering algorithms were designed and deployed. Based on different considerations, the algorithms were used to find reasonable metering rates through optimizing linear or nonlinear functions. With the development of real-time surveillance systems (e.g., various detectors that lead to an improvement in data collection and processing), and optimization skills (e.g., linear-quadratic optimization technique and hierarchical decomposition algorithm), solving a large-scale nonlinear optimization problem is no longer a difficult task. However, explicit relationships

between adjustable or controllable system parameters and system performance have to be obtained in order to analyze detailed modeling information. Real-world systems are often too complex to allow such a detailed description.

In optimization problems, the gradient of the objective function with respect to the decision variables needs to be attained exactly, while the solution can be optimized by setting the gradient of the objective function equal to zero and solving it. However, the process to compute the gradient of a complicated objective function is often difficult. An efficient optimization method is thus desirable to be developed. The SPSA algorithm has significant advantages in solving multivariate optimization problems whose gradient of the objective function is often difficult to be derived. Such advantage makes the SPSA an ideal candidate methodology to optimize the dynamic ramp metering control problem. In this study, SPSA was applied to optimize metering rates with the use of the microscopic traffic simulation model CORSIM. Detailed description of the SPSA algorithm may be found in Spall (1992, 1998, and 2000), Kleinman, et al. (1998), and Ting, et al. (1998).

The SPSA algorithm, a recursive optimization technique for finding local optimizers of linear or nonlinear objective functions, was first introduced and developed by Spall (1992). Based on the measurement of the objective function (not on the measurement of the gradient of the objective function), SPSA is an easily implemented and highly efficient gradient approximation algorithm. SPSA computes the positively and negatively perturbed objective function values in each iteration. SPSA is like other Kiefer and Bolfowitz stochastic approximation algorithms, such as the Finite Difference Stochastic Approximation (FDSA), in that SPSA requires only measurements (possibly noisy) of an objective function to form gradient estimates and converge to a local optimum. However, SPSA differs significantly from FDSA in requiring only two objective function evaluations per gradient estimate, whereas FDSA requires $2p$

evaluations, where p is the number of system parameters being estimated. This gives SPSA a significant advantage in high-dimensional problems, especially when evaluating the objective function is expensive or time-consuming (Ting, et al., 1998).

The SPSA algorithm uses objective function measurements to iteratively update system control parameters until the objective function can reach the local optimization (as shown in Figure 3.2). Let $L(\lambda)$ with vector λ be the objective function to be optimized by a set of system optimized parameters λ (e.g., the ramp metering rates and mainline traffic flow in the freeway system). If $L(\lambda)$ is a differentiable function with respect to λ , $g(\lambda)$ represents the gradient of $L(\lambda)$ and shown in Equation 3.13.

$$g(\lambda) = \frac{\partial L(\lambda)}{\partial \lambda} = 0 \quad (3.13)$$

Finding the approximate optimal solution of Equation 3.13 is the major responsibility of SPSA. Assume that the measurement of the objective function $y(\lambda)$ is represented by Equation 3.14 for any λ :

$$y(\lambda) = L(\lambda) + \text{noise} \quad (3.14)$$

There is no direct measurement of the gradient $g(\lambda)$ that can be expressed in an equation. The SPSA algorithm gives an initial guess of the optimal λ represented by $\hat{\lambda}_0$ and uses $y(\lambda)$ to update λ recursively until the optimal solution λ_h^* is approximated. In the approximation process, SPSA iteratively produces a sequence of estimates (e.g., $\hat{\lambda}_0, \hat{\lambda}_1, \hat{\lambda}_2, \dots, \hat{\lambda}_{h+1}$) generated by each iteration. The configuration of the developed SPSA algorithm is shown in Figure 3.2.

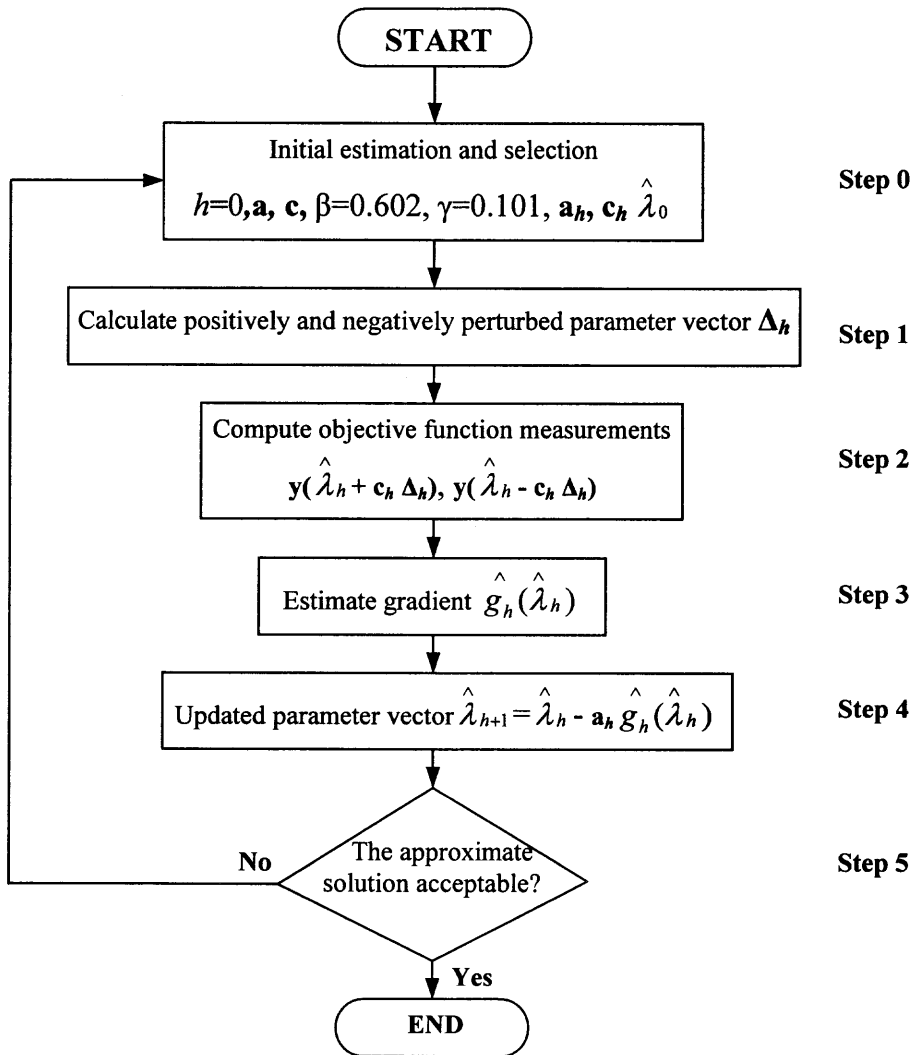


Figure 3.2 The configuration of the SPSA algorithm.

Step 0: Initialization

Set counter index h equal to 0. Pick initial guess $\hat{\lambda}_0$ and non-negative coefficients, \mathbf{a} , \mathbf{c} , β and γ in the SPSA gain sequences as shown in Equations 3.15 and 3.16. The initial guess $\hat{\lambda}_0$ depends on the practical scenario. As a rule-of-thumb, a large \mathbf{a} can enhance performance in the later iterations by producing a larger step size, while it will be effective to set \mathbf{c} at some small positive number. Choosing $\beta \leq 1.0$ usually yields better finite-sample performance through

maintaining a larger step size. Theoretically valid and recommended values for β and γ are 0.602 and 0.101, respectively (Spall, 1998).

$$\mathbf{a}_h = \mathbf{a}(h+1)^{-\beta} \quad (3.15)$$

$$\mathbf{c}_h = \mathbf{c}(h+1)^{-\gamma} \quad (3.16)$$

Step 1: Generate Simultaneous Perturbation Vector

Generate a p -dimensional random vector Δ_h where each of the p components of Δ_h is independently generated from a zero-mean probability distribution. An effective (and theoretically valid) choice for each component of Δ_h is to use a Bernoulli ± 1 distribution with probability of $\frac{1}{2}$ for each ± 1 outcome. Since uniform and normal random variables have infinite inverse moments, they are not allowed for the elements of Δ_h .

Step 2: Evaluate Objective Function

Obtain two measurements of the objective function $L(\lambda)$ based on a simultaneous perturbation around the current $\hat{\lambda}_h$ (e.g., $y(\hat{\lambda}_h + \mathbf{c}_h \Delta_h)$ and $y(\hat{\lambda}_h - \mathbf{c}_h \Delta_h)$) with the \mathbf{c}_h and Δ_h obtained from Steps 0 and 1, respectively.

Step 3: Approximate Gradient

Generate the simultaneous perturbation approximation to the (unknown) p -

dimensional gradient $\hat{\mathbf{g}}_h(\hat{\lambda}_h)$:

$$\hat{\mathbf{g}}_h(\hat{\lambda}_h) = \begin{bmatrix} \frac{y(\hat{\lambda}_h + \mathbf{c}_h \Delta_h) - y(\hat{\lambda}_h - \mathbf{c}_h \Delta_h)}{2 \mathbf{c}_h \Delta_{h1}} \\ \frac{y(\hat{\lambda}_h + \mathbf{c}_h \Delta_h) - y(\hat{\lambda}_h - \mathbf{c}_h \Delta_h)}{2 \mathbf{c}_h \Delta_{h2}} \\ \vdots \\ \frac{y(\hat{\lambda}_h + \mathbf{c}_h \Delta_h) - y(\hat{\lambda}_h - \mathbf{c}_h \Delta_h)}{2 \mathbf{c}_h \Delta_{hp}} \end{bmatrix} \quad (3.17)$$

where Δ_{hi} is the i^{th} component of the Δ_h vector. In Equation 3.17, the denominators change in the p components of $\hat{g}_h(\hat{\lambda}_h)$. The numerators indicate the simultaneous perturbation of all components of $\hat{\lambda}_h$.

Step 4: Update $\hat{\lambda}_h$

Use the standard stochastic approximation form

$$\hat{\lambda}_{h+1} = \hat{\lambda}_h - \mathbf{a}_h \hat{g}_h(\hat{\lambda}_h) \quad (3.18)$$

to update $\hat{\lambda}_h$ to a new value $\hat{\lambda}_{h+1}$.

Step 5: Iteration or Termination

Return to **Step 1** and increase the counter index from h to $h+1$. Terminate the algorithm if the difference between successive iterations is less than a pre-set value that should be small enough to guarantee accuracy. The $\hat{\lambda}_h$ found in the last iteration is the optimum, called λ^* (proof provided in Appendix C).

The SPSA algorithm is very general and can be applied in many different situations to optimize many different kinds of objective functions. For instance, $L(\lambda)$ could be the function dealing with total throughput, while λ could represent the optimal ramp metering rates at different segments in a freeway network. The constraints can be imposed by adding penalty functions in the objective. The flexibility of the algorithm stems from the fact that only objective function measurements are required, instead of full objective function or gradient information. The objective function measurements required by the SPSA algorithm can come from a real system as well as from a computer simulation of a real world probabilistic system.

3.3 Dynamic Multi-ramp Metering Control with SPSA

In practice, traffic volumes feeding into a freeway network vary over space and time. The dynamic ramp metering control with SPSA, which reflects real world traffic and geometric situations, integrates the developed ramp metering control model and the developed SPSA algorithm discussed in Sections 3.1 and 3.2. The dynamic ramp metering control principle is shown in Figure 3.3. Given an initial time interval, the feasible range of metering rates as discussed in Section 3.1 need to be determined first. Then, the input data for SPSA calculation are collected from the studied simulation model. With the application of SPSA, the optimized multi-ramp metering rates are obtained. To apply the ramp metering control, it should be verified that the optimized ramp metering rates are in the feasible range. If the optimized ramp metering rates are out of the feasible range, minimum or maximum ramp metering rates can be set for implementing ramp metering control. After the optimization achieves ramp metering control, the control procedure is iterated for the next time interval and it terminates when the last time interval is reached.

In the dynamic multi-ramp metering control with SPSA, the multiple ramp metering rates subject to dynamic traffic conditions and capacity constraints (e.g. on-ramp volumes, mainline capacity and the boundaries of feasible metering rates, etc.) are optimized by the SPSA algorithm, while the input data for optimizing metering rates can be obtained from the simulation results. In this study, the simulation result of the previous time interval will be used as the input data for determining the optimal metering rates in the next time interval.

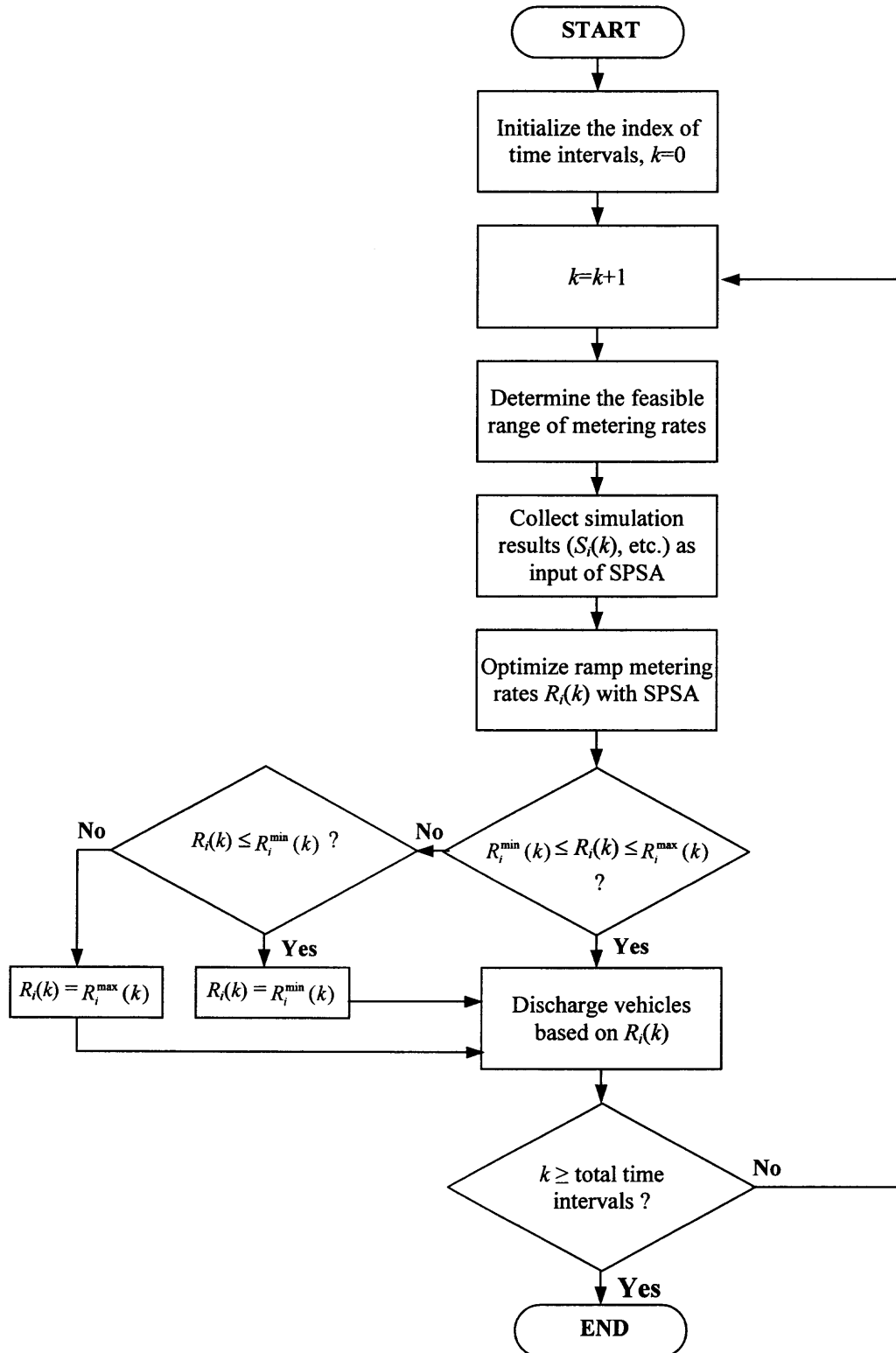


Figure 3.3 The configuration of proposed dynamic metering control model.

3.4 Summary

The proposed dynamic ramp metering control model was developed based on basic assumptions (e.g., the steady traffic flow on the mainline, the first-come first-released rule, and the average vehicle length). The SPSA algorithm can be applied to optimize the objective total throughput function and iteratively update system control parameters until the objective function approximated the optimization solution. The procedure of the recursive optimization technique was introduced in detail. Subject to the constraints (e.g., the density and capacity of the link, and the feasible range of metering rates), the ramp metering control model was optimized through the implementation of the SPSA algorithm.

CHAPTER 4

CASE STUDY

4.1 Site Identification

The case study is designed to demonstrate the benefit of the dynamic ramp metering control model and the efficiency of the SPSA solution algorithm in approximating the optimal solutions. The study site for implementing the developed dynamic metering control model is a 12-mile segment of eastbound I-80 in New Jersey, which starts from milepost (MP) 29.2 and ends at MP 41.1. The typical segment without freeway-to-freeway connectors contains seven on-ramps and five off-ramps supporting the entry and exit flows, which will make evaluation results and recommendation applicable to similar sites and other corridors without much difficulty. The daily traffic is over 100,000 vehicles. The mainline speed limit is 65 mph, while the speed on ramps ranges from 20 to 40 mph. The configuration of the study site is shown in Figure 4.1.

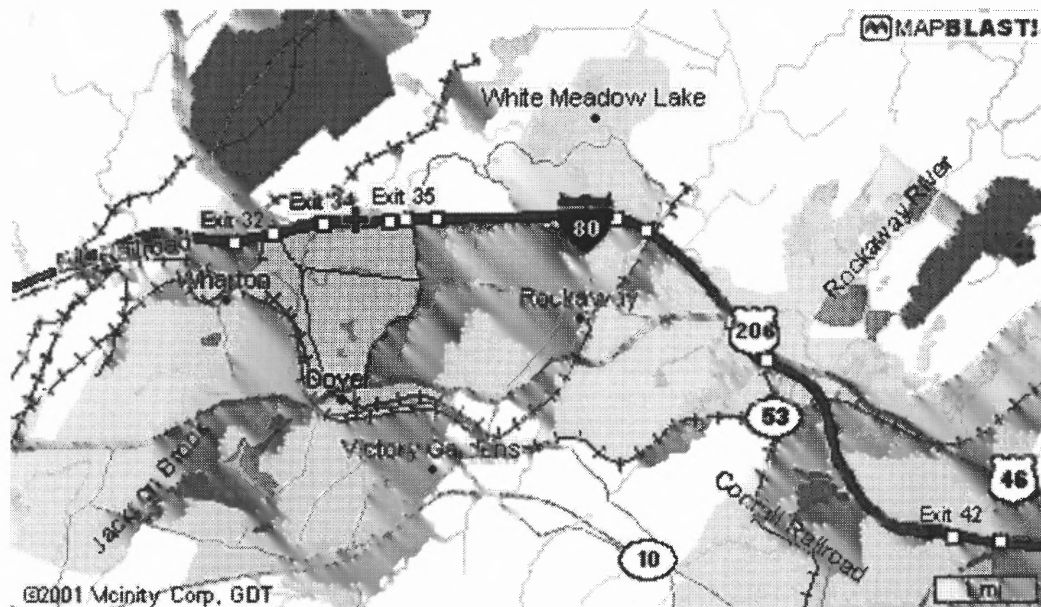


Figure 4.1 Map of the study site.

Although there are no ramp meters installed on freeways in New Jersey, the recommended site was selected based on the availability of data. Most of the data for this study site were provided by NJDOT for developing a simulation model.

4.2 Site Visit

Several field trips were made to get a general overview and observe local traffic operations. The collected geometric and traffic conditions are shown in Figures A.1 through A.8 of Appendix A. It was found that the traffic on westbound I-80 was very light during the morning peak period. Heavy congestion was observed on eastbound I-80, especially at the ramp junction of Route 513/Hibernia Avenue (Figures A.1, A.2 and A.3). Figure A.4 shows heavy traffic at the ramp junction of Route 661 & Mount Hope, while conditions at two ramps at the junction of Route 615 & Howard Boulevard are shown in Figures A.5 and A.6. Figures A.7 and A.8 show the geometric and link-node diagrams respectively for the study site.

4.3 Data

To develop a comprehensive dynamic ramp metering control model for the I-80, the required types of data should include:

- Geometric data,
- Mainline volumes and speeds,
- Ramp volumes and speeds, and
- Origin/Destination (O/D) demand or turning percentage.

NJDOT was the principal data provider while some information was obtained from reports (Garmen Associates, 1991; Parsons Brinckerhoff Quade & Douglas Inc., 1997). The collected geometric data include: (1) freeway link lengths and number of lanes, (2) ramp locations, lengths, and number of lanes, (3) lengths and number of auxiliary lanes, (4) locations where geometry changes, (5) grades, and (6) radius of the curvature. All geometric data, summarized in Table 4.1, were collected from construction plans, provided by NJDOT. All traffic data for eastbound I-80 were collected during weekdays in the peak period 6:00 AM - 9:00 AM and are shown in Table 4.2, while Origin/Destination (O/D) demand distributions are summarized in Table 4.3. These data will be applied for developing a simulation model to evaluate the benefits of ramp metering control for the study site. Table 4.2 shows that the average speeds on the segments from milepost (MP) 34.6 to 39.6 were very low. One of the main reasons that led to congestion during the peak hour would be the higher merging volumes from on-ramps (e.g., MP 34.6 and MP 37.9).

Table 4.1 Geometric Data

Link Name	Type	Length (ft)	Through Lanes (#)	Auxiliary Lane						Through Destination Node	Curve Radius (ft)	Grade (%)
				One		Two		Three				
				Type	Length (ft)	Type	Length (ft)	Type	Length (ft)			
(8300,300)	F	0	3	-	-	-	-	-	-	301	0	0
(300,301)	F	5808	3	D	400	-	-	-	-	302	5000	1
(301,302)	F	1320	3			-	-	-	-	303	0	0
(302,303)	F	1056	3	A	400	-	-	-	-	340	0	0
(303,340)	F	14942	3	A	400	D	400	-	-	341	7500	0
(340,341)	F	5370	3	-	-	-	-	-	-	351	7500	0
(341,351)	F	2930	3	A	1000	A	800	D	400	352	0	0
(351,352)	F	1470	4	-	-	-	-	-	-	371	0	2
(352,371)	F	10200	4	A	650	D	650	-	-	372	0	1
(371,372)	F	1050	4	-	-	-	-	-	-	373	2000	-2
(372,373)	F	1100	4	A	640	-	-	-	-	381	2000	0
(373,381)	F	5770	4	A	650	D	650	-	-	391	6000	0
(381,391)	F	4326	4	-	-	-	-	-	-	411	3500	0
(391,411)	F	6280	4	A	935	-	-	-	-	8411	5000	-2
(301,305)	R	845	1	-	-	-	-	-	-	8305	500	0
(8306,206)	R	0	1	-	-	-	-	-	-	306	600	0
(206,306)	R	729	1	-	-	-	-	-	-	302	600	0
(306,302)	R	400	1	-	-	-	-	-	-	303	600	0
(8307,207)	R	0	1	-	-	-	-	-	-	307	0	0
(207,307)	R	387	1	-	-	-	-	-	-	303	2500	0
(307,303)	R	400	1	-	-	-	-	-	-	340	2500	0
(340,346)	R	1192	1	-	-	-	-	-	-	8346	500	0
(8345,245)	R	0	2	-	-	-	-	-	-	345	1100	0
(245,345)	R	1250	2	-	-	-	-	-	-	341	1100	0
(345,341)	R	400	2	-	-	-	-	-	-	351	1100	0
(351,355)	R	600	1	-	-	-	-	-	-	8355	1100	0
(8356,256)	R	0	1	-	-	-	-	-	-	356	0	0
(256,356)	R	300	1	-	-	-	-	-	-	352	0	0
(356,352)	R	400	1	-	-	-	-	-	-	371	0	0
(371,375)	R	829	1	-	-	-	-	-	-	8375	0	0

Note: A: acceleration lane, D: deceleration land, F: freeway, R: ramp

4.4 Simulation

Computer simulation is one of the most important tools in evaluating traffic operations under different control strategies. It is possible to predict the effect of traffic control and the performance of Transportation Systems Management (TSM) strategies if a transportation network can be replicated by means of a simulation model. The prediction of the effect could be expressed in terms of measures of effectiveness (MOEs), which include average speeds, number of vehicle stops, delays, vehicle-hours of travel, vehicle-miles of travel, fuel consumption, and pollutant emissions. While the MOEs provide insight into the effect of the applied strategy on the traffic stream, they also provide the basis for optimizing that strategy.

There is a great deal of skepticism as to whether metering can be successfully implemented. Several previous studies (Lindley, 1988; Blumentritt, et al., 1981; Deepak, et al., 1978; Hallenbeck, et al., 1991; Nsour, et al., 1995, MNDOT, 1994; and Chien, et al., 1998) focused on the success of metering control systems in various cities and how their guidelines and criteria could be modified and potentially applied locally, especially for short ramps. The goal of this study is to assess the potential effects of implementing the proposed dynamic metering control model on a segment of eastbound I-80, New Jersey. To achieve the objectives, a state-of-the-art simulation model CORSIM was selected for evaluating metering control strategies by quantifying metering impacts on traffic operations on freeways. A simulation approach, rather than an actual field testing approach, was chosen for the following reasons.

- Computer simulation is less costly. Some MOEs (e.g., throughput and delay), while cannot be measured in the field due to time and cost constraints, can be

easily approximated with simulation. It is relatively inexpensive to obtain data from simulation outputs.

- With computer simulation, the disruption of traffic operations caused by field experiments will be completely avoided. For different traffic schemes, experimentation with various combinations of diverted traffic volumes, ramp metering rates, and origin and destination demand distributions are impractical in field study, especially for incident-based congestion.
- When significant physical changes to the facility are required in many schemes, which are not acceptable for experimental purposes, computer simulation could be easily used.
- Evaluation of the operational impact of future traffic demand has to be conducted by using simulation or an equivalent analytical tool. In addition, many variables can be held constant, and results could be quickly obtained.
- The availability of traffic simulation models greatly expands the opportunity for the development of new and innovative TSM concepts and designs. Planners and engineers are no longer restricted by the lack of a mechanism for testing ideas prior to field demonstration. Furthermore, because simulation models produce information that allows designers to identify the weakness in concepts and designs, they provide the basis to identify the optimal form of candidate approaches. Thus, the eventual field implementation will have a high probability of success.

4.5 Network Modeling

The network of the study site begins from MP 29.2 and ends at MP 41.1 of eastbound I-80, which contains seven on-ramps and five off-ramps. As shown in Table 4.4, control, geometric and traffic data are main data required by CORSIM. The geometric configuration and link-node diagram are as shown in Figures A.7 and A.8, respectively.

Table 4.4 Required Data for CORSIM Simulation Model

Item	Control Data	Geometric Data	Traffic Data
1	number of the time periods	number of lanes	vehicle volume
2	duration of each time period	length of links	vehicle speed
3	time interval duration	grade of link	traffic O/D
4	Desired output	curve radius of link	vehicle type

The first step of network modeling with CORSIM is to determine the relationship among links and nodes. A link connects two nodes, which represents a directional freeway or ramp segment. For entry and exit links, a dummy node is placed between the entry or exit node and the internal node, which allows for the collection of traffic statistics on the links.

The network was coded along the mainline considering critical points such as interchanges, potential ramp meter locations, curvature/superelevation change, and entry or exit points. The developed simulation model contains eight entry nodes, six exit nodes, 14 dummy nodes and 19 internal nodes, while eight entry links, six exit links and 32 internal links connect the 47 total nodes. The detail link-node identification numbers of the study network are summarized in Table 4.5.

Table 4.5 Links and Nodes of the Simulation Network

Link						Node						
Entry	Internal				Exit	Entry	Dummy		Internal			Exit
8300,300	300,301	371,372	207,307	371,375	305,8305	8300	300	375	301	372	376	8305
8306,206	301,302	372,373	307,303	372,376	346,8346	8306	305	276	302	373	377	8346
8307,207	302,303	373,381	340,346	376,276	355,8355	8307	206	277	303	381	395	8355
8345,245	303,340	381,391	245,345	277,377	375,8375	8345	207	385	340	391	-	8375
8356,256	340,341	391,411	345,341	381,385	276,8376	8356	346	295	341	306	-	8411
8376,276	341,351	301,305	351,355	372,376	411,8411	8376	245	411	351	307	-	-
8377,277	351,352	206,306	256,356	295,395	-	8377	355	-	352	345	-	-
8395,295	352,371	306,302	356,352	395,391	-	8395	256	-	371	356	-	-

4.6 Calibration and Validation

As mentioned before, simulation is a viable approach to conduct a feasibility study for evaluating various ramp metering control strategies considering time varying demand. To conduct a credible simulation analysis, one must be confident that simulation results represent real world traffic operations reasonably well. Therefore, a procedure for calibrating and validating of the simulation model should be carefully performed.

Before implementing a ramp metering control plan at the study site, it is essential to demonstrate that traffic engineers have done the best design for the plan. To achieve this goal, the calibrated and validated simulation model used for emulating traffic conditions on I-80, plays an important role to evaluate candidate ramp metering control plans and assess the corresponding impact on the study site.

The impact incurred by implementing different ramp metering control plans can be assessed by simulated MOEs including volume, total delay, and average speed. Then, the best plan that achieves the optimal objective can be identified.

To calibrate the simulation model, the MOEs generated by CORSIM must be compared with field data to ensure that simulation results can represent realistic traffic operations of the study site.

4.6.1 Data Collection and Processing

Two data sets collected from the study site during different time periods were used for calibrating and validating the simulation model. The traffic volume and average speed data used for calibrating the developed simulation model were collected in the field. Table 4.6, for example, shows the volume and speed data collected during 7:00 am - 8:00 am on link 302-303. The traffic volume data used for validating the simulation model were collected during 8:00 am - 9:00 am from the same data stations. The average volume and speed on this link was 4260 vph and 47.9 mph, respectively. However, only traffic volumes were provided by data stations at MP 35.1, MP 35.2, and MP 38.1, as shown in Table 4.7.

Table 4.6 Volume & Speed Data (Link 302-303, MP 30.2, 7:00 am-8:00 am)

Date	Right Lane		Middle Lane		Left Lane	
	Volume(vphpl)	Speed(mph)	Volume(vphpl)	Speed(mph)	Volume(vphpl)	Speed(mph)
10/11/99	1117	60.5	1691	63.2	1779	64.5
10/12/99	1001	37.3	1325	44	1292	44.2
10/13/99	1310	42.2	1589	45.8	1684	46.4
10/14/99	1195	39.7	1475	43.4	1580	43.5
Average	1156	45	1520	49.1	1584	49.7

Table 4.7 Volume Data (8:00 am-9:00 am, May 26, 1999)

Volume (vphpl)	Location of Data Stations		
	MP 35.1	MP 35.2	MP 38.1
	1598	1755	1560

4.6.2 Model Calibration

The data describing freeway geometry, traffic conditions (volumes, speeds and turning movement) and facility locations (e.g., locations of ramps and warning signs) were the major input of CORSIM. Traffic operations during a peak hour (7:00am-8:00am) on the eastbound of I-80 were simulated. After comparing simulation results with field data, discrepancies were found and reduced by calibrating parameters in CORSIM. The parameters, such as car-following sensitivity factor (defined by time headway between vehicles), lane change parameter, minimum separation for vehicle generation, collision avoidance time period and the percentage of cooperative drivers, were adjusted to fine tune the simulated driving behavior.

There is no certain way to identify the impact from an individual parameter change when changing several parameters at a time, due to the interdependent influence among those parameters and the simulation results. Therefore, the impact of each parameter on simulation results was investigated. To identify the key parameters influencing the simulation results, sensitivity analysis for various parameters was conducted. The calibrated values of parameters are shown in Tables 4.8 and 4.9.

Table 4.8 Car-Following Sensitivity Factor

Driver Type	1	2	3	4	5	6	7	8	9	10
Default Value (hundredth of a second)	150	140	130	120	110	100	90	80	70	60
Calibrated Value (hundredth of a second)	130	120	110	100	90	80	70	60	50	40

Table 4.9 Other Calibrated Parameters

Parameter	Default Value	Calibrated Value
Minimum separation for generation of vehicles (tenth of a second)	18	12
Parameter for collision avoidance time period (%)	1	2
Percentage of cooperative drivers (%)	20	60

Figures 4.2, 4.3 and 4.4 shown below demonstrate the sensitivity of calibrated parameter to the simulation results. Decreasing the values of the car-following sensitivity factor could achieve larger traffic volumes and higher speeds due to shorter gaps allowable between vehicles. With more cooperative drivers, traffic volumes on ramps and their speeds might increase because more vehicles were able to merge into the traffic stream on the mainline.

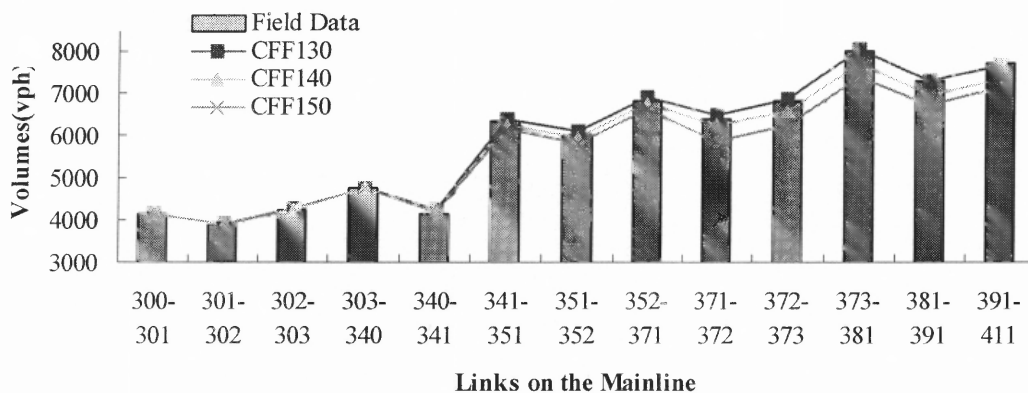


Figure 4.2 Traffic volumes on different links for various car following sensitivity factors (CFF).

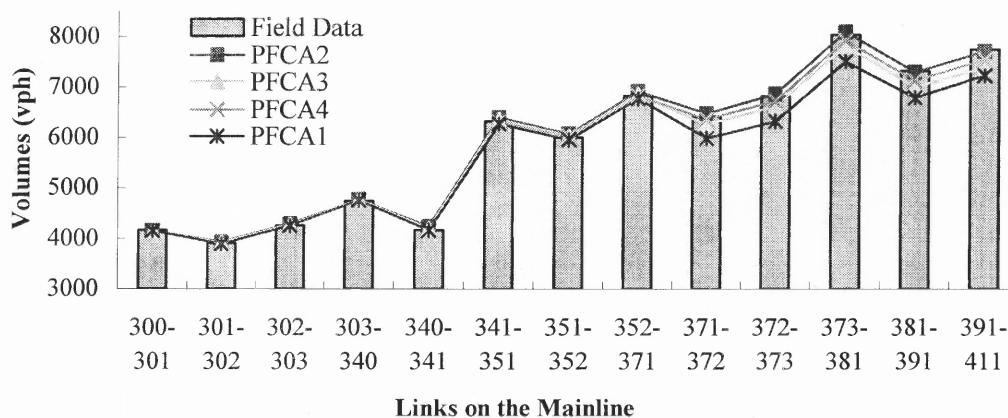


Figure 4.3 Traffic volumes on different links for various collision avoidance time periods (PFCA).

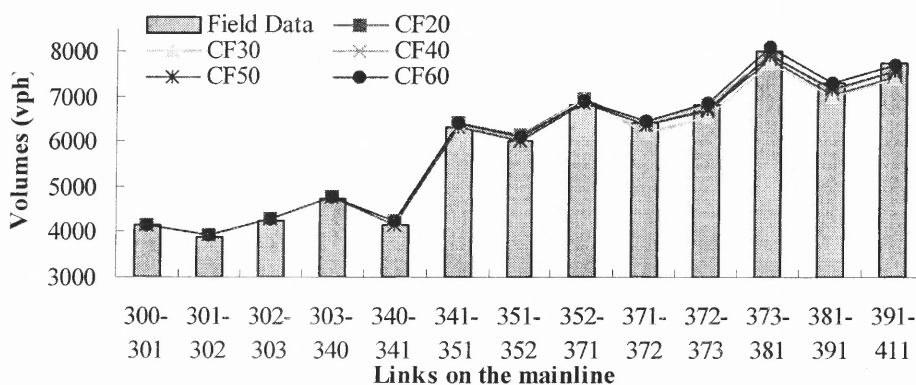


Figure 4.4 Traffic volumes on different links for various courtesy factors (CF).

For describing the turning movement of vehicles in the network, card type 25 in CORSIM gives the turning percentages for every link with an off-ramp. However, the O/D percentage of vehicles generated based on card type 25 significantly deviates from the actual O/D percentage of the network. Thus, card type 74 (O/D) was used to adjust the turning movements to each off-ramp. After the adjustment the simulation result shows the same O/D percentage as shown in Table 4.3.

The calibration procedure adopted in this study is composed by the following comparisons: (1) graphical comparison, (2) aggregate comparison, and (3) statistical comparison.

(1) Graphical Comparison

The graphical comparison is a subjective validation approach, which is especially useful for testing the results generated by the simulation model preliminarily. It makes the comparison easy and visible.

(2) Aggregate Comparison

Aggregated means and standard deviations give a general indication of system performance in the real world and in simulation. However, they do not present an accurate trend or an indication of how variables perform over time, what patterns are created, or how much individual measurements deviate. Aggregate comparison along with the graphical comparisons of scattered plots, reveals the similarities and discrepancies of the magnitude and changing pattern for variables.

(3) Statistical Comparison

The statistical analysis is crucial for validating the proposed model based on sample data collected from the study site and simulation. It can be used for accessing the accuracy of the model, testing various hypotheses and determining the degree of

correlation between field data and simulation results. The following indices are used for statistical comparison.

- Mean Absolute Percent Error (MAPE)

MAPE measures the percentage error between simulation results and field data and can be estimated by Equation 4.1:

$$\text{MAPE} = \frac{1}{n} \sum_{i=1}^n \frac{|S_i - O_i|}{O_i} * 100\% \quad (4.1)$$

where n , S_i and O_i are sample size, observation i of simulation output, and observation i of field measurement, respectively.

- Root Mean Square Error (RMSE)

RMSE denotes the error between simulation results and field data and can be estimated by Equation 4.2:

$$\text{RMSE} = \sqrt{\frac{1}{n} \sum_{i=1}^n (S_i - O_i)^2} \quad (4.2)$$

where n , S_i and O_i have been defined in Equation 4.1.

Figures 4.5 and 4.6 show that both the simulated and the field observed traffic volumes at various sections on the mainline were quite close to each other. Note that the field traffic volume on each link was derived based on two data stations on the mainline (approximately at MP 30.2 and MP 35.2) because the volumes reported from other data stations were inconsistent with the field data and were not used for calibration.

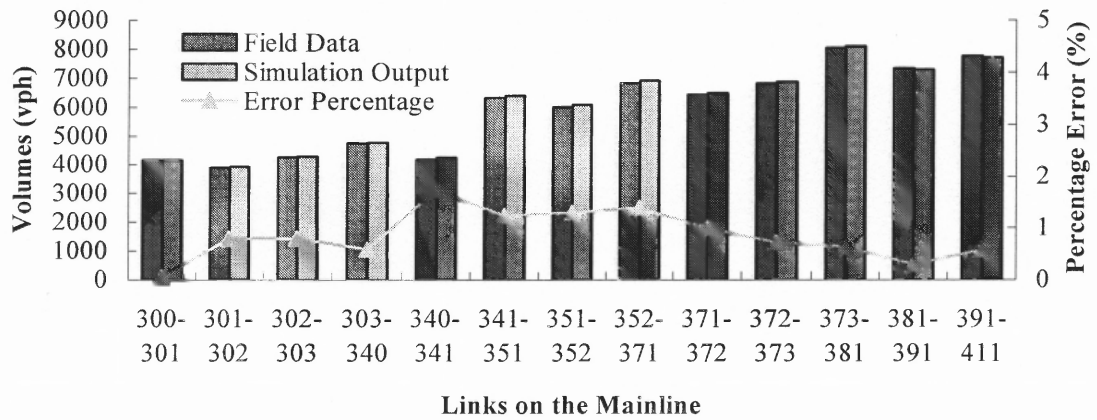


Figure 4.5 Field data vs. simulated data (Mainline).

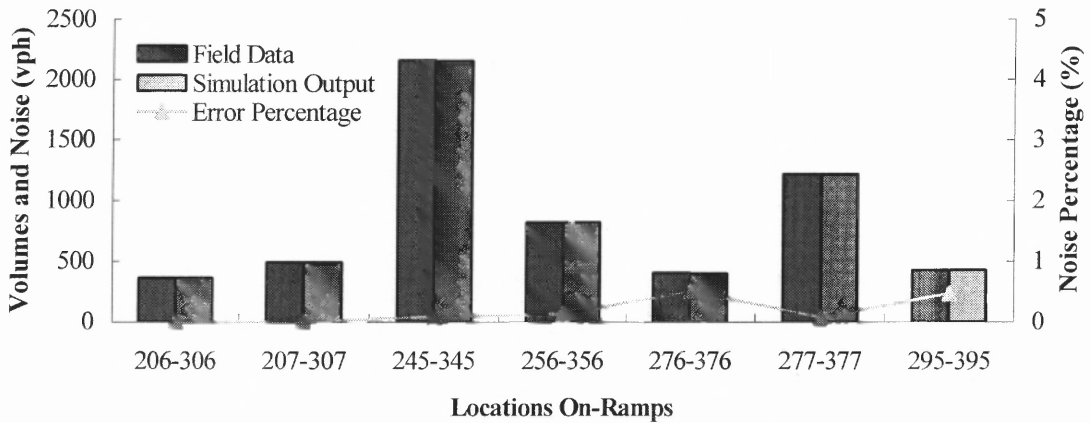


Figure 4.6 Field data vs. simulated data (On-ramps).

4.6.3 Model Validation

To insure that the model could produce reliable and accurate estimates of real network traffic conditions on a system-wide basis, model validation is required. The calibrated model was validated through comparing simulation outputs with their field counterparts. It should be noted that the data set used to validate the model was different from that used to calibrate the model. In this study, volumes on the same links collected during different time periods were used to validate the model. The preliminary test of traffic volumes was conducted by graphically comparing the values of field observations and simulation results.

The statistical analysis was conducted by calculating MAPE and RMSE for the field and simulated traffic volumes on mainline links. The MAPE and RMSE of traffic volumes were plotted in Figures 4.7 and 4.8, respectively. Figure 4.7 shows that for 364 simulation outputs, the MAPE ranged from 0% to 1.5%. In Figure 4.8, the RMSE of traffic volumes ranged from 0 veh to 35 veh. The simulation model demonstrated its capability to emulate traffic volumes operating on the studied network.

Regarding the speed data, only the station at MP 30.2 provided speed information. A comparison of actual and simulated data generate a MAPE of 1.54% and RMSE of 0.97 mph. This indicates that the simulation model could accurately simulate vehicle speeds at the survey point.

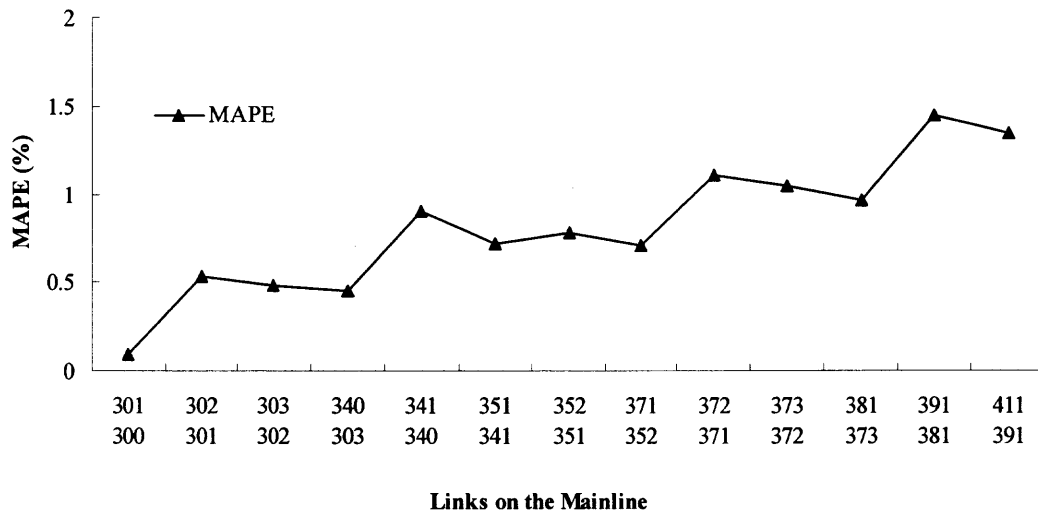


Figure 4.7 MAPE of volumes on the mainline.

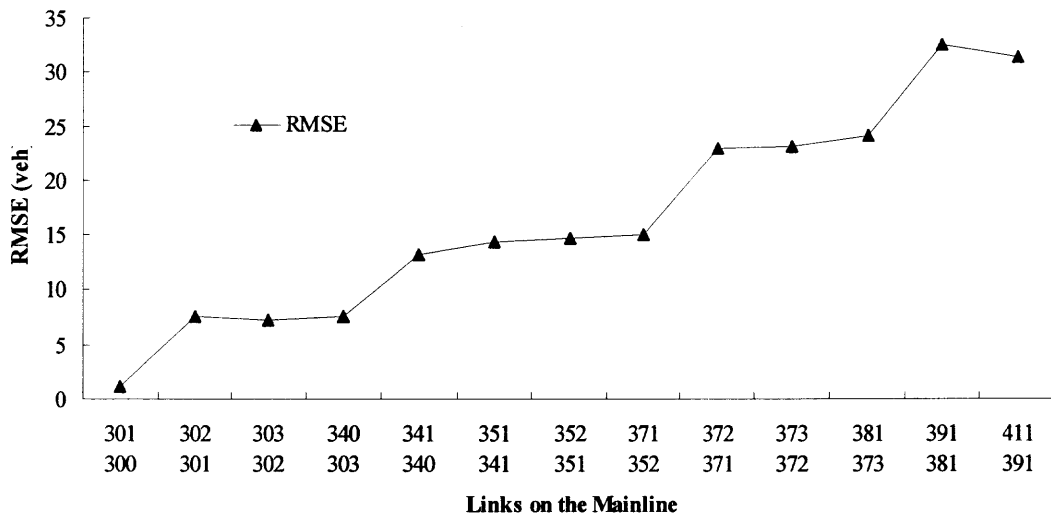


Figure 4.8 RMSE of volumes on the mainline.

4.7 Summary

A 12-mile study site with seven on-ramps and five off-ramps along eastbound I-80 from milepost 29.2 to 41.1 was identified. Field investigation showed that the traffic on eastbound I-80 was heavy and led to congestion during the morning peak period. For this study, geometric data (e.g., link length, auxiliary lanes for on/off ramps, and etc.), traffic data (e.g., volumes and speeds on the mainline and ramps), and origin/destination demand were collected.

The advantages of computer simulation were discussed in this chapter. The network of the study site was modeled by CORSIM. The developed simulation model was calibrated and validated based on the field data collected from I-80. By comparing the simulation outputs to the field data, the validity of the simulation model was demonstrated. Both the graphical and aggregate comparison showed that the developed simulation model could adequately simulate traffic operations on eastbound I-80.

Statistical analysis on MAPE and RMSE indicated that the differences between simulation outputs and data collected from the field were very small. Thus, the simulation model is capable of simulating traffic operations in the study site and generating reliable results.

CHAPTER 5

SYSTEM EVALUATION

5.1 Evaluation of Ramp Metering Control

It is necessary to evaluate the performance of ramp metering control on the study network, and then to determine the ramps where the proposed metering control model can be applied. As mentioned earlier, ramp metering control can be referred to the control of vehicles entering a freeway mainline from one or more entrance ramps. For improving freeway operation, the proposed ramp metering control is to minimize the interference of entering traffic from the ramp to the mainline traffic. To evaluate ramp metering control, constraints, such as locations of ramp meters and ramp storage capacities, should be considered; In addition, the potential ramps suitable for metering control should be identified. The CORSIM model developed in Chapter 4 is applied here to evaluate pre-timed and demand/capacity control strategies, since those are the most widely applied metering methods for static and demand responsive system.

5.1.1 Constraints

As ramp meters restrict the number of vehicles merging into the mainline traffic, queues may be formed at the metered ramps. Since different ramps have different geometric conditions and vehicle arrivals are stochastic, it is crucial to ensure adequate storage capacities at the metered ramps. Therefore, an analysis of ramp meter locations and their corresponding storage capacities should be conducted before the simulation analysis. Subject to such constraints, feasible metering rates that do not cause overflow situations should be estimated at each ramp.

(1) Locations of Ramp Meters

Considering the safety aspects of the merging operation, the location of the ramp meter should be determined by the minimum distance required for a stopped vehicle to accelerate along the lane and smoothly merge into the mainline traffic stream. That minimum distance can be obtained from Equation 5.1.

$$d = 0.5at^2 + V_0t \quad (5.1)$$

where a represents vehicle acceleration rate that is defined as

$$a = \frac{V_t - V_0}{t} \quad (5.2)$$

where V_t and V_0 are the average speed on the mainline and the initial speed of a vehicle released by a ramp meter, respectively. For a stopped vehicle, V_0 is zero. Since a , V_t , and V_0 are known, the time t required for the vehicle accelerating from the ramp meter to the on-ramp gore can thus be determined. By substituting a , t , and V_0 into Equation 5.1, d can be obtained.

In this study, the acceleration rates for passenger cars, carpool vehicles, buses, and trucks were assumed to be 6.8, 3.8, 3.5 and 3.2 mph/sec (embedded in CORSIM), respectively. The meter location was determined by the truck acceleration rate (3.2 mph/sec) which is the most constraining. The lengths of the auxiliary acceleration lanes of the ramps at the study site are listed in Table 5.1, and the suggested ramp meter locations are summarized in Table 5.2.

Table 5.1 Length of the Auxiliary Lane on the Freeway

Link	302-303	303-340	341-351	352-371	372-373	373-381	391-411
Length (feet)	400	400	1000	650	640	650	935

Table 5.2 Distance from Meter Location to the On-ramp Gore

Metered Node	306	307	345	356	376	377	395
Actual Location (feet)	400	400	400	320	330	320	50*

*: The minimum distance from the meter to the on-ramp gore suggested by Ramp Meter Design Guidelines (CALTRANS, 1991)

An example for determining the suggested meter locations is discussed next. Link 372-373 had an auxiliary acceleration lane of 640 ft. In order for a truck to accelerate from a stop at the meter to the average mainline speed (e.g., 65 mph), the required acceleration time t was

$$t = \frac{V_t - V_0}{a} = \frac{65 - 0}{3.2} = 20.13 \text{ seconds.}$$

By substituting t into Equation 5.2, the minimum distance was

$$\begin{aligned} d &= 0.5at^2 + V_0t \\ &= 0.5 \times 3.2 \times (5280/3600) \times 20.13^2 + 0 \times 20.13 \\ &= 951 \text{ feet} \end{aligned}$$

Apparently, the auxiliary acceleration lane was not long enough. The ramp meter has to be located at least 311 feet (951 minus 640 feet) before the on-ramp gore. To insure safety, the ramp meter at node 376 was located 330 feet away from the on-ramp gore. The above ramp meter location was determined based on an assumed average mainline

speed of 65mph. If the average mainline speed decreases, the distance between the meter location and on-ramp gore decreases.

(2) Ramp Storage Capacity

In general, ramps provide the necessary linkages between freeways and local streets or arterials. To avoid vehicle spillback onto surface streets from a ramp metering signal, the ramp storage capacity has to be taken into consideration.

The storage capacities for potential metered ramps are shown in Table 5.3. At node 306, for example, the maximum queue length of 729 feet was measured from the entrance of the on-ramp to the meter location. By assuming an average vehicle length of 20 feet, the queue storage capacity was 36 vehicles. The constraint of this ramp was represented by $L_q \leq 36$. The minimum metering rate $R_i^{\min}(k)$ (370 vph) could be solved by Equation 3.12, if the mean arrival rate m was 360 vph. Thus, the resulting headway was 9.7 (e.g., $3600/370$) seconds per vehicle.

In CORSIM, the suggested minimum metering headway is 4 seconds. Thus, the maximum metering rate is 900 vphpl ($3600/4 = 900$). Based on the collected data, the entry flows at metering nodes 377 and 345 were 1216 and 1080 vphpl, respectively, while the corresponding vehicle headways were 2.96 and 3.31 seconds per vehicle. Since the metering headways are both less than the minimum 4.0 seconds, the headway has to be set at 4.0 seconds and the queues on both ramps would easily extend over the entrance of the ramp. Thus, ramp metering control was not recommended on both ramps.

Table 5.3 Storage Capacity of On-ramps

Item	Node					Unit(s)
	306	307	356	376	395	
m	360	489	819	400	430	vph
$R_i^{\min}(k)$ (metering rate)	370	513	860	416	448	vph
τ	0.973	0.953	0.952	0.962	0.960	-
L_q (set as maximums)	36	19	19	24	23	vehicles
Max Queue Length	729	387	380	475	455	feet
Average Vehicle Length	20	20	20	20	20	feet
Queue Storage Capacity	36	19	19	24	23	vehicles
Pre-timed Headway	9.7	7.0	4.2	8.7	8.0	seconds/vehicle

5.1.2 Simulation Analysis and Evaluation

Ramp metering control was evaluated by performing extensive simulation with CORSIM. The benefits expected from the implementation of ramp metering control are increasing throughput and/or decreasing delay. To generate unbiased estimates, ten simulation runs with different random number seeds were performed for each of the three scenarios: no control, pre-timed control, and demand-capacity control situations. The benefits of alternate strategies are evaluated and discussed next.

(1) No Control

Without ramp metering control, vehicles entering the mainline stream from ramps would not be regulated. Under this situation, the network-wide MOEs, such as total throughput and total delay, were obtained based on one-hour simulation. The total throughput was 9,613 vph, while the total delay was 17,199 vehicle-minutes, which would be used as base results for comparing other metering control strategies.

(2) Pre-timed Metering Control

Although the simulation of the pre-timed metering control strategy was used on individual on-ramps, the simulated network-wide MOEs were analyzed. The applied metering rates were selected subject to the storage constraint of each ramp and the minimum ramp metering rate derived from Equation 3.12. As mentioned earlier, the maximum ramp metering rate in CORSIM was 900 vphpl. Thus, the upper and lower bounds of metering rates for each ramp could be determined. If the metering rate derived from Equation 3.12 is not in the feasible range, metering control on that ramp at that moment will not be recommended.

To obtain the optimal pre-timed metering rate, a numerical search method was applied. A series of simulation runs with different metering rates were performed. The boundaries of metering headways and all the simulated metering headways at different ramps are calculated and presented in Table 5.4. It is found that there were feasible solutions for metering control at nodes 306, 307, 356, 376 and 395. Thus, they are recommended as the candidate places to implement ramp metering control.

Table 5.4 Pre-timed Metering Headways

Ramp Meter Site (Node)		306	307	345	356	376	377	395
Pre-timed Headway Range (Seconds/veh)	Min	4.0	4.0	4.0	4.0	4.0	4.0	4.0
		6.0	4.7	-	-	5.0	-	5.0
		8.0	5.5	-	4.1	6.0	-	6.0
		9.0	6.3	-	-	7.0	-	7.0
	Max	9.7	7.0	-	4.2	8.7	-	8.0

All simulation results are summarized in Table 5.5. The highlighted numbers in Table 5.5 represent the best metering rates that the minimum network-wide delay could be achieved. The achieved minimum delays were all less than that under no ramp control. The benefits of pre-timed ramp metering control on those ramps were thus quantified.

Ideally, the optimal metering rate was expected to achieve maximum throughput and minimum delay at the same time. However, this was not achieved and that may be reasonable and consistent with real world traffic operations.

Table 5.5 MOEs under Pre-timed Metering Control and No Control Situations

Node	Pre-timed Headway (seconds)	Total Throughput (vph)			Total Delay (veh-min)		
		No Control (1)	Pre-timed (2)	[(2)-(1)]/(1) (%)	No Control (3)	Pre-timed (4)	[(4)-(3)]/(3) (%)
306	9.7	9613	9572	-0.43	17199	17429	1.34
	9.0	9613	9638	0.26	17199	16962	-1.38
	8.0	9613	9611	-0.02	17199	16812	-2.25
	6.0	9613	9627	0.15	17199	17010	-1.10
	4.0	9613	9581	-0.33	17199	17789	3.43
307	7.0	9613	9625	0.12	17199	17172	-0.16
	6.3	9613	9617	0.04	17199	16971	-1.33
	5.5	9613	9624	0.11	17199	17037	-0.94
	4.7	9613	9629	0.17	17199	17058	-0.82
	4.0	9613	9584	-0.30	17199	17268	0.40
356	4.2	9613	9507	-1.10	17199	17306	0.62
	4.1	9613	9507	-1.10	17199	16694	-2.94
	4.0	9613	9560	-0.55	17199	18254	6.13
376	8.7	9613	8650	-10.02	17199	17356	0.91
	7.0	9613	9598	-0.16	17199	17089	-0.64
	6.0	9613	9623	0.10	17199	16939	-1.51
	5.0	9613	9602	-0.11	17199	16843	-2.07
	4.0	9613	9605	-0.08	17199	17067	-0.77
395	8.0	9613	9617	0.04	17199	17026	-1.01
	7.0	9613	9585	-0.29	17199	17348	0.87
	6.0	9613	9620	0.07	17199	16968	-1.34
	5.0	9613	9636	0.24	17199	16323	-5.09
	4.0	9613	9587	-0.27	17199	17734	3.11

- At node 306, if the pre-timed metering headway was 9 sec/vehicle the total throughput increased 0.26%, while the total delay was reduced by 1.38%. However, if the pre-timed headway was 8 sec/vehicle, the total delay was further reduced (to 2.25%), but the total throughput was slightly decreased.
- At node 307, if the pre-timed headway was 4.7 sec/vehicle the total throughput increased, and the total delay was reduced. If the pre-timed headway was 6.3 sec/vehicle, the total delay was reduced, but the throughput did not.

- At node 356, when pre-time metering control was applied, the total throughput was always less than that under no control. When the pre-timed metering headway was at 4.1 sec/vehicle, the total delay was reduced. Node 356 is not recommended for pre-timed meter control if the objective is to increase the total throughput.
- At node 376, if the pre-timed headway was 6.0 sec/vehicle, the total throughput could be increased and the total delay reduced. If the pre-timed headway was 5.0 sec/vehicle, the total delay was reduced, while the total throughput was reduced.
- At node 395, if the pre-timed headway was 5.0 sec/vehicle, increased total throughput and reduced total delay were achieved simultaneously.

The simulation results indicated that the greatest benefit in reducing delay and increasing throughput usually could not be achieved simultaneously (except at node 395). Future research should give more attention to the analysis of the tradeoff between increased delay and increased throughput. Figures A.9 through A.16 of Appendix A show the simulation results for pre-timed metering control at nodes 306, 307, 376, and 359.

(3) Demand/Capacity Metering Control

Demand/capacity control, being a demand responsive control strategy, can respond to real time traffic conditions to effectively reduce congestion. It requires that the total traffic volume from both mainline traffic and vehicles released from the metered on-ramp should not exceed the designated freeway capacity. Therefore, before designing a demand/capacity metering control system, an evaluation of freeway capacity, immediately downstream of the metered on-ramp, should be conducted. By definition, the freeway capacity is the maximum hourly volume at which vehicles can be reasonably expected to

traverse a point or uniform segment of a lane during a given time period under prevailing freeway traffic conditions. Traffic counts can be obtained from the surveillance systems (e.g., detectors, CCTV) installed on the freeway. The maximum metering rate is subject to the capacity constraint, while the minimum metering rate considered here is to ensure that queuing vehicles do not spillback onto local streets. Also, the metering headway is always set at four seconds or greater according to the suggestion of CORSIM's developers.

To determine the maximum ramp metering rate which will not exceed the capacity of the freeway, the mainline capacity should be investigated first. According to the *Highway Capacity Manual* (HCM, 1997), the capacity of the freeway should not be more than 2200 vphpl when the free flow speed is 65 mph. (Vehicle is used in this dissertation instead of passenger car equivalent. If heavy vehicles are present, the indicated numbers should be adjusted.) If the calibrated values of the car-following factor are from 40 to 130 hundreds of a second, the simulated freeway capacity of CORSIM can increase up to 2950 vphpl. To analyze optimal metering rates under various freeway capacities, the maximum ramp metering rates were estimated based on freeway capacities ranging between 1800 and 3000 vphpl. The metering headways corresponding to various freeway capacities were calculated based on collected demand data summarized in Table 5.6, where the highlighted values indicate the feasible metering rates. Simulation results for implementing metering control at every individual ramp are shown in Table 5.7.

As discussed before, metering control would not recommended at nodes 345 and 377 due to possible vehicles spillback onto local streets. The range (4.0 ~ 4.2 seconds) of the metering headway at node 356 was not wide enough for implementing demand/capacity control, but pre-timed control might be a suitable alternative.

After applying the demand/capacity control strategy at nodes 306, 307, 376, and 395, the simulated network-wide delay was less than that without metering control, while

After applying the demand/capacity control strategy at nodes 306, 307, 376, and 395, the simulated network-wide delay was less than that without metering control, while the total throughput increased. Table 5.8 shows that delay could be significantly reduced under demand/capacity metering control at nodes 307, 376, and 395. However, the corresponding throughputs were increased at nodes 307 and 395. As shown in Table 5.9, increased throughputs can be achieved with demand/capacity control at all four nodes. The corresponding delays were reduced when demand/capacity control was implemented at nodes 307, 376, and 395, but increased at node 306. Similar to the pre-timed control, the demand/capacity control could not achieve maximum total throughput and minimum total delay simultaneously. Again, the tradeoff between the increased delay and increased capacity should be considered in the future.

Figures A.17 through A.24 in Appendix A show the simulation results on average delay and total throughput before and after the demand/capacity metering control at nodes 306, 307, 376, and 395.

Table 5.6 Metering Headway for Demand/Capacity Control

Capacity on Mainline (pcphpl)	Metering Headway (seconds) at nodes				
	306	307	356	376	395
3000	2.12	2.29	2.40	2.51	2.88
2900	2.25	2.44	2.57	2.69	3.12
2800	2.40	2.62	2.77	2.93	3.44
2700	2.57	2.83	3.00	3.16	3.77
2600	2.77	3.06	3.26	3.49	4.22
2500	3.00	3.35	3.60	3.84	4.83
2400	3.28	3.68	4.00	4.36	5.52
2300	3.60	4.09	4.52	4.92	6.52
2200	4.01	4.63	5.12	5.68	7.95
2100	4.52	5.29	5.93	6.84	10.33
2000	5.15	6.26	7.13	8.29	14.50
1900	6.04	7.58	8.95	10.90	26.29
1800	7.24	9.54	11.94	15.41	80.36
Feasible Headway Range (seconds)	4.0~9.7	4.0~7.0	4.0~4.2	4.0~8.7	4.0~8.0

Table 5.7 MOEs under Demand/Capacity Control and No Control Situations

Metered Node	Capacity (veh/hr.pl)	Controlled Headway on Ramp (seconds/veh)	On-ramp Metering Rate Range (seconds/veh)		Total Throughput (veh/hour)		Total Delay (veh-min)	
			Min	Max	No Control	D/C*	No Control	D/C
306	2200	4.01	4.0	9.7	9613	9620	17199	17451
	2100	4.52			9613	9606	17199	17092
	2000	5.15			9613	9593	17199	17303
	1900	6.04			9613	9620	17199	17158
	1800	7.24			9613	9610	17199	17170
307	2300	4.09	4.0	7.0	9613	9614	17199	16730
	2200	4.63			9613	9620	17199	17008
	2100	5.29			9613	9626	17199	16587
	2000	6.26			9613	9636	17199	16660
376	2400	4.36	4.0	8.7	9613	9611	17199	16461
	2300	4.92			9613	9631	17199	17009
	2200	5.68			9613	9596	17199	16844
	2100	6.84			9613	9588	17199	17715
	2000	8.29			9613	9608	17199	16841
395	2600	4.22	4.0	8.0	9613	9583	17199	16878
	2500	4.83			9613	9629	17199	16647
	2400	5.52			9613	9599	17199	16807
	2300	6.52			9613	9592	17199	17274
	2200	7.95			9613	9613	17199	17090

*: D/C refers to Demand/Capacity Control.

Table 5.8 Benefits of Demand/Capacity Control (Reduced Delay)

Metered Node	Controlled Headway (seconds/veh)	Total Throughput (veh/hour)			Total Delay (veh-min)		
		No Control (1)	D/C* (2)	[(1)-(2)]/(1) (%)	No Control (3)	D/C (4)	[(4)-(3)]/(3) (%)
306	4.52	9613	9606	-0.07	17199	17092	-0.62
307	5.29	9613	9626	0.14	17199	16587	-3.56
376	4.36	9613	9611	-0.02	17199	16461	-4.29
395	4.83	9613	9629	0.17	17199	16647	-3.21

*: D/C refers to Demand/Capacity Control.

Table 5.9 Benefits of Demand/Capacity Control (Increased Throughput)

Metered Node	Controlled Headway (seconds/veh)	Total Throughput (veh/hour)			Total Delay (veh-min)		
		No Control (1)	D/C* (2)	[(1)-(2)]/(1) (%)	No Control (3)	D/C (4)	[(4)-(3)]/(3) (%)
306	4.01	9613	9620	0.07	17199	17451	1.47
307	6.26	9613	9636	0.24	17199	16660	-3.13
376	4.92	9613	9631	0.19	17199	17009	-1.10
395	4.83	9613	9629	0.17	17199	16647	-3.21

*: D/C refers to Demand/Capacity Control.

5.1.3 Summary

In Section 5.1, the ramp meter location and the ramp storage capacity were calculated. The CORSIM model developed in Chapter 4 was applied for testing and evaluating pre-timed and demand/capacity metering control strategies. After conducting a simulation analysis, benefits such as reduced total delay and increased total throughput were quantified. It was found that in most cases there was no metering rate that could simultaneously minimize the total delay and maximize the total throughput simultaneously. The potential ramps suitable to metering control were determined. Future studies could determine the best situations (the range of traffic volumes) for applying pre-timed and demand/capacity control.

The analysis conducted in this section demonstrates that ramp metering control is a potential strategy to improve traffic operations on the study site. In addition, it is desired to develop an effective multi-ramp metering control algorithm, which will optimize time-dependent metering rates for multiple ramps.

5.2 Model Testing

Before the developed dynamic multi-ramp metering control model is applied at the metered ramps in the studied network, testing of the proposed model should be performed. The test site in the network was identified as shown in Figure 5.1 where a three-lane mainline, a one-lane on-ramp, and a one-lane off-ramp were included.

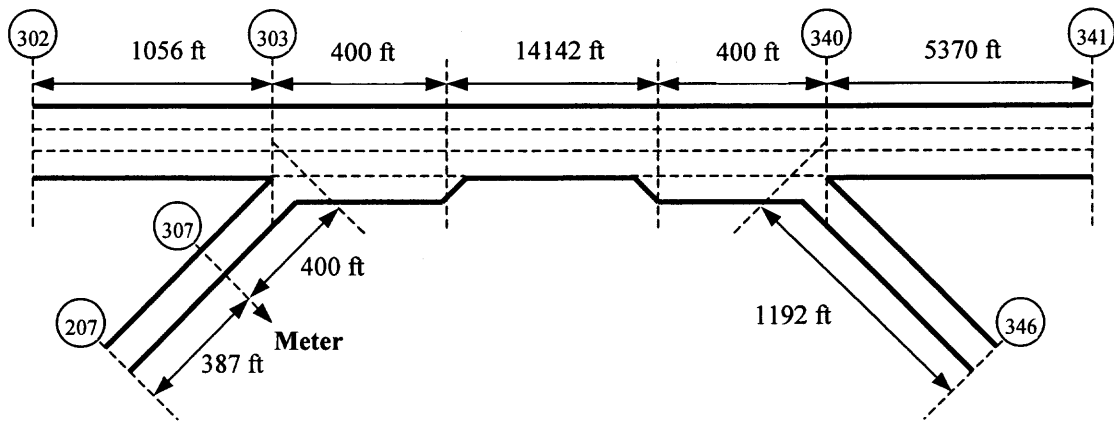


Figure 5.1 Configuration of the study site at node 307.

5.2.1 Constraints

The developed dynamic multi-ramp metering control model was applied on the test site where only one metered ramp at node 307 was involved. The suggested ramp meter location was 400 feet from the on-ramp gore, which guaranteed that vehicles could be discharged from the ramp and smoothly merge onto the mainline. The ramp storage capacity was 19 vehicles based on the available space on the ramp of 387 feet and the average vehicle length of 20 feet.

5.2.2 Testing Cases

Considering dynamic system control for the real-time application, the time dependent demand of I-80 over a series of time intervals was simulated with CORSIM. In this study, the traffic operations (with and without the proposed system control) were simulated using 16 time intervals with 3-min duration each. To assess the benefits of the developed metering control model and analyze the range of entry flows that are suitable for applying metering control, various demand distributions were used and are discussed in the following three cases.

Case 1: Base Traffic Condition Collected from NJDOT

Case 1 was designed to evaluate the benefits of the developed multi-ramp metering control model under existing traffic condition shown in Table 5.10. The entry and ramp flows both varied over the 16 intervals.

Case 2: Increasing Entry Volume with Fixed Ramp Flow

To analyze the range of entry flows that might benefit from the proposed metering control, Case 2 was designed to increase the entry flow from 2960 vph to 5960 vph at a rate of 200 vph per interval, while the flow passing through node 307 was fixed and 489 vph for every interval (Table 5.10).

Case 3: Fixed Entry Volume with Increasing Ramp Flow

Since the demand at the on-ramp changes over time, the optimal metering rate is also time dependent. This case assumed that the ramp demand approaching node 307 increased from 240 vph to 900 vph, while the entry flow was fixed and 4160 vph over the evaluation period (see Table 5.10).

Table 5.10. Traffic Demand Distribution for the Three Test Cases

Index of Interval*	Entry Flow at Node 301 (vph)			Ramp Flow at Node 307 (vph)		
	Case 1	Case 2	Case 3	Case 1	Case 2	Case 3
1	1472	2960	4160	173	489	240
2	3523	3160	4160	414	489	262
3	5082	3360	4160	597	489	286
4	4446	3560	4160	523	489	313
5	3962	3760	4160	466	489	341
6	3291	3960	4160	387	489	373
7	2626	4160	4160	309	489	407
8	2429	4360	4160	286	489	445
9	2331	4560	4160	274	489	486
10	2371	4760	4160	279	489	530
11	2453	4960	4160	288	489	579
12	2553	5160	4160	300	489	633
13	2703	5360	4160	318	489	691
14	2898	5560	4160	341	489	755
15	2315	5760	4160	272	489	824
16	1769	5960	4160	208	489	900

*: The duration of each interval is three minutes.

5.2.3 Data Collection

As discussed in Section 3.1, the mainline density $\rho_i(k)$ can be determined by $\rho_i(k-1)$ and other parameters presented in Equation 3.3. According to the Highway Capacity Manual (1997), the mainline density should not exceed the maximum value of 45 vehs/mi/ln when the free flow speed is 65 mph. If $\rho_i(k)$ is greater than 45 vehs/ln-mile, the $R_i(k)$ is set to the default value $R_i^{\min}(k)$.

A computer program coded in FORTRAN was developed to optimize ramp metering rates with SPSA by minimizing the objective function of Equation 3.7. The input data (e.g., $\theta_i(k)$, $\rho_i(k-1)$, $q_0(k)$, $S_i(k)$, $Q_i(k)$ and $R_i(K)$) either were initialized at the beginning time interval, collected in real-time, or estimated from historical data. Using the SPSA algorithm to search for optimal ramp metering rates, parameters **a** and **c** are set at 100 and 3 respectively for a larger iteration step size. Parameters β and γ have the effective and valid values at 0.602 and 0.101 respectively for a steady convergence during the optimization process. The optimal metering rates over the 16 intervals for the three cases are summarized in Table 5.11.

Table 5.11 Optimal Metering Rates for Various Test Cases

Index of Interval*	Case 1 (vph)	Case 2 (vph)	Case 3 (vph)
1	240	794	612
2	781	794	627
3	900	794	640
4	900	815	689
5	854	836	713
6	766	858	740
7	674	881	778
8	645	881	835
9	633	881	880
10	638	881	900
11	663	881	900
12	680	881	900
13	699	881	900
14	723	881	900
15	631	881	900
16	240	881	900

*: The duration of each interval is three minutes.

As mentioned earlier, the optimal metering rate obtained in each interval was based on the simulation output generated in the previous interval. Thus, a shorter interval could increase the precision of the control, but the computation effort would increase. In reality, an appropriate interval length should be determined so that the maximum benefit of ramp metering control can be achieved. In this study, the interval lengths were identical and equal to three minutes.

The output data (e.g., link volume, accumulated vehicle-mile, and average delay) for each time interval were collected. Since CORSIM only generated accumulated statistics, the MOEs in each interval need to be recalculated. A macro in MS-Excel was developed to efficiently retrieve data from simulation outputs, and then estimate the net benefit of each interval. Two MOEs, total delay and total throughput were selected for evaluating the benefit of ramp metering control. The network-wide total delay (veh-min) was obtained from the total vehicle-miles multiplied by average delay (min/mi), while the total throughput was obtained by summing the exiting volumes in the end of each interval. The benefit assessment of the dynamic multi-ramp metering control with SPSA was conducted by comparing total throughput and delay with and without the developed dynamic ramp metering control model.

5.2.4 Analysis and Evaluation

The total before and after delay and throughput were analyzed for Case 1 and the results are shown in Figure 5.2. The maximum total throughput benefit was 6.2% at the fifth interval, while the maximum total delay benefit was 3% at the fourth interval. The benefits of delay and throughput maximizations could not be achieved at the same metering rate. There were not benefits in some intervals with less demand, which suggests that the developed model might work well when traffic gets congested.

In Case 2, after implementing the developed dynamic ramp metering control model, simulation results showed that the total throughput increased from the 3rd to the 9th interval (see Figure 5.3), while total delay was reduced from the 8th to the 15th interval. The maximum achieved delay was 6.17% below that under no control. This analysis demonstrated that the developed dynamic ramp control model could increase the total throughput when the entry flow ranged from 3360 vph to 4560 vph with fixed ramp flow of 489 vph. The total delay could be reduced if the entry flow ranged between 4360 vph and 5960 vph. This suggests that the throughput benefit could be achieved with the developed metering control while traffic conditions on the mainline were congested but before reaching saturation.

In Case 3, after implementing the developed metering control total throughput increased in most intervals except the last one with the highest vehicle demand of 900 vph (the metering control for the upper bound demand on the ramp might not meet the ramp storage constraint). It was found that the developed control model was more sensitive to increase throughput when the ramp demand ranged from 373 vph to 579 vph as shown in Figure 5.4. Meanwhile, a delay benefit was obtained from the 1st to 12th intervals. It indicated that the total delay would decrease before traffic reached saturation.

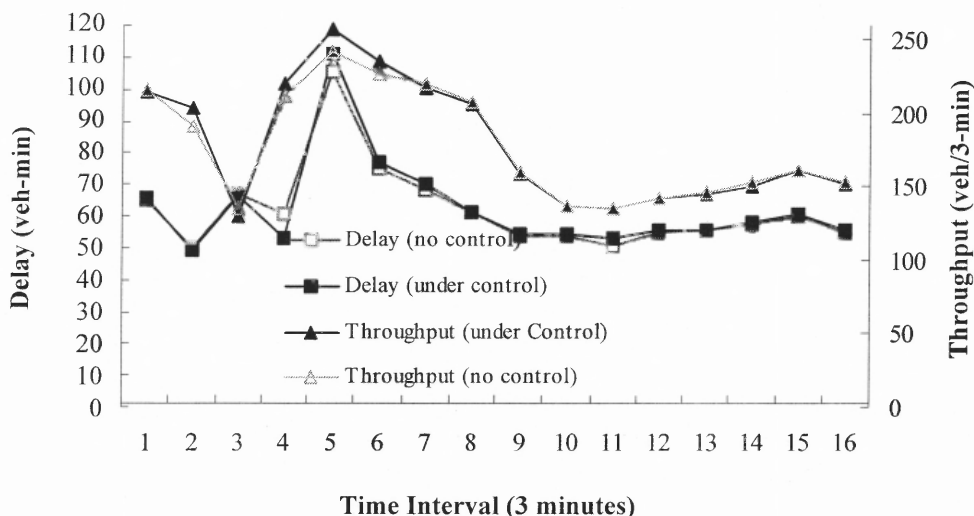


Figure 5.2 Total delay and total throughput over time (Case 1).

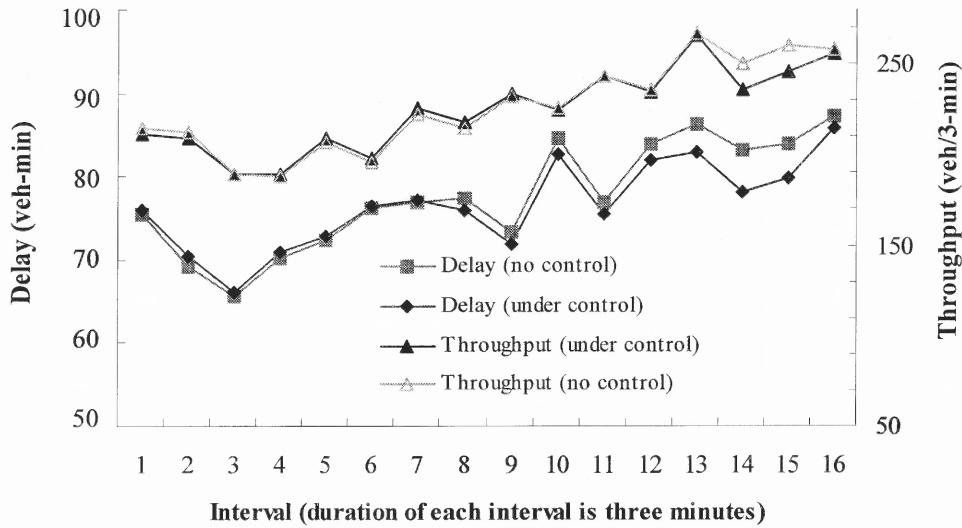


Figure 5.3 Total delay and total throughput over time (Case 2).

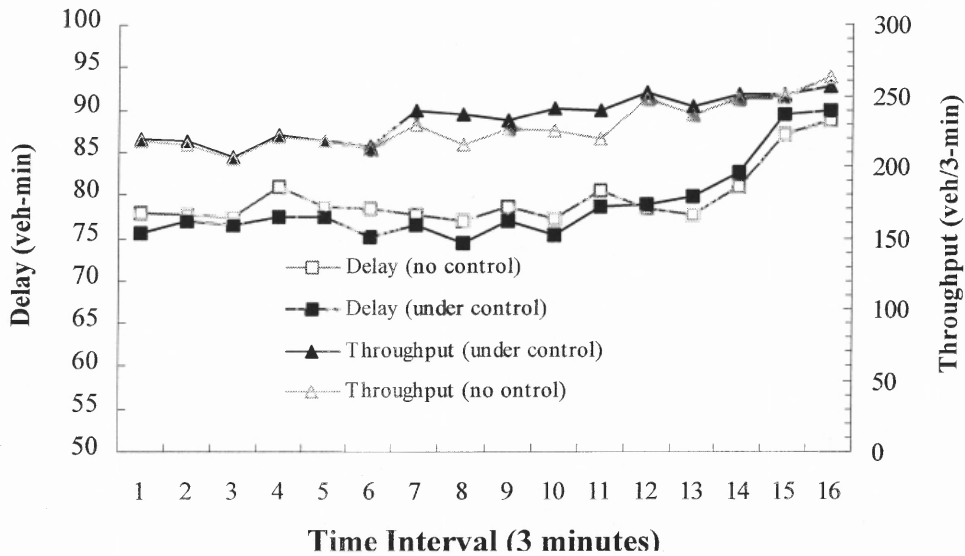


Figure 5.4 Total delay and total throughput over time (Case 3).

5.3 Individual Ramp Control

The analysis and evaluation of Section 5.2.4 indicated that the developed model might work well when the traffic was getting congested. To evaluate the potential application of the developed model at an individual ramp or multiple ramps on the entire network and find the range of feasible metering rates, a traffic distribution as shown in Table 5.12 was designed corresponding to each of the 16 intervals. The entry flow (at link 300-301) increased by 200 vph in every interval with fixed demand at all on-ramps.

Under the traffic conditions shown in Table 5.12, the developed model was applied at metered nodes 306, 307, 356, 376 and 395, respectively. Similar to the test cases in Section 5.2, the 48-minute simulation period was divided into 16 intervals. The constraints discussed in Section 5.1.1 are also in effect for individual ramp control. The optimal metering rates for control at each ramp were obtained and were listed in Table 5.13. The network-wide simulation and analysis were conducted as follows.

With the application of the developed dynamic multi-ramp metering control model to each individual ramp (e.g., at node 306), simulation results (see Table 5.14) showed that the total throughput from interval 3 to 9 could increase by 6.63% (greater than 5%). However, the increased total throughput for all 16 time intervals was 0.39% (less than 5%). This analysis demonstrates that the developed dynamic ramp metering control was efficient, while the entry flow ranged from 3360 vph to 4560 vph.

Table 5.15 shows the total delay with metering control. At node 306 the total delays were reduced from the 8th to the 15th time interval. With control, the reduction of the total delay was 8.92% for the 8 intervals and 5.26% for all 16 intervals. Thus, it is beneficial to use the proposed metering control at node 306 and particularly when the

entry flow ranged between 4360 and 5760 vph. After considering also the results for the other metered ramps (nodes 307, 356, 376 and 395), a summary Table 5.16 can be developed indicating the entry flows for which vehicle metering will be most effective.

Table 5.12 Traffic Demand Distribution

Interval*	Entry Flow	Node 306	Node 307	Node 345	Node 356	Node 376	Node 377	Node 395
	vph							
1	2960	360	489	2159	819	400	1216	430
2	3160							
3	3360							
4	3560							
5	3760							
6	3960							
7	4160							
8	4360							
9	4560							
10	4760							
11	4960							
12	5160							
13	5360							
14	5560							
15	5760							
16	5960							

*: The duration of each interval is three minutes.

Table 5.13 Optimal Metering Rates (vph) for Individual Ramps

Interval*	Node 306	Node 307	Node 356	Node 376	Node 395
1	705	794	895	737	766
2	705	794	895	737	766
3	705	794	895	737	766
4	720	815	900	753	783
5	735	836	900	771	802
6	751	858	900	789	822
7	767,	881	900	808	842
8	779	881	900	820	842
9	779	881	900	820	842
10	779	881	900	820	842
11	779	881	900	820	842
12	779	881	900	820	842
13	779	881	900	820	842
14	779	881	886	819	774
15	779	881	874	758	761
16	779	881	862	744	748

*: The duration of each interval is three minutes.

Table 5.14 Network-wide Total Throughput for Individual Ramp Control

Interval*	Entry Flow (vph)	Before (veh/3min)	After (veh/3min)				
			Node 306	Node 307	Node 356	Node 376	Node 395
1	2960	467	445	430	437	441	449
2	3160	492	451	473	456	447	458
3	3360	437	459	477	481	469	454
4	3560	448	473	471	460	476	451
5	3760	438	484	465	457	455	485
6	3960	422	452	459	482	476	472
7	4160	442 (0%)	478 (8.14%)	459 (3.85%)	465 (5.20%)	475 (7.47%)	473(7.01%)
8	4360	448	461	476	469	483	467
9	4560	450	484	446	468	445	464
10	4760	482	463	487	495	475	479
11	4960	498	489	478	489	478	491
12	5160	512	489	486	483	515	485
13	5360	509	530	516	493	506	501
14	5560	532	499	525	510	517	516
15	5760	537	503	523	518	495	529
16	5960	542	527	516	503	523	509
Total (1-16)		7656	7686	7687	7665	7675	7682
%		0.00	0.39	0.40	0.11	0.25	0.34
Total (3-9)		3085	3289	3253	3282	3278	3265
%		0.00	6.63	5.46	6.37	6.27	5.84

*: The duration of each interval is three minutes.

Table 5.15 Network-wide Total Delay for Individual Ramp Control

Interval*	Entry Flow (vph)	Before (veh-min)	After (veh-min)				
			Node 306	Node 307	Node 356	Node 376	Node 395
1	2960	614.5	595.2	613.8	623.0	627.6	617.4
2	3160	619.7	652.8	620.7	647.7	629.3	607.0
3	3360	560.3	624.9	601.7	605.5	637.9	637.4
4	3560	655.0	590.5	530.0	642.6	628.4	682.7
5	3760	624.0	540.4	575.8	648.0	603.1	599.0
6	3960	527.2	629.1	558.8	667.5	605.7	645.2
7	4160	623.9	672.2	674.2	639.9	645.0	674.0
8	4360	742.5	678.8	650.9	692.9	682.8	744.0
9	4560	836.0	669.6	825.9	813.3	728.5	754.9
10	4760	981.4	948.1	850.3	820.3	930.6	785.9
11	4960	973.0	876.9	936.7	953.4	892.5	903.1
12	5160	1170.2	966.5	1081.1	1071.7	1024.0	1092.8
13	5360	1278.9	1053.9	1112.8	1089.5	1076.1	1102.5
14	5560	1338.6	1251.2	1185.5	1249.6	1230.4	1295.3
15	5760	1469.0	1349.1	1350.4	1382.4	1412.7	1281.8
16	5960	1554.1	1702.0	1484.8	1615.2	1462.1	1618.2
Total (1-16)		14568.2	13801.3	13653.3	14162.5	13816.5	14041.5
%		0	-5.26	-6.28	-2.78	-5.16	-3.62
Total (3-9)		4568.8	4405.6	4417.2	4709.6	4531.3	4737.3
%		0	-3.57	-3.32	3.08	-0.82	3.69
Total (8-15)		10343.6	9496.2	9478.4	9688.3	9439.6	9578.7
%		0.00	-8.92	-9.13	-6.76	-9.58	-7.99

*: The duration of each interval is three minutes.

Table 5.16 Suggested Entry Flows of Mainline for the Proposed Control Model

Item		Node Number				
		306	307	356	376	395
Entry Flow (vph)	For Increasing Total Throughput	3360~4560	3360~4560	3360~4560	3360~4560	3360~4560
	For Reducing Total Delay	4360~5760	4360~5960*	4360~5760	4360~5960*	4360~5760

*: The suggested entry flow may be greater than 5960.

5.4 Dynamic Multi-ramp Metering Control

In this section, the developed dynamic ramp metering control is applied simultaneously for multiple metered ramps (e.g., nodes 306, 307, 356, 376 and 395). Similar to the situation of individual ramp control discussed in Section 5.3, the 48-minute simulation duration was divided into 16 intervals. The constraints discussed in Section 5.1.1 are also in effect for multiple ramp control. The metering rates were jointly optimized with the developed SPSA algorithm and shown in Table 5.17. The coordination among the controlled ramps was considered to achieve the ultimate benefit for the studied network.

Based on an entry flow of 4160 vph on the mainline, the total throughput after control is 482 veh/3min representing a 9.05% increase over the non-controlled case as shown in Table 5.18. Comparing the results with and without control from the third to ninth interval (Table 5.18 and Figure 5.5), the accumulated total throughput after multiple ramp control increased by 8.07%. However, the accumulated total throughput over all intervals increased by only 1.16%. Table 5.18 and Figure 5.6 show that after multiple ramp control, the accumulated total delay from the eighth to fifteenth interval was reduced by 9.73%, while the accumulated total delay over all intervals was reduced by 5.68%. Thus, multiple ramp control was more efficient to increase total throughputs when the mainline traffic entry flow ranged from 3360 vph to 4560 vph, and more efficient to reduce total delay when the entering volume of the mainline was from 4360 vph to 5760 vph. It was also found that multiple ramp control was more efficient than individual ramp control in increasing the total throughput of the network (Tables 5.14 and 5.18).

Table 5.17 Optimal Metering Rates and Headways for Multi-ramp Control

Time Interval*	Node 306	Node 307	Node 356	Node 376	Node 395
	Metering Rate, vph (Headway, in seconds)				
1	650 (5.54)	766 (4.70)	900 (4.00)	753 (4.78)	799 (4.51)
2	650 (5.54)	766 (4.70)	900 (4.00)	753 (4.78)	799 (4.51)
3	650 (5.54)	766 (4.70)	900 (4.00)	753 (4.78)	799 (4.51)
4	664 (5.42)	766 (4.70)	900 (4.00)	769 (4.68)	816 (4.41)
5	680 (5.29)	766 (4.70)	900 (4.00)	787 (4.57)	835 (4.31)
6	696 (5.17)	776 (4.64)	900 (4.00)	805 (4.47)	855 (4.21)
7	712 (5.06)	799 (4.51)	900 (4.00)	824 (4.37)	875 (4.11)
8	724 (4.97)	799 (4.51)	900 (4.00)	824 (4.37)	875 (4.11)
9	723 (4.98)	799 (4.51)	900 (4.00)	824 (4.37)	875 (4.11)
10	719 (5.01)	754 (4.77)	900 (4.00)	900 (4.00)	889 (4.05)
11	713 (5.05)	747 (4.82)	900 (4.00)	900 (4.00)	900 (4.00)
12	709 (5.08)	742 (4.85)	900 (4.00)	900 (4.00)	900 (4.00)
13	705 (5.11)	737 (4.88)	891 (4.04)	900 (4.00)	900 (4.00)
14	693 (5.19)	721 (4.99)	881 (4.09)	900 (4.00)	900 (4.00)
15	681 (5.29)	705 (5.11)	869 (4.14)	867 (4.15)	900 (4.00)
16	668 (5.39)	689 (5.22)	860(4.19)	887 (4.06)	900 (4.00)

*: The duration of each interval three minutes

Table 5.18 Results of Multi-ramp Control

Interval*	Entry Flow (vph)	Total Throughput (veh/3min)		Total Delay (veh-min)	
		Before	After	Before	After
1	2960	467	432	614.5	603.7
2	3160	492	431	619.7	641.6
3	3360	437	449	560.3	623.7
4	3560	448	475	655.0	638.2
5	3760	438	519	624.0	610.3
6	3960	422	447	527.2	599.3
7	4160	442, (0%)	482, (9.05%)	623.9	687.6
8	4360	448	487	742.5	715.0
9	4560	450	477	836.0	719.8
10	4760	482	494	981.4	874.4
11	4960	498	461	973.0	859.2
12	5160	512	454	1170.2	1049.3
13	5360	509	553	1278.9	1089.3
14	5560	532	516	1338.6	1184.9
15	5760	537	543	1469.0	1364.9
16	5960	542	529	1554.1	1480.0
Total (1-16), (percentage, %)		7656, (0.00)	7745, (1.16)	14568.2, (0.00)	13741.3, (-5.68)
Total (3-9), (percentage, %)		3085, (0.00)	3334, (8.07)	4568.8, (0.00)	4594.0, (0.55)
Total (8-15), (percentage, %)		4510, (0.00)	4514, (0.10)	10343.6, (0.00)	9336.9, (-9.73)

*: The duration of each interval is three minutes.

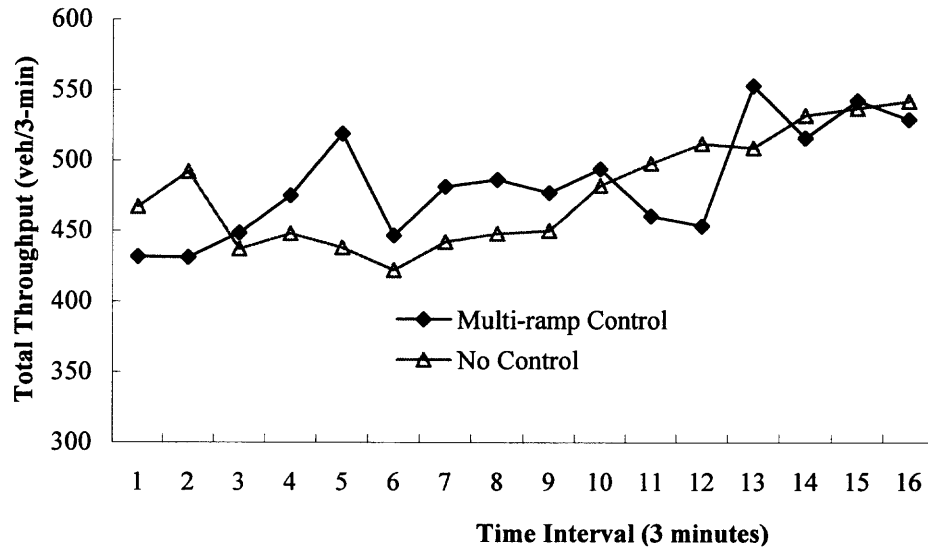


Figure 5.5 Total throughput over time (multi-ramp control).

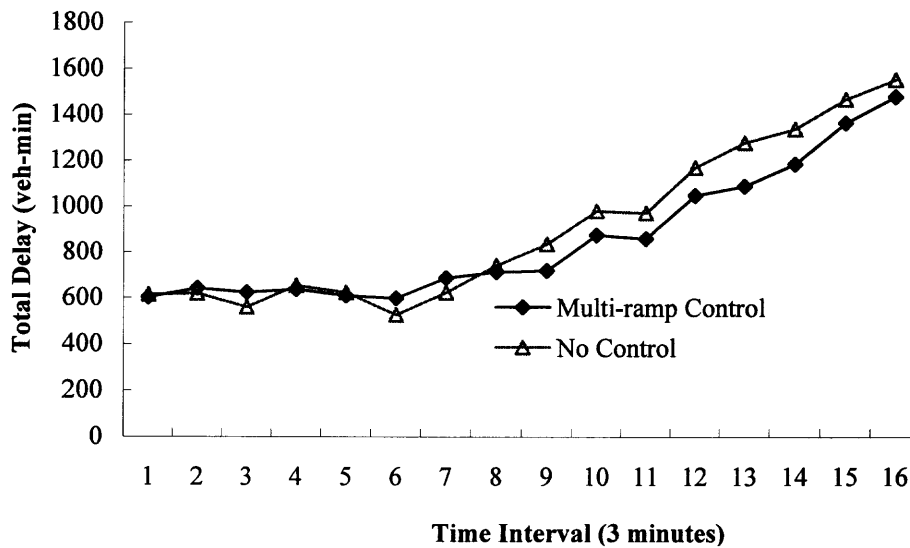


Figure 5.6 Total delay over time (multi-ramp control).

5.5 Road User Cost

During peak hours, congestion forces traffic to operate under a “queue” situation even under “Forced Flow” conditions. Queuing situations impose four major related road user cost components: stopping Vehicle Operating Cost (VOC), stopping delay, queue delay, and queue idling VOC. The queue delay and queue idling VOC component accounts for approximately 90% of the total road user costs associated with the “Forced Flow” condition. Thus, to simplify the calculations, only queue delay and queue idling VOC components are recommended to be estimated (NJDOT, 2001).

Queue delay is the additional time necessary to creep through the queue under forced flow conditions (congestion situations), while queue idling VOC is the additional vehicle operating costs associated with “stop and go” driving in the queue. The operating costs include fuel, engine oil, maintenance, and depreciation. The Road User Cost (RUC) can be calculated based on delay and vehicle operation as in Equation 5.5.

$$C = D[P_C(V_C + I_C) + P_T(V_T + I_T)] \quad (5.5)$$

where D : the total delay;

V_C : the value of time for cars (\$12.75/hour, NJDOT, 2001);

V_T : the value of time for trucks (\$21.25/hour, NJDOT, 2001);

I_C : the idling cost rate for cars (\$0.68/hour, NJDOT, 2001);

I_T : the idling cost rate for trucks (\$0.78/hour, NJDOT, 2001);

P_C : the percentage of cars in the traffic flow;

P_T : the percentage of trucks in the traffic flow;

Table 5.19 shows the road user cost and benefit analysis for multi-ramp control. The total benefit from delay reduction is \$196.99 over the control period (16 time intervals). The annual benefit of road user cost for savings can be approximately

estimated. Assuming that there are two peak hours (morning and evening) every weekday with 4560 vph average entry flow on the mainline, the benefit during each three-minute interval is \$27.67 (Table 5.19), and there are 20 intervals per hour. Thus, the annual benefit under this assumption is:

$$\begin{aligned} & \text{Peak Hours Benefit per Workday} \times \text{Workdays per Year} \\ & = (2 \times 20 \times 27.67) (\$/\text{day}) \times 260 (\text{days/year}) = 287,560 (\$/\text{year}). \end{aligned}$$

Table 5.19 Road User Costs and Benefits for Multi-ramp Control

Interval	Entry Flow (vph)	<i>D</i> (Before) (veh-h)	<i>D</i> (After) (veh-h)	<i>C</i> (Before) (\$)	<i>C</i> (After) (\$)	Benefit (save) (\$)
1	2960	10.24	10.06	146.35	143.78	2.57
2	3160	10.33	10.69	147.59	152.81	-5.22
3	3360	9.34	10.40	133.44	148.54	-15.10
4	3560	10.92	10.64	156.00	152.00	4.00
5	3760	10.40	10.17	148.62	145.35	3.26
6	3960	8.79	9.99	125.56	142.73	-17.17
7	4160	10.40	11.46	148.59	163.76	-15.17
8	4360	12.38	11.92	176.84	170.29	6.55
9	4560	13.93	12.00	199.11	171.43	27.67
10	4760	16.36	14.57	233.74	208.25	25.48
11	4960	16.22	14.32	231.74	204.63	27.10
12	5160	19.50	17.49	278.70	249.91	28.79
13	5360	21.32	18.16	304.59	259.43	45.16
14	5560	22.31	19.75	318.81	282.20	36.61
15	5760	24.48	22.75	349.87	325.07	24.79
16	5960	25.90	24.67	370.13	352.49	17.65
Total (1-16)		242.81	229.02	3469.68	3272.70	196.99

Note: *D* is the total delay; *C* is the road user cost. Cost and benefits calculation is based on 2001 prices (NJDOT). The duration of each interval is three minutes.

5.6 Fuel Consumption and Emissions

The fuel consumption was increased by 34.72 % on ramps after the multi-ramp metering control (Table 5.20). However, the fuel consumed on the whole network was increased by just 1.33%. Emissions of reactive hydrocarbons (HC), carbon monoxide (CO), and nitrogen oxides (NO_x) from vehicles have the potential to adversely impact human health and the environment. The implementation of multi-ramp control did not lead to significant increases of HC and NO_x (0.44% and 1.20%, respectively) in the study network, while CO was reduced by 0.69 %. Dramatic increased emissions from vehicles

on ramps (NC, 226.48%; CO 164.08%; and NO_x, 233.01%) were observed after control. However, these increased emissions contributed minimally to the network since the traffic volume on ramps is a small proportion of the total.

Table 5.20 Fuel Consumption and Emissions Analysis for Joint Ramp Control

Item		Before	After	%
Fuel (gallons)	Mainline	475.6	479.1	0.73
	Ramp	8.6	11.6	34.72
	Total	484.2	490.7	1.33
HC (grams)	Mainline	277.8	273.2	-1.65
	Ramp	2.6	8.4	226.48
	Total	280.4	281.6	0.44
CO (grams)	Mainline	20079.1	19653.8	-2.12
	Ramp	173.5	458.2	164.08
	Total	20252.6	20112.0	-0.69
NO _x (grams)	Mainline	1167.5	1149.2	-1.56
	Ramp	13.9	46.4	233.01
	Total	1181.4	1195.6	1.20

5.7 Sensitive Analysis

5.7.1 Short Ramp

When an on-ramp lacks physical storage area, the performance of ramp metering control will be affected. To verify this and investigate how a short ramp might affect metering control, the benefits of the metering control under different ramp storage capacities were analyzed. Ramp metering control at node 307 as shown in Figure 5.1 is used for this purpose. The maximum queue length on link 207-307 was increased from 387 feet to 987 feet by 100 feet, while the mainline and ramp flows remained the same (4160 vph and 489 vph, respectively).

The optimal metering rates found by applying SPSA for this case are summarized in Figure 5.7. The optimal metering rate decreased as the ramp storage area increased. However, when the ramp storage was more than 887 feet, the optimal metering rates would not change. Figure 5.8 shows the total delay and throughput benefits versus ramp

storage length over the entire 48-minute simulation interval before and after metering control. Comparing with the base situation where the ramp storage length was 387 feet, it was found that total throughput increased when the ramp storage increased, especially when extending the ramp storage from 387 feet to 587 feet. In addition to the benefit on throughput, the total delay can be reduced when the ramp storage is longer than 787 feet. This indicated that increasing ramp storage could improve the efficiency of the developed dynamic metering control model.

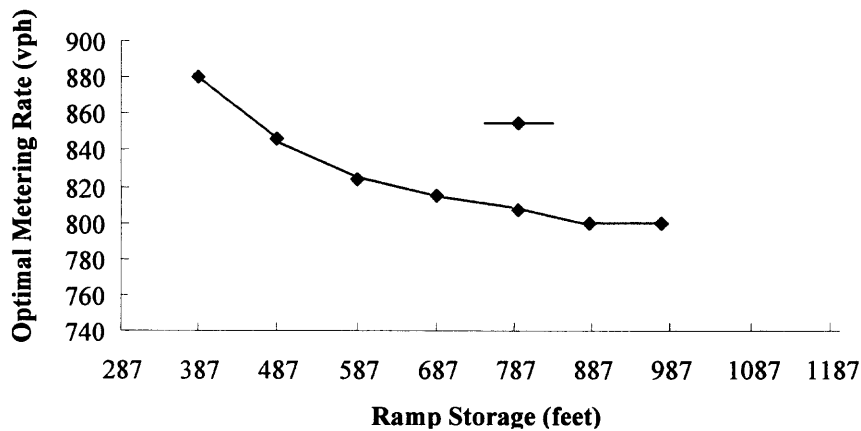


Figure 5.7 Optimal metering rate with SPSA vs. ramp storage area (node 307).

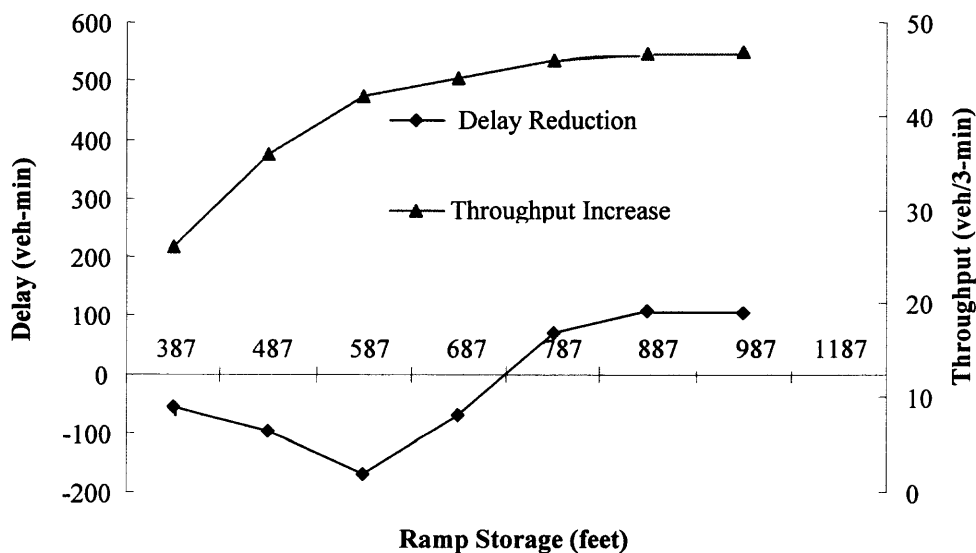


Figure 5.8 The benefit of total delay and total throughput (node 307).

5.7.2 Control at Different Groups of Metered Ramps

In this section, the developed model was applied to different groups of multiple metered ramps. The purpose of this analysis is to determine the best control strategy in terms of the combination of ramps to be controlled (among nodes 306, 307, 356, 376 and 395). The traffic distribution is shown in Table 5.12. The constraints discussed in Section 5.1.1 are applicable here also. Four cases were designed for this comparison analysis. In Case A, ramps at both nodes 306 and 307 were controlled with the developed model. Case B applied the developed model to three ramps at nodes 306, 307, and 356 simultaneously. Case C involved four metered ramps that were at node 306, 307, 356, and 376. Case D is as discussed in Section 5.3, where the developed model was implemented on all ramps. The simulation results are summarized in Tables 5.21 and 5.22.

Table 5.21 Network-wide Total Throughput for Multiple Ramps Control

Interval*	Entry Flow (vph)	Before (veh/3min)	Total Throughput (veh/3min)			
			Case A	Case B	Case C	Case D
1	2960	467	441	443	446	432
2	3160	492	466	466	465	431
3	3360	437	472	478	480	449
4	3560	448	476	474	478	475
5	3760	438	478	475	473	519
6	3960	422	459	470	475	447
7	4160	442	472	473	477	482
8	4360	448	472	475	480	487
9	4560	450	469	472	469	477
10	4760	482	479	488	488	494
11	4960	498	487	491	492	461
12	5160	512	491	492	501	454
13	5360	509	527	519	519	553
14	5560	532	516	517	521	516
15	5760	537	517	521	518	543
16	5960	542	525	521	525	529
Total (1-16)		7656	7748	7774	7807	7749
%		0.00	1.20	1.55	1.97	1.21
Total (3-9)		3085	3299	3317	3332	3336
%		0.00	6.92	7.51	8.01	8.14

*: The duration of each interval is three minutes.

As shown in Table 5.21, for Cases A, B, C, and D, the network-wide accumulated total throughput increased from the third to the ninth interval by 6.92%, 7.51%, 8.01%, and 8.14%, respectively. The results indicate that the developed model was more efficient in increasing total throughput by controlling all five ramp simultaneously. Table 5.22 shows that the network-wide total delay accumulated from the eighth to the fifteenth interval was reduced by 8.80%, 8.15%, 9.00%, and 9.73% for cases A, B, C, and D, respectively. It also shows that simultaneous metering control at all ramps would reduce total delay the most.

Table 5.22 Network-wide Total Delay for Multiple Ramps Control

Interval*	Entry Flow (vph)	Before	Total Delay (veh-min)			
		(veh-min)	Case A	Case B	Case C	Case D
1	2960	614.5	599	605	602	604
2	3160	619.7	631	634	625	642
3	3360	560.3	607	605	605	624
4	3560	655.0	554	582	585	638
5	3760	624.0	552	582	579	610
6	3960	527.2	588	612	603	599
7	4160	623.9	667	656	645	688
8	4360	742.5	659	668	664	715
9	4560	836.0	742	764	747	720
10	4760	981.4	893	867	875	874
11	4960	973.0	901	916	902	859
12	5160	1170.2	1018	1034	1023	1049
13	5360	1278.9	1077	1079	1071	1089
14	5560	1338.6	1212	1223	1217	1185
15	5760	1469.0	1344	1355	1361	1365
16	5960	1554.1	1587	1595	1554	1480
Total (1-16)		14568.2	13631	13776	13658	13741
%		0.00	(6.43)	1.06	(0.86)	0.61
Total (8-15)		10343.6	9433	9500	9413	9337
%		0.00	-8.80	-8.15	-9.00	-9.73

*: The duration of each interval is three minutes.

5.7.3 Optimal Simulation

The developed SPSA was utilized to obtain approximate optimal ramp metering rates, while the optimal control was simulated with the developed CORSIM model. When metering control could not release all arrival vehicles at a ramp in a time period, a queue

developed on the ramp. This situation frequently took place at ramps with heavy traffic, or when the metering rates were not high enough to discharge the queue. The sensitivity analysis was conducted by investigating the optimization performance during simulation. The simulation analysis for the optimal metering control at node 356 under the traffic conditions shown in Table 5.12 was used. The focus area mainly included an on-ramp, one off-ramp, and the mainline (i.e., links 256-356, 356-352, 371-375, 351-352, 352-371, and 371-372 as shown in Figure A.8).

Table 5.23 shows simulation results for optimal metering control at the metered ramp (node 356). The highlighted numbers (arrival plus queue) in the table were greater than the corresponding optimal metering rates at node 356. Simulation control did not release all arrived vehicles at intervals 4 through 16. A progressively increasing queue was formed at these intervals, and it exceeded the SPSA optimal rate at intervals 14, 15 and 16.

Table 5.23 Simulation Results after Optimal Metering Control at Node 356

Interval*	Entry Flow (vph)	Arrival Rate	Departure Rate	Queue after Control	Arrival plus Queue	SPSA Optimal Rate
		(vph)	(vph)	(vph)	(vph)	(vph)
1	2960	819	819	0	819	895
2	3160	819	819	0	819	895
3	3360	819	819	0	819	895
4	3560	819	815	3	822	900
5	3760	819	815	3	822	900
6	3960	819	814	3	822	900
7	4160	819	814	5	824	900
8	4360	819	810	5	824	900
9	4560	819	804	9	828	900
10	4760	819	800	15	834	900
11	4960	819	790	19	838	900
12	5160	819	778	29	848	900
13	5360	819	746	41	860	900
14	5560	819	710	73	892	886
15	5760	819	700	109	928	874
16	5960	819	700	119	938	862

*: The duration of each interval is three minutes.

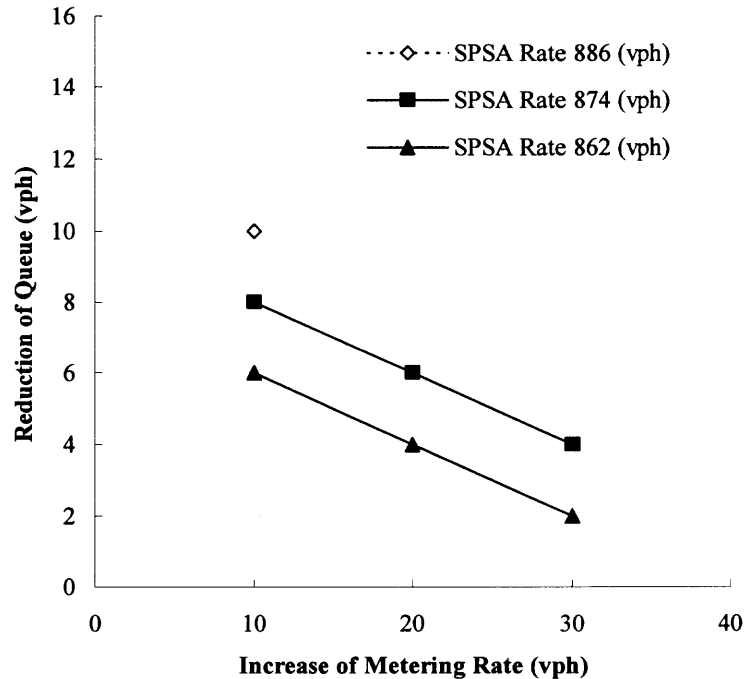


Figure 5.9 Metering rate change vs. queue reduction (node 356).

To improve this situation, the metering rates that were optimized with SPSA needed to be adjusted. The relationship between the change of optimal rates and the change of queues at node 356 is presented in Figure 5.9. As the optimal metering rates increase, the vehicle departure rate increases, the queue is reduced and the congested situation at the ramp is alleviated. In Table 5.24, the maximum of the increased throughput was the highlighted value (i.e., 0.5, 0.6, and 2.3 veh/3min) for the corresponding optimal rates (i.e., 886, 874, and 862 vph) found by SPSA. The delay was increased as the ramp metering rate increased. It is suggested that the optimal rates of 886, 874, and 862 vph be changed to 896, 874, and 962 vph, respectively. Under the new metering rates, the optimization simulation would improve the performance of the developed dynamic ramp metering control model.

Table 5.24 Change of the Throughput and Delay with Adjusted Optimal Rates

Optimal Metering Rate with SPSA (vph)	Adjustment of Optimal Rates (vph) at Node 356			Suggested Metering Rate (vph)
	+10	+20	+30	
	Throughput (veh/3min) / Delay (veh-min)			
886	0.5 / 2.0	0 / 2.0	0 / 2.0	886+10=896
874	0.6 / 11.0	-1.0 / 17.0	-1.0 / 17.0	874 +10=884
862	0.6 / -28.0	2.3 / 41.0	2.0 / 133.0	862+20=882

Note: The change of throughput (veh/3min) and the change of delay (veh-min) in the table are derived from the comparison of simulations before and after adjustment of optimal rates. The average values in the table are from ten simulation runs in three-minute intervals.

5.8 Summary

After analyzing the locations of ramp meters and the storage capacity of the metered ramp, the ramp metering control under different metering control strategies (e.g., pre-timed and demand/capacity control) was studied. The benefits, such as increased total throughput and reduced total delay were observed after the application of metering control. The potential metered ramps thus were determined.

The feasibility to implement the proposed dynamic multi-ramp metering control model was investigated through simulation of the traffic operation at the study site. The proposed model could be implemented in individual and multiple ramp control systems to maximize the total throughput. Evaluation of the simulated MOEs (e.g., throughput and delay) indicated that the proposed model could effectively improve the performance of traffic operations on I-80 under certain traffic situations. It was found that multiple ramp control would be more effective than individual ramp control.

In addition, the road user cost, fuel consumption and emissions (HC, CO, and NO_x) for the joint ramp metering control system were estimated. The sensitive analysis for the developed model included cases of short ramps, combination control, and optimal simulation.

CHAPTER 6

CONCLUSIONS AND FUTURE RESEARCH

In this study, the developed dynamic ramp metering control model was applied in a case study and was shown of a viable way that could efficiently manage traffic operations on freeways, and capable of eliminating, or at least reducing, congestion at the study site. The potential benefit of ramp metering control was discussed in detail. The constraints (e.g., meter signal locations, ramp storage capacities, lower and upper bounds of ramp metering rates) were formulated based on geometric and traffic conditions. CORSIM was selected to simulate traffic operations under various metering control conditions. The proposed SPSA algorithm was developed and applied to optimize dynamic ramp metering rates by maximizing the total throughput. The total throughput and total delay at the study site under time-varying traffic conditions and different ramp metering control strategies were simulated and analyzed. Conclusions and recommendations are presented next.

6.1 Conclusions and Recommendations

The major findings of this study are:

- Unrestrained merging traffic from ramps at the study site frequently resulted in bottlenecks during the peak hours. When the sum of mainline volume and entry ramp volume exceeded mainline capacity, congestion and queues were formed. Thus, the freeway capacity decreased and delay increased.

- The feasible ramp metering rates were found to be between 240 and 900vph. Subject to the ramp's storage constraint, the suggested lower bounds of metering rates on all potential ramps might be higher than 240 vph and were shown in Table 5.3. For example, the suggested lower bounds of metering rates at nodes 306, 307, 356, 376, and 395 were 370, 513, 870, 416 and 448 vph, respectively. If the ramp storage area increased, the feasible range of metering rates increased and the benefit of metering control could be further improved.
- A calibrated and validated CORSIM model was developed based on the data collected on eastbound I-80. The simulation model demonstrated its capability to mimic realistic traffic operations at the study site. It could be extensively applied to evaluate traffic operations under various ramp metering control strategies.
- Simulation results indicated that for metering control at a single ramp, the performance of pre-timed control at node 395 outperformed that at other nodes. The total delay could be reduced by 5.09%. For demand/capacity metering, the control at node 376 outperformed that at other nodes. The total delay could be reduced by 4.29%. Ramp metering could provide a higher and more predictable level of service on the freeway. It also improved the efficiency of traffic operations by smoothing the traffic stream on the mainline.
- The potential metered ramps connecting eastbound I-80 and Howard Boulevard South (node 306), Howard Boulevard North (node 307), Mount Hope Avenue (node 356), Hibernia Avenue (node 376), and E Main Street (node 395) were identified as been suitable for metering control at the study site. The ramps on

eastbound I-80 connecting Route 15 (MP 34.6) and Hibernia Avenue (MP 37.9) were not recommended for metering control due to insufficient storage space on the ramps.

- The effectiveness of metering control under a given set of traffic conditions was increased in terms of the reduced total delay or the increased total throughput. However, the optimal metering control did not minimize the total delay and maximize the total throughput simultaneously.
- A dynamic multi-ramp metering control model was developed and applied to single-ramp and multi-ramp conditions, considering a peak demand of 4160 vph on the mainline. While optimizing single ramp control, simulation results showed that the maximum total throughput could be increased by 8.14% (control at node 306 as shown in Table 5.14). While optimizing multi-ramp control, the total throughput was increased by 9.05% (as shown in Table 5.18).
- Considering time-varying traffic conditions (Table 5.12) and under single ramp control, simulation results of the developed dynamic multi-ramp metering control model showed that the total throughput could be increased by 6.63% and total delay reduced by 9.58% (Tables 5.14 and 5.15). Under multi-ramp control, the total throughput was increased by 8.07%, and a considerable reduction of 9.73% in total delay was achieved (Table 5.18). Therefore, multi-ramp control outperformed single ramp control in maximizing total throughput, and reducing total delay.

- While developing the dynamic multi-ramp metering control model, the non-linear relationship among control parameters in a large-scale network increased the level of difficulty in optimizing the ramp metering control problem. The developed simultaneous perturbation stochastic approximation (SPSA) algorithm was demonstrated to be efficient in solving the multivariate optimization problem formulated in this study.
- The developed SPSA solution algorithm could be applied to jointly optimize metering rates for multiple ramps in real-time by maximizing the total throughput. The developed dynamic multi-ramp metering control model could capture dynamic traffic flow changes over time and space, which was more efficient to increase total throughput when the range of mainline traffic entry flow was between 3360 vph and 4560 vph, and was more efficient to reduce total delay when the entering volume of the mainline was between 4360 vph and 5760 vph as shown in Table 5.18.
- The developed CORSIM model under optimal ramp metering rates control would not always release all vehicles arriving at the ramp during a time period. This led to the building up of long queues on the ramp over time. The ideal control result could not be achieved due to the stochastic and large number of vehicles at the ramp, or lower ramp metering rates.
- In this study, the optimal metering rates in the current time interval were determined based on the simulation from the previous time interval. Thus, the optimal metering rates were derived for the traffic conditions at the previous time

interval, which could not reflect the real-time condition. To mitigate this, two methods are suggested to be preformed. The first to shorten the time interval. Then the change between traffic conditions in the current and previous time intervals will be minimal. The second is to use real-time and predicted traffic if sufficient instrumentation and modeling capability is available.

- The choice of parameters (e.g., \mathbf{a} , \mathbf{c} , β and γ) is critical to the performance of SPSA. A large \mathbf{a} can enhance performance in the later iterations by producing a larger step size, while it will be effective to set \mathbf{c} as some small positive number. Choosing $\beta \leq 1.0$ usually yields better finite-sample performance through maintaining a larger step size. In this study, \mathbf{a} , \mathbf{c} , β and γ were 100, 3, 0.602 and 0.101, respectively.

6.2 Future Research

- The capacity of short ramp storage constraint imposed in this study prevented queuing vehicles on ramps from spilling back onto local streets, and no vehicle diversion was assumed. In practice, vehicle diversion will occur when the freeway becomes congested and should be considered in the future.
- Although the developed CORSIM model simulated traffic operations of eastbound I-80, it did not include the traffic on arterials (e.g., NJ State Routes 10 and 46) near the study site and the signalized intersection control that might affect the traffic flow on the freeway. It is essential that the study should be extended to cover the whole I-80 corridor so that the impacts of traffic control at ramps and intersections can be jointly considered.

- The analysis of simulation results showed that achieving maximum total throughput did not always achieve minimum total delay. The tradeoff between reduced delay and increased throughput should be considered in the future.
- While applying the dynamic multi-ramp metering control with SPSA, the traffic demand including O/D flow was assumed to be fixed. With the application of ITS, traffic volumes can be detected in real-time, and may provide a reliable input to reflect actual traffic variation over time. If such data are available, they should be incorporated in the model.
- The developed model is a system-wide dynamic multi-ramp metering control model that can be used to handle a series of ramps in a traffic responsive mode. To process collected real-time data, optimize metering rates, and execute the control mechanism through ramp meters, the optimization of ramp metering rates is often carried by centralized or decentralized computer systems. However, the system-wide models often lead to hierarchical non-linear optimization programming. The effectiveness of the centralized control versus the decentralized control should be evaluated in the future.
- In the dynamic multi-ramp metering control with SPSA, the objective function was to maximize the total throughput. Other objective, such as total delay, vehicle emissions and fuel consumption, and local congestion can be considered by enhancing the developed objective function (Equation 3.6) and modifying the developed SPSA.

- The M/M/1 queuing model applied in this study assumed exponential vehicle arrivals and departures with one server. However, vehicles on ramps will more likely be discharged into the mainline deterministically under metering control. Thus, the M/D/1 model (exponentially distributed arrivals and deterministic departures with one server) used in the dynamic metering control model should be studied.
- The SPSA solution algorithm was successfully applied to search for optimal ramp metering rates in the developed dynamic ramp metering model. Its efficiency should be compared with that of other algorithms such as fuzzy logic control and artificial neural networks.
- In this study, the performance of the control model was evaluated off-line with the use of simulation data. On-line control analysis and field implementation should be conducted to enhance the applicability and credibility of the developed model.
- Closure of an entrance ramp represents the most restrictive form of metering but is the least popular because of considerable public opposition. Closure may mitigate serious weaving problems. In this study, ramp closure was not considered as a control strategy. However, it should be analyzed while traffic diversion on local streets is considered.

APPENDIX A

FIGURES

Appendix A consists of study site photos presenting traffic and geometric situations, the overview figures of the modeling network, and the analysis figures of simulation results with and without metering control.



Figure A.1 Mainline I-80 (Route 513/Hibernia Avenue).



Figure A.2 Ramp 1 on I-80 (Route 513/Hibernia Avenue).



Figure A.3 Ramp 2 on I-80 (Route 513/Hibernia Avenue).



Figure A.4 Ramp on I-80 (Route 66/Mount Hope).



Figure A.5 Ramp 1 on I-80 (Route 615/Howard Boulevard).



Figure A.6 Ramp 2 on I-80 (Route 615/Howard Boulevard).

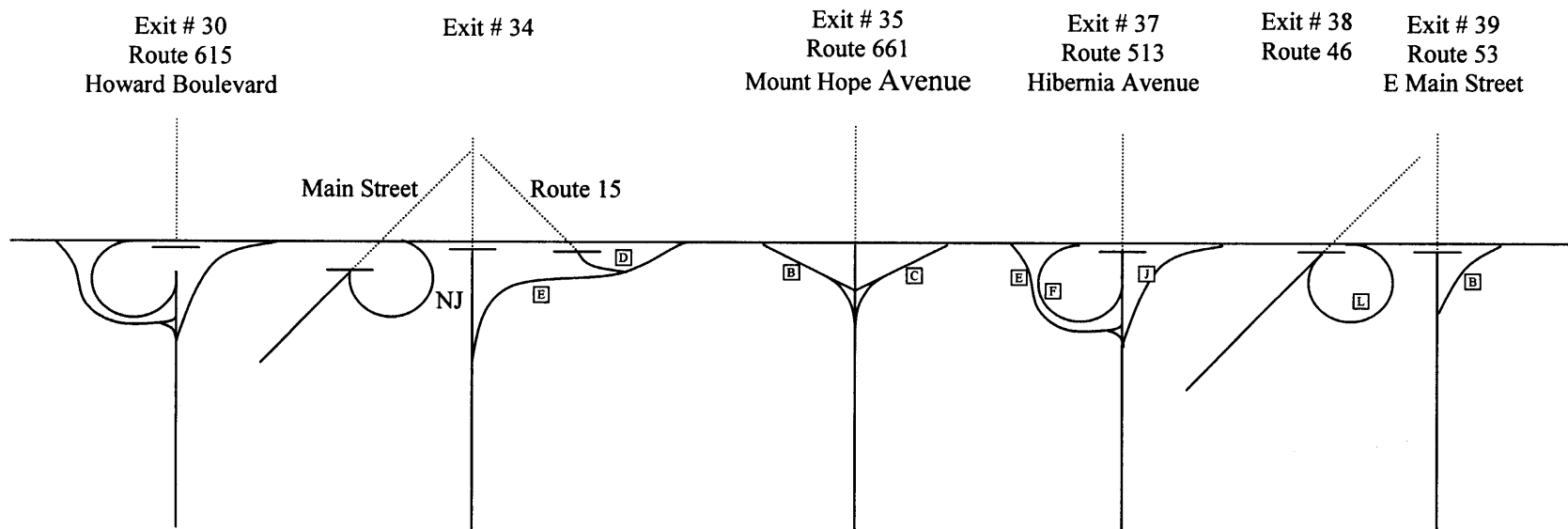


Figure A.7 Geometric diagram of eastbound I-80 mileposts 30 – 42.

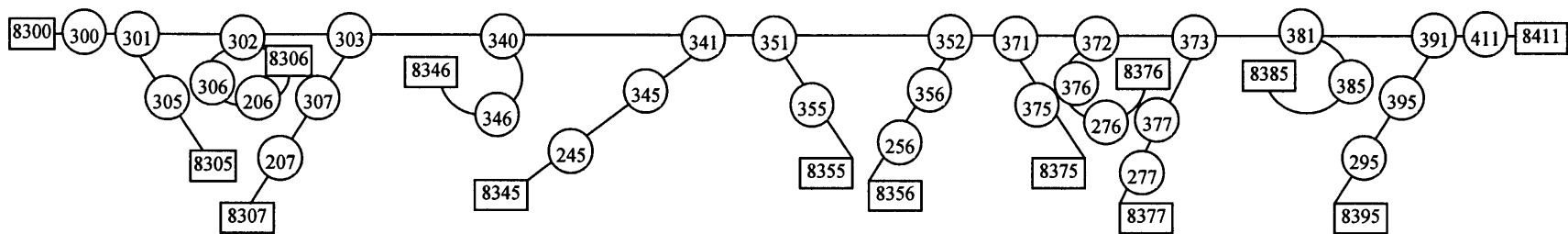


Figure A.8 Link – Node diagram converted from Figure A.7.

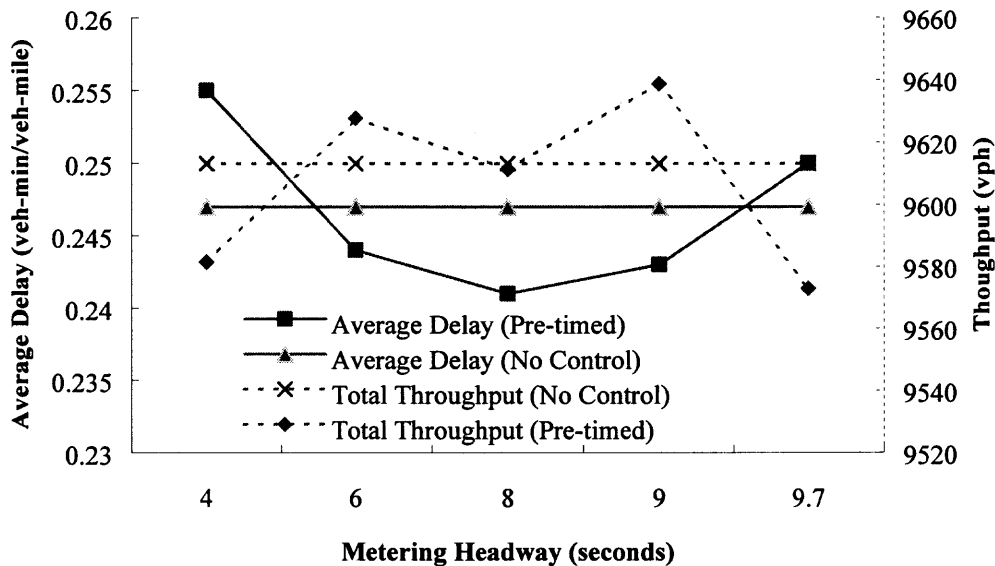


Figure A.9 Average delay and total throughput vs. metering headway (Pre-timed metering control at node 306).

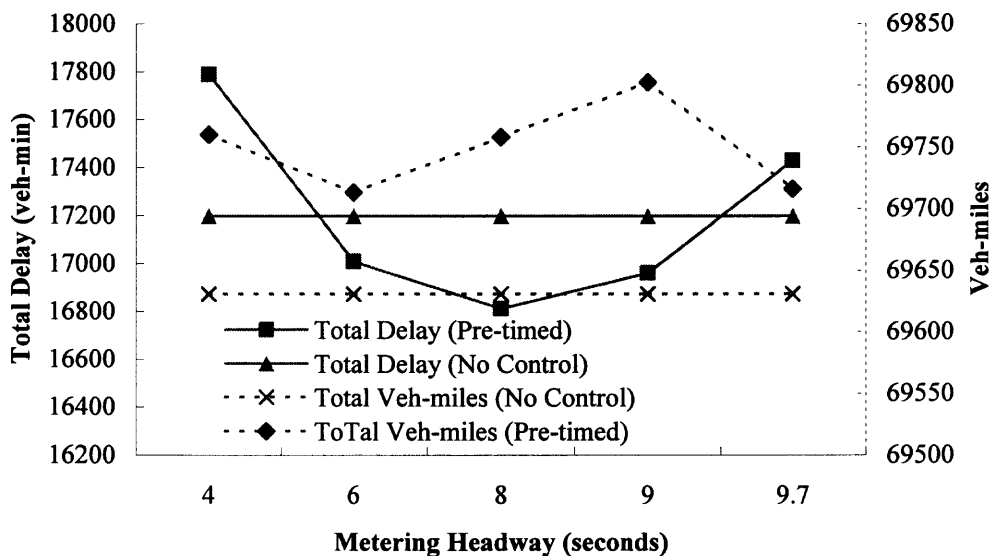


Figure A.10 Total delay and veh-miles vs. metering headway (Pre-timed metering control at node 306).

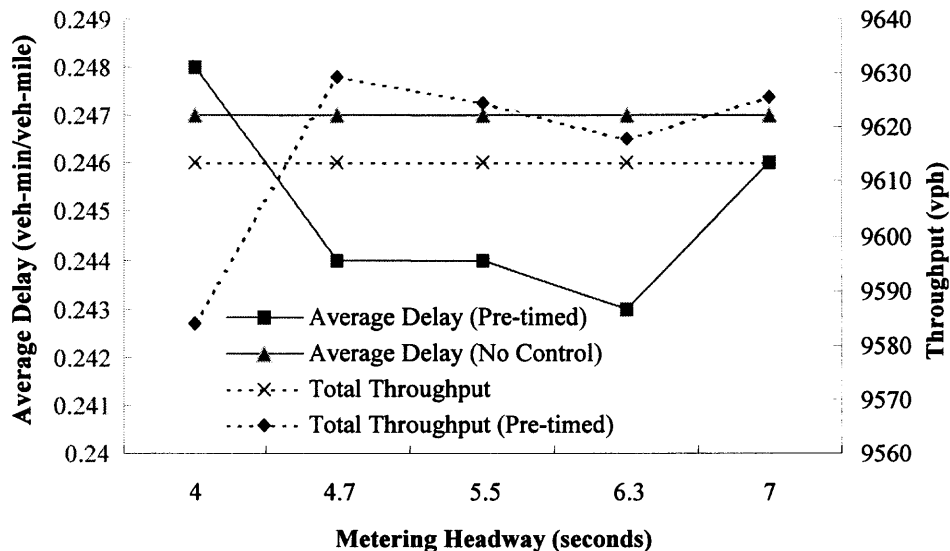


Figure A.11 Average delay and total throughput vs. metering headway (Pre-timed metering control at node 307).

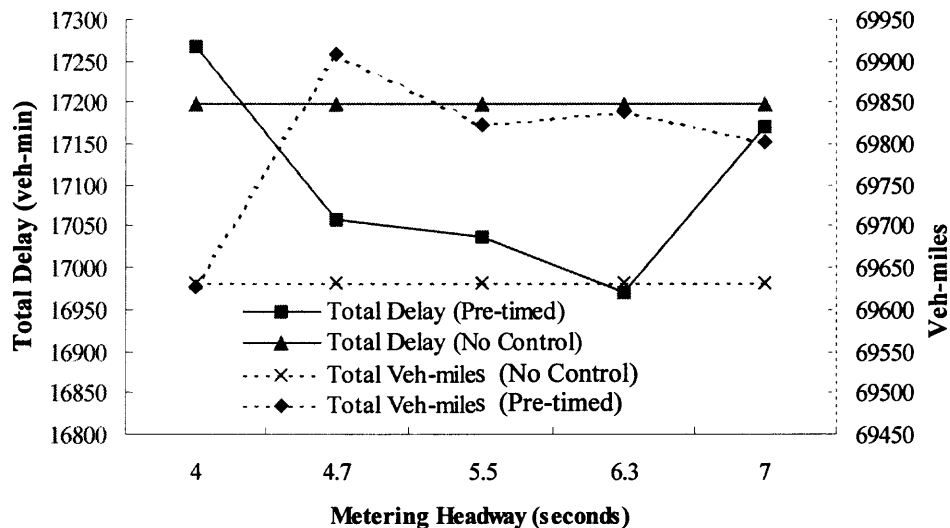


Figure A.12 Total delay and veh-miles vs. metering headway (Pre-timed metering control at node 307).

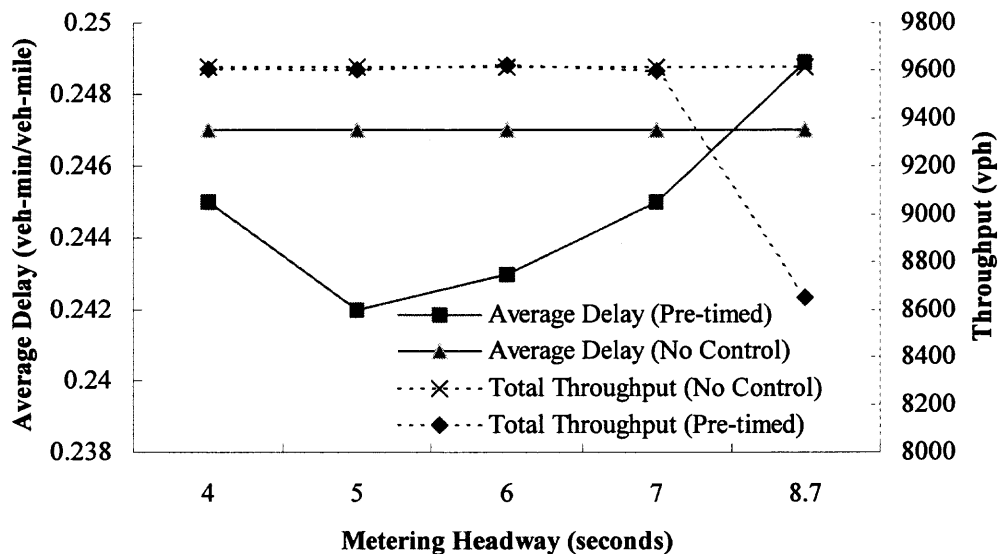


Figure A.13 Average delay and total throughput vs. metering headway (Pre-timed metering control at node 376).

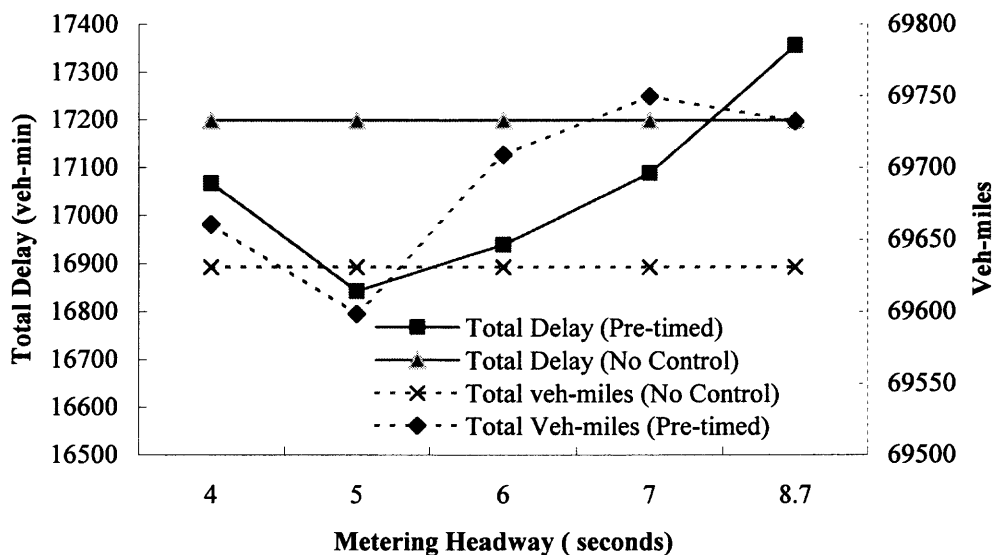


Figure A.14 Total delay and veh-mile vs. metering headway (Pre-timed metering control at node 376).

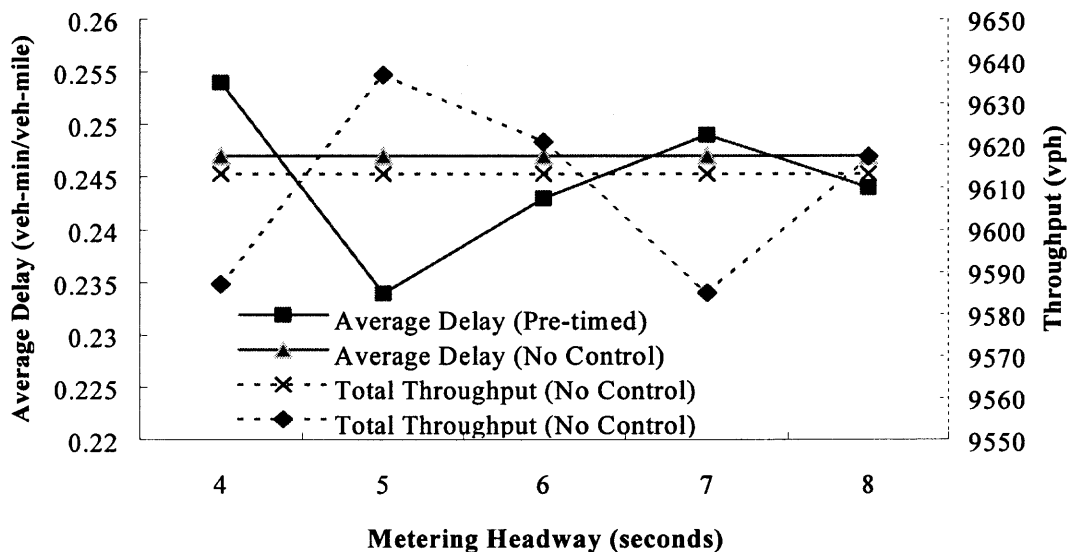


Figure A.15 Average delay and total throughput vs. metering headway (Pre-timed metering control at node 395).

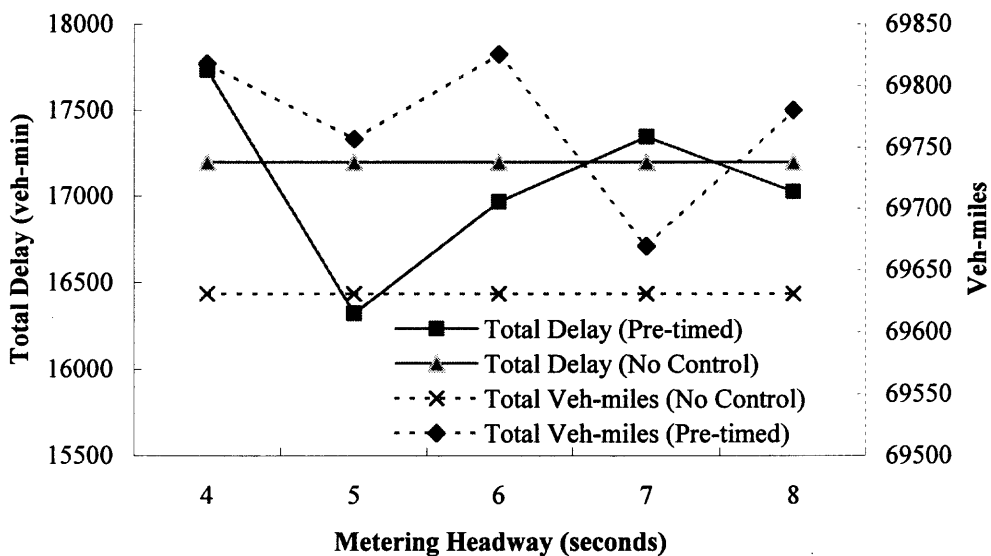


Figure A.16 Total delay and veh-miles vs. metering headway (Pre-timed metering control at node 395).

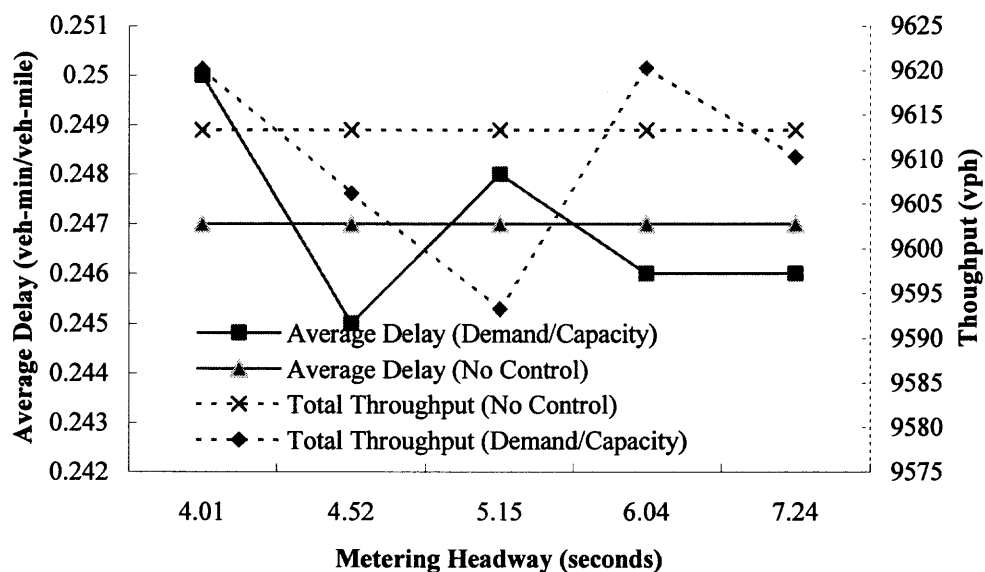


Figure A.17 Average delay and total throughput vs. metering headway (Demand/Capacity control at node 306).

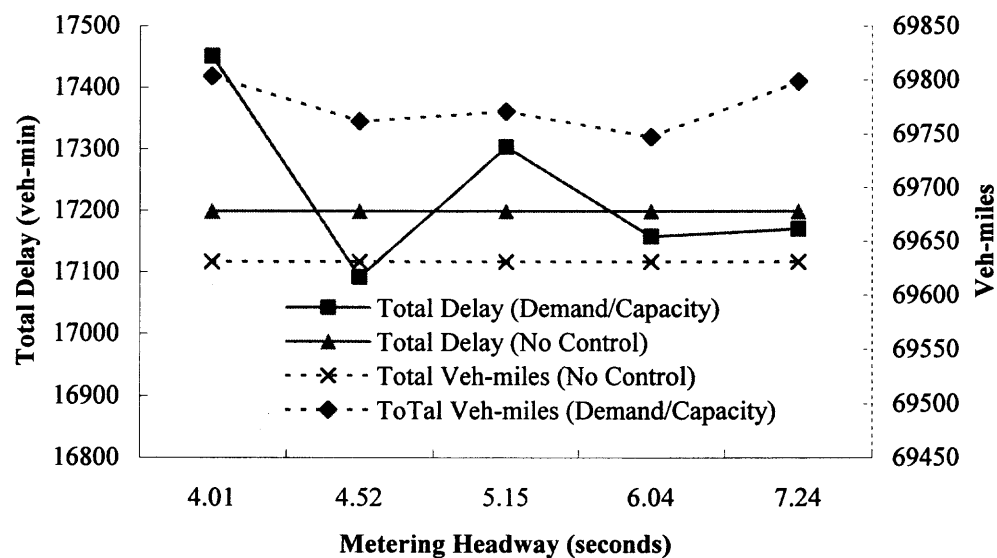


Figure A.18 Total delay and veh-miles vs. metering headway (Demand/Capacity control at node 306).

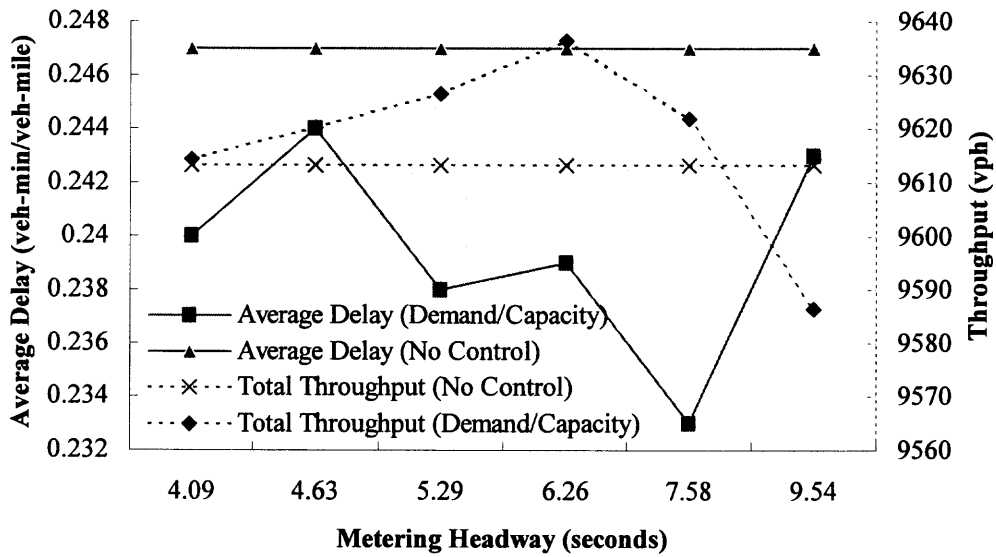


Figure A.19 Average delay and total throughput vs. metering headway (Demand/Capacity control at node 307).

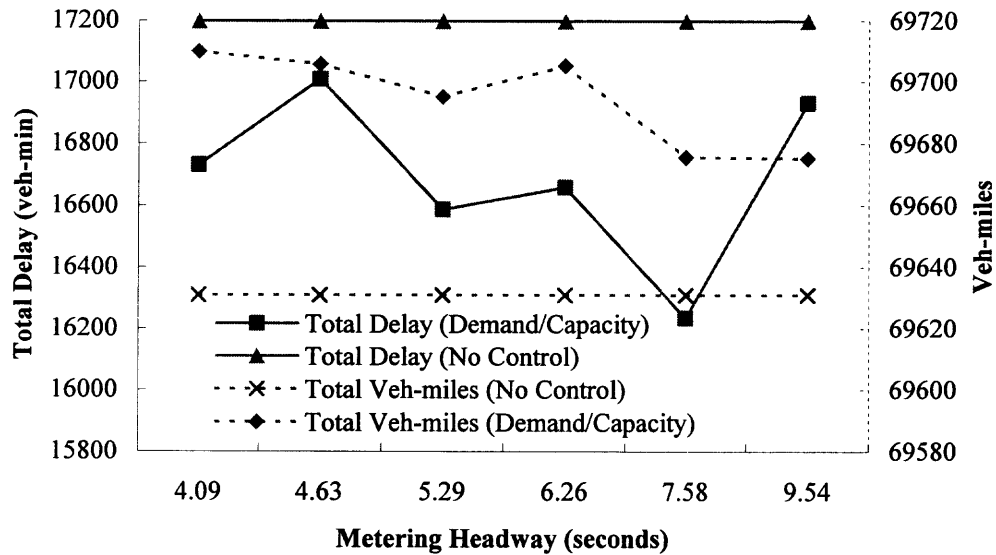


Figure A.20 Total delay and veh-miles vs. metering headway (Demand/Capacity control at node 307).

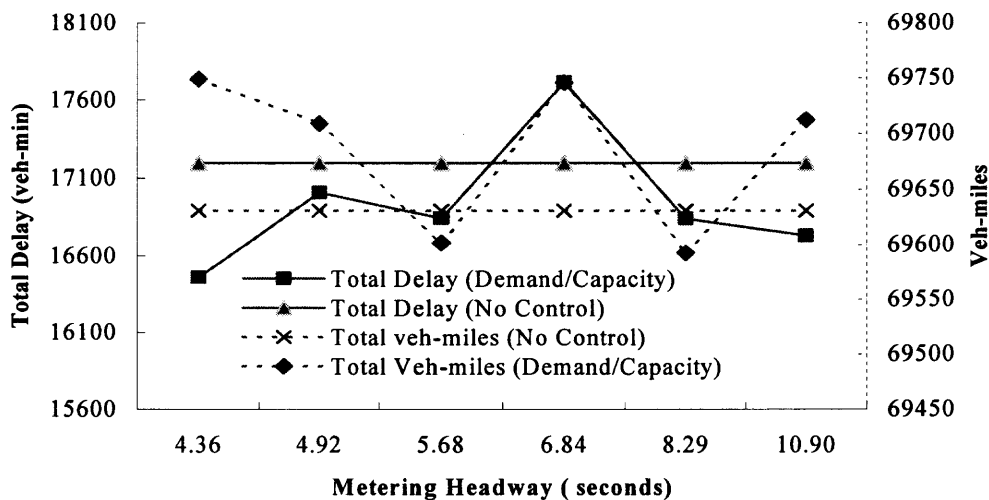


Figure A.21 Average delay and total throughput vs. metering headway (Demand/Capacity control at node 376).

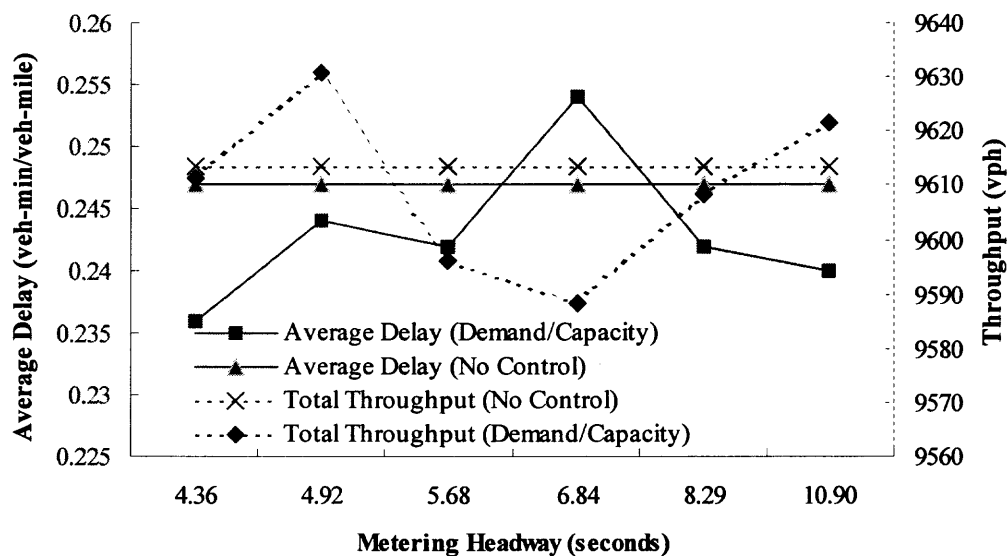


Figure A.22 Total delay and veh-miles vs. metering headway (Demand/Capacity control at node 376).

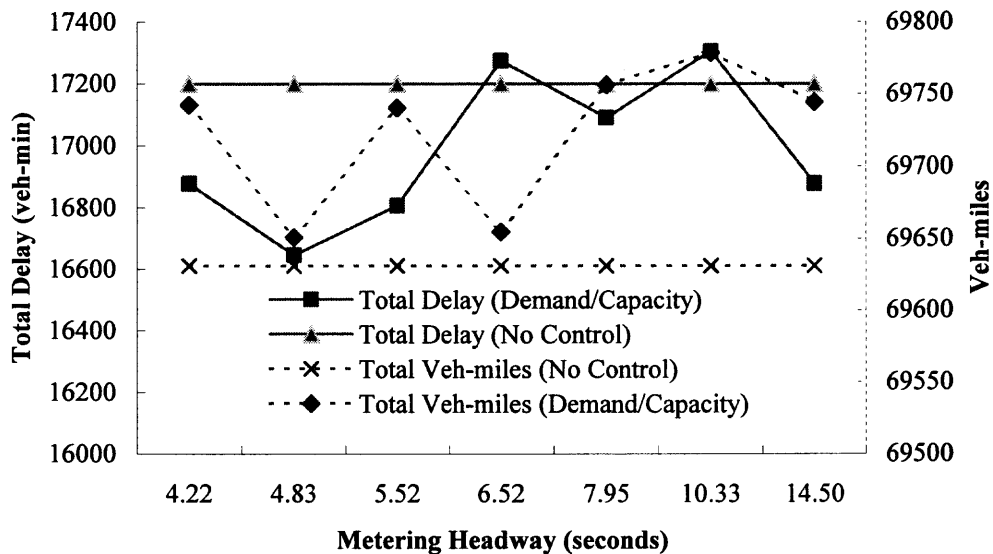


Figure A.23 Average delay and total throughput vs. metering headway (Demand/Capacity control at node 395).

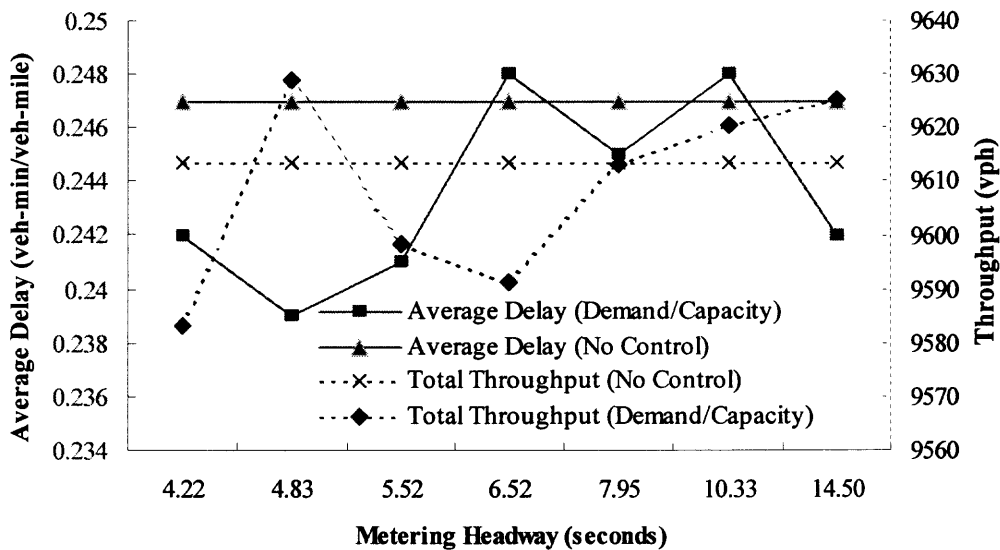


Figure A.24 Total delay and veh-miles vs. metering headway (Demand/Capacity control at node 395).

APPENDIX B
CORSIM INPUT FILES

In this Appendix, two typical CORSIM input files are listed. File 1 is the CORSIM model without ramp metering control, while File 2 is the CORSIM model with multiple ramp metering control. Detailed comments about the various components of the files are also included.

FILE 1: NO RAMP METERING CONTROL CORSIM MODEL

EVALUATION OF THE POTENTIAL FOR USING RAMP METERING
IN THE ATMS OF THE I-80 SHOWCASE CORRIDOR

SPONSOR
NEW JERSEY DEPARTMENT OF TRANSPORTATION

A Sample Comment for No Ramp Metering Control CORSIM Model
This data set introduces basic features of CORSIM and provides
comments of coding for the study site. This data set reflect
the real world case of I-80

```

8300--300--301-----302--303--340-----341--351-----352--
      \      /      /      \      /      \      /
      350    306  307    346    345    355    356
      \      /      /      \      /      \      /
      8305   206  207    8346   245    8355   256
      /      /      /      \      /      \      /
      8306  8307          8345          8356

--371-----372--373--381-----391--351--411--8411
  \      /      /      \      /      \      /
  375    376  377    385    395    355
  \      /      /      \      /      \      /
  8375   276  277    8385   295    8355
  /      /      /      \      /      \      /
  8376  8377          8395

```

Record Type 00 must be the first record type. These records are comment cards that include alphanumeric information that the user wants to print on the first page of the output report. To insert comment cards in the data set, use blank record types (i.e., Columns 78-80 are blanks).

Record Types 01 through 05 are called control records. These five records are required for each data set and entered only in the first time period.

Ramp Metering 03 25 01 Inst. of Trans., NJIT 1
by Noreen Zayas, Yuqing Ding, Jiangtao Luo and Xiaobo Liu

Record type 01 is the run identification card. It is used to indicate the use propose (e.g. Ramp Metering), date of run (3/25/01), name of the agency (e.g., Inst. of Trans., NJIT). Notice that 4 columns (45-48) are allocated for the year representation.

```
1 0 60 7981 10 0 0 0 8 000 7781 0721 2
```

Record type 02 is the run control card. The '1' in column 8 indicates that a simulation run will be performed. The '0' in column 12 indicates that off-line incident detection, point processing and MOE estimation are not

desired in this run. '60' is the maximum number of minutes of fill time prior to simulation. Simulation starts whether equilibrium is attained or not at the end of 60 minutes. Columns 22-29 (the '7981' in columns 26-29 ending with 1 is used to generate vehicle entry headway. The '10' in columns indicates fuel and emissions option for FRISIM. The '8' in column 52 specifies the model whose data appears after record type 02. The '8' denotes that the model is FRESIM. The '000' in columns 54-56 denotes the clock time (in military time) at the beginning of the simulation. Columns 61-68 ('7781), and 69-76 ('0721') provide the values for random number seeds.

180 180 180 180 180 180 180 180 180 180 180 180 180 180 180 180

3

Record type 03 gives the time period specifications. The '180' indicates the duration of the each time period. In this run there are 16 time periods.

180

4

Record type 04 indicates the duration of the time step and the time interval per time period. The '60' is the duration of the time interval. The time step duration is specified in columns 12 to 16. Since in this run it is blank, the default value of 1 second is used. Notice that when both the NETSIM and FRESIM models are used this entry must be left blank. The '180' in columns 17-20 indicates the time interval duration of 180 seconds (3 minutes). Time interval duration controls the frequency by which cumulative simulation statistical results can be obtained.

9

5

Record type 05 is the reports and graphics card. This card can be used to generate cumulative output and intermediate output.

In this test case, the FRESIM sub-network is coded first. Although the order in which sub-networks are input does not affect the simulation run, all of the records for a sub-network must be input in numerical order.

MP30-34 Mainline

8300 300 301	0 3	1	19
300 301 302 58080	3 92 400	1 9	19
301 302 303 13200	3	1	19
302 303 340 10560	3 91 400	1	19
303 340 341149420	3 91 400 92 400	1 9	19
MP34-42			
340 341 351 53700	3	1	19
341 351 352 29300	3 91 1000101 800 92 400	1 9	19
351 352 371 14700	4	1	19
352 371 372102000	4 91 510 92 510	1 9	19
371 372 373 10500	4	1	19
372 373 381 11000	4 91 640	1	19
373 381 391 57700	4 91 650 92 650	1 9	19
381 391 411 43260	4	1	19
391 4118411 62800	4 91 935	1	19
MP30-34 Ramps			
301 3058305 8451	1	1	19
8306 206 306	1 1	1	19
206 306 302 7291	1	1	19
306 302 303 4001	1	9	19

373	381	6000	65	5750	20
381	391	3500	65		20
391	411-2	5000	65		20
MP30-34 Ramp					
301	305	500	25		20
8306	206	600	25		20
206	306	600	25		20
306	302	600	25		20
8307	207		25		20
207	307	2500	25		20
307	303	2500	25		20
340	346	500	25		20
MP34-42 Ramp					
8345	245	1100	30		20
245	345	1100	40		20
345	341	1100	30		20
351	355	1100	30		20
8356	256		30		20
256	356		30		20
356	352		30		20
371	375		20		20
8376	276	350	20		20
276	376	350	20		20
376	372	350	20		20
8377	277	500	20		20
277	377	500	20		20
377	373	500	20		20
381	385	350	20		20
8395	295		25		20
295	395		25		20
395	391		25		20

Record Type 20 represents freeway link operations. A Record Type 20 is required for each link specified with a Record Type 19. Columns 1-4 include the link's upstream node number, and Columns 5-8 include the downstream node number. Columns 9-10, 11-12, and 13-16 specify the link's grade, super elevation, and radius of curvature, respectively. In this run, those columns were left blank, which indicates that default values are acceptable. Columns 21-22 show the desired free-flow speed (in miles per hour), which ranges from 20 to 65 mph in this run. Some of the links have an entry in Columns 29-33, which represents the distance (in feet) to the point at which drivers begin to react to the off-ramp exiting from this link. In FRESIM, this point is referred to as a warning sign. However, it does not mean the location of a physical sign. There is no entry if the link in question does not have an off-ramp destination.

MP30-34					
8300	300	301	100		25
300	301	302	94	305	6
301	305	8305	100		25
301	302	303	100		25
8306	206	306	100		25
206	306	302	100		25
302	303	340	100		25
8307	207	307	100		25
207	307	303	100		25
307	303	340	100		25
303	340	341	88	346	12
340	346	8346	100		25

8377 2771216 10 50
8395 295 430 9 50

Record Type 50 describes the traffic volume (in vehicles per hour) entering the FRESIM network. Columns 1-4 include the upstream node number, and columns 5-8 include the downstream node number. Columns 9-12 show the volume. The number in columns 13-16 specifies the percentage of trucks entering from the entry node.

130 120 110 100 90 80 70 60 50 40 68

Record Type 68 describes car-following sensitivity factor. The car-following model in FRESIM (the Pitt Car-Following Model) is based on the premise that drivers' desire to follow the car in front of them at a desired separation. In this example, there are 10 sensitivity factors from 130 to 40 (in hundredth of a second) for 10 driver types (Types 1 through 10). For instance, in this example, Columns 1-4 ('130') indicate that the new factor value is 130 hundredths of a second of ZFOLK(1) for driver type 1, while the '120' in Columns 5-8 indicate 120 hundredths of a second of ZFOLK(2) for driver type 2.

30 12 2 60 70

Record Type 70 describes lane change parameters, minimum separation for vehicle generation, and maximum non-emergency deceleration for FRESIM. The '30' in Columns 1-4 indicates the time (30 tenths of a second) to complete a lane change. The '12' in Columns 5-8 indicates the minimum separation (12 tenths of a second) for generation of vehicles. The '2' in Column 12 indicates that drivers need 2 seconds for collision avoidance. The '60' in Columns indicates that there are 60% of drivers desiring to yield the right-of-way to lane-changing vehicles attempting to merge ahead of them.

MP30-42 OD Table

300 301	6 300 340	11 300 351	3 300 371	5 300 381	6 300 411	69	74
302 340	13 302 351	2 302 371	5 302 381	6 302 411	74		74
303 340	14 303 351	2 303 371	5 303 381	6 303 411	73		74
341 351	8 341 371	6 341 381	7 341 411	79			74
352 371	8 352 381	8 352 411	84				74
372 381	12 372 411	88					74
373 381	12 373 411	88					74
391 411	100						74

Record Type 74s represent origin-destination. Columns 1-4 and 5-8 include the link's upstream and the downstream node number, respectively. All of these columns are described as follows:

Entry 1:

Column 1-4: origin node number

Entry 2:

Column 5-8: destination node number

Entry 3:

Column 11-12: percentage of vehicles that are entering through the origin node specified in Entry 1 and will travel to the destination node specified in Entry 2.

Entry 4-6:
 Column 13-24: Same as Entry 1-3 but for another
 O/D exchange

Entry 7-9:
 Column 25-36: Same as Entry 1-3 but for another
 O/D exchange

Entry 10-12:
 Column 37-38: Same as Entry 1-3 but for another
 O/D exchange

Entry 13-15:
 Column 49-60: Same as Entry 1-3 but for another
 O/D exchange

Entry 16-18:
 Column 61-72: Same as Entry 1-3 but for another
 O/D exchange

170

Record Type 170 is the sub-network delimiter. It indicates,
 in this case, the end of the FRESIM sub-network data.

2 2 2

172

Record Type 172 represent environmental tables.
 The '2' in Columns 1-4 indicates that HC emission rate in
 the table is be modified. The '2' in Columns 5-8 indicates
 the vehicle performance index. The '2' in Columns 9-12
 indicates the vehicle performance index 2 specified in
 Columns 5-8 had the same fuel or emission rate as another
 vehicle performance index.

MP30-42

8300			195
300	9016	7692	195
301	13549	9031	195
302	14753	9131	195
303	15900	9231	195
340	21427	10011	195
341	25430	9747	195
351	28353	10065	195
352	29805	10373	195
371	39915	11605	195
372	40880	11340	195
373	41614	10725	195
381	43528	6083	195
391	45754	3107	195
411	50392	671	195
8411			195
8305			195
305	13905	8621	195
8306	15173	8876	195
306	14572	8866	195
206	15050	8750	195
8307			195
207	15453	8804	195
307	15603	8974	195
346	21205	9230	195
8346			195
8345			195
245	24160	9255	195
345	25054	9680	195
355	28875	9851	195
8355			195

8356																			195
256	29310	9878																	195
356	29522	10090																	195
375	40330	10887																	195
8375																			195
8376																			195
276	40470	11048																	195
376	40594	11294																	195
8377																			195
277	41042	10886																	195
377	41391	10831																	195
385	43172	5863																	195
8385																			195
8395																			195
295	45259	3107																	195
395	45714	3107																	195

Record type 195, defines the node coordinates. Columns 1-4 denote the intersection node number. Columns 7-12 refer to the X coordinate and columns 15-20 indicate the Y coordinate.

300	301	2																	196
303	340	1																	196
340	341	2																	196
371	372	1																	196
372	373	1																	196
373	381	1																	196
381	391	2																	196
391	411	1																	196
301	305	2																	196
306	302	1																	196
206	306	1																	196
307	303	1																	196
207	307	1																	196
340	346	1																	196
345	341	1																	196
245	345	1																	196
351	355	1																	196
376	372	1																	196
276	376	1																	196
377	373	1																	196
277	377	1																	196
381	385	1																	196

Record Type 196s specify the optional geometric data. These records are needed to graphically depict curved links and overpasses. Columns 1-4 and 5-8 define the upstream and downstream node numbers, respectively. Column 12 defines the link curvature in the direction of flow along that link. A '1' indicates a clockwise curvature; a '2' indicates counterclockwise curvature; and a '0' indicates no curvature.

0	8																		210
---	---	--	--	--	--	--	--	--	--	--	--	--	--	--	--	--	--	--	-----

Record type 210 is the time period delimiter. The '0' in Columns 1-4 indicates that there is (are) other time period(s) follows. If '1' is in Columns 1-4, it indicates that this is the final time period and all simulation data have been entered. In the example, there are total 16 time periods.

0 8	210
MP30-34	
8300 300 301 100	25
300 301 302 94 305 6	25
301 3058305 100	25
301 302 303 100	25
8306 206 306 100	25
206 306 302 100	25
302 303 340 100	25
8307 207 307 100	25
207 307 303 100	25
307 303 340 100	25
303 340 341 88 346 12	25
340 3468346 100	25
MP34-42	
340 341 351 100	25
341 351 352 95 355 5	25
351 352 371 100	25
352 371 372 94 375 6	25
371 372 373 100	25
372 373 381 100	25
373 381 391 91 385 9	25
381 391 411 100	25
391 4118411 100	25
8345 245 345 100	25
245 345 341 100	25
345 341 351 100	25
351 3558355 100	25
8356 256 356 100	25
256 356 352 100	25
356 352 371 100	25
371 3758375 100	25
8376 276 376 100	25
276 376 372 100	25
376 372 373 100	25
8377 277 377 100	25
277 377 373 100	25
377 373 381 100	25
381 3858385 100	25
8395 295 395 100	25
295 395 391 100	25
395 391 411 100	25
Time Period 3	
MP30-34	
8300 3003326 6	50
8306 206 360 4	50
8307 207 489 8	50
MP34-42	
8345 2452159 9	50
8356 256 819 8	50
8376 276 400 5	50
8377 2771216 10	50
8395 295 430 9	50
MP30-42 OD Table	
300 301 6 300 340 11 300 351 3 300 371 5 300 381 6 300 411 69	74
302 340 13 302 351 2 302 371 5 302 381 6 302 411 74	74
303 340 14 303 351 2 303 371 5 303 381 6 303 411 73	74
341 351 8 341 371 6 341 381 7 341 411 79	74
352 371 8 352 381 8 352 411 84	74
372 381 12 372 411 88	74
373 381 12 373 411 88	74
391 411 100	74

0 8	170
MP30-34	210
8300 300 301 100	25
300 301 302 94 305 6	25
301 3058305 100	25
301 302 303 100	25
8306 206 306 100	25
206 306 302 100	25
302 303 340 100	25
8307 207 307 100	25
207 307 303 100	25
307 303 340 100	25
303 340 341 88 346 12	25
340 3468346 100	25
MP34-42	
340 341 351 100	25
341 351 352 95 355 5	25
351 352 371 100	25
352 371 372 94 375 6	25
371 372 373 100	25
372 373 381 100	25
373 381 391 91 385 9	25
381 391 411 100	25
391 4118411 100	25
8345 245 345 100	25
245 345 341 100	25
345 341 351 100	25
351 3558355 100	25
8356 256 356 100	25
256 356 352 100	25
356 352 371 100	25
371 3758375 100	25
8376 276 376 100	25
276 376 372 100	25
376 372 373 100	25
8377 277 377 100	25
277 377 373 100	25
377 373 381 100	25
381 3858385 100	25
8395 295 395 100	25
295 395 391 100	25
395 391 411 100	25
Time Period 4	
MP30-34	
8300 3003560 6	50
8306 206 360 4	50
8307 207 489 8	50
MP34-42	
8345 2452159 9	50
8356 256 819 8	50
8376 276 400 5	50
8377 2771216 10	50
8395 295 430 9	50
MP30-42 OD Table	
300 301 6 300 340 11 300 351 3 300 371 5 300 381 6 300 411 69	74
302 340 13 302 351 2 302 371 5 302 381 6 302 411 74	74
303 340 14 303 351 2 303 371 5 303 381 6 303 411 73	74
341 351 8 341 371 6 341 381 7 341 411 79	74
352 371 8 352 381 8 352 411 84	74
372 381 12 372 411 88	74
373 381 12 373 411 88	74

373 381 12 373 411 88	74
391 411 100	74
	170
0 8	210
MP30-34	
8300 300 301 100	25
300 301 302 94 305 6	25
301 3058305 100	25
301 302 303 100	25
8306 206 306 100	25
206 306 302 100	25
302 303 340 100	25
8307 207 307 100	25
207 307 303 100	25
307 303 340 100	25
303 340 341 88 346 12	25
340 3468346 100	25
MP34-42	
340 341 351 100	25
341 351 352 95 355 5	25
351 352 371 100	25
352 371 372 94 375 6	25
371 372 373 100	25
372 373 381 100	25
373 381 391 91 385 9	25
381 391 411 100	25
391 4118411 100	25
8345 245 345 100	25
245 345 341 100	25
345 341 351 100	25
351 3558355 100	25
8356 256 356 100	25
256 356 352 100	25
356 352 371 100	25
371 3758375 100	25
8376 276 376 100	25
276 376 372 100	25
376 372 373 100	25
8377 277 377 100	25
277 377 373 100	25
377 373 381 100	25
381 3858385 100	25
8395 295 395 100	25
295 395 391 100	25
395 391 411 100	25
Time Period 6	
MP30-34	
8300 3003960 6	50
8306 206 360 4	50
8307 207 489 8	50
MP34-42	
8345 2452159 9	50
8356 256 819 8	50
8376 276 400 5	50
8377 2771216 10	50
8395 295 430 9	50
MP30-42 OD Table	
300 301 6 300 340 11 300 351 3 300 371 5 300 381 6 300 411 69	74
302 340 13 302 351 2 302 371 5 302 381 6 302 411 74	74
303 340 14 303 351 2 303 371 5 303 381 6 303 411 73	74
341 351 8 341 371 6 341 381 7 341 411 79	74
352 371 8 352 381 8 352 411 84	74

372 381 12 372 411 88	74
373 381 12 373 411 88	74
391 411 100	74
0 8	170
MP30-34	210
8300 300 301 100	25
300 301 302 94 305 6	25
301 3058305 100	25
301 302 303 100	25
8306 206 306 100	25
206 306 302 100	25
302 303 340 100	25
8307 207 307 100	25
207 307 303 100	25
307 303 340 100	25
303 340 341 88 346 12	25
340 3468346 100	25
MP34-42	
340 341 351 100	25
341 351 352 95 355 5	25
351 352 371 100	25
352 371 372 94 375 6	25
371 372 373 100	25
372 373 381 100	25
373 381 391 91 385 9	25
381 391 411 100	25
391 4118411 100	25
8345 245 345 100	25
245 345 341 100	25
345 341 351 100	25
351 3558355 100	25
8356 256 356 100	25
256 356 352 100	25
356 352 371 100	25
371 3758375 100	25
8376 276 376 100	25
276 376 372 100	25
376 372 373 100	25
8377 277 377 100	25
277 377 373 100	25
377 373 381 100	25
381 3858385 100	25
8395 295 395 100	25
295 395 391 100	25
395 391 411 100	25
Time Period 7	
MP30-34	
8300 3004160 6	50
8306 206 360 4	50
8307 207 489 8	50
MP34-42	
8345 2452159 9	50
8356 256 819 8	50
8376 276 400 5	50
8377 2771216 10	50
8395 295 430 9	50
MP30-42 OD Table	
300 301 6 300 340 11 300 351 3 300 371 5 300 381 6 300 411 69	74
302 340 13 302 351 2 302 371 5 302 381 6 302 411 74	74
303 340 14 303 351 2 303 371 5 303 381 6 303 411 73	74
341 351 8 341 371 6 341 381 7 341 411 79	74

352 371	8	352 381	8	352 411	84	74						
372 381	12	372 411	88			74						
373 381	12	373 411	88			74						
391 411	100					74						
0	8					170						
MP30-34						210						
8300 300 301	100					25						
300 301 302	94	305	6			25						
301 3058305	100					25						
301 302 303	100					25						
8306 206 306	100					25						
206 306 302	100					25						
302 303 340	100					25						
8307 207 307	100					25						
207 307 303	100					25						
307 303 340	100					25						
303 340 341	88	346	12			25						
340 3468346	100					25						
MP34-42												
340 341 351	100					25						
341 351 352	95	355	5			25						
351 352 371	100					25						
352 371 372	94	375	6			25						
371 372 373	100					25						
372 373 381	100					25						
373 381 391	91	385	9			25						
381 391 411	100					25						
391 4118411	100					25						
8345 245 345	100					25						
245 345 341	100					25						
345 341 351	100					25						
351 3558355	100					25						
8356 256 356	100					25						
256 356 352	100					25						
356 352 371	100					25						
371 3758375	100					25						
8376 276 376	100					25						
276 376 372	100					25						
376 372 373	100					25						
8377 277 377	100					25						
277 377 373	100					25						
377 373 381	100					25						
381 3858385	100					25						
8395 295 395	100					25						
295 395 391	100					25						
395 391 411	100					25						
Time Period 8												
MP30-34												
8300 3004360	6					50						
8306 206 360	4					50						
8307 207 489	8					50						
MP34-42												
8345 2452159	9					50						
8356 256 819	8					50						
8376 276 400	5					50						
8377 2771216	10					50						
8395 295 430	9					50						
MP30-42 OD Table												
300 301	6	300 340	11	300 351	3	300 371	5	300 381	6	300 411	69	74
302 340	13	302 351	2	302 371	5	302 381	6	302 411	74			74
303 340	14	303 351	2	303 371	5	303 381	6	303 411	73			74

341 351	8	341 371	6	341 381	7	341 411	79	74				
352 371	8	352 381	8	352 411	84			74				
372 381	12	372 411	88					74				
373 381	12	373 411	88					74				
391 411	100							74				
								170				
0	8							210				
MP30-34												
8300 300 301	100							25				
300 301 302	94	305	6					25				
301 3058305	100							25				
301 302 303	100							25				
8306 206 306	100							25				
206 306 302	100							25				
302 303 340	100							25				
8307 207 307	100							25				
207 307 303	100							25				
307 303 340	100							25				
303 340 341	88	346	12					25				
340 3468346	100							25				
MP34-42												
340 341 351	100							25				
341 351 352	95	355	5					25				
351 352 371	100							25				
352 371 372	94	375	6					25				
371 372 373	100							25				
372 373 381	100							25				
373 381 391	91	385	9					25				
381 391 411	100							25				
391 4118411	100							25				
8345 245 345	100							25				
245 345 341	100							25				
345 341 351	100							25				
351 3558355	100							25				
8356 256 356	100							25				
256 356 352	100							25				
356 352 371	100							25				
371 3758375	100							25				
8376 276 376	100							25				
276 376 372	100							25				
376 372 373	100							25				
8377 277 377	100							25				
277 377 373	100							25				
377 373 381	100							25				
381 3858385	100							25				
8395 295 395	100							25				
295 395 391	100							25				
395 391 411	100							25				
Time Period 9												
MP30-34												
8300 3004560	6							50				
8306 206 360	4							50				
8307 207 489	8							50				
MP34-42												
8345 2452159	9							50				
8356 256 819	8							50				
8376 276 400	5							50				
8377 2771216	10							50				
8395 295 430	9							50				
MP30-42 OD Table												
300 301	6	300 340	11	300 351	3	300 371	5	300 381	6	300 411	69	74
302 340	13	302 351	2	302 371	5	302 381	6	302 411	74			74

303 340 14 303 351 2 303 371 5 303 381 6 303 411 73	74
341 351 8 341 371 6 341 381 7 341 411 79	74
352 371 8 352 381 8 352 411 84	74
372 381 12 372 411 88	74
373 381 12 373 411 88	74
391 411 100	74
0 8	170
MP30-34	210
8300 300 301 100	25
300 301 302 94 305 6	25
301 3058305 100	25
301 302 303 100	25
8306 206 306 100	25
206 306 302 100	25
302 303 340 100	25
8307 207 307 100	25
207 307 303 100	25
307 303 340 100	25
303 340 341 88 346 12	25
340 3468346 100	25
MP34-42	
340 341 351 100	25
341 351 352 95 355 5	25
351 352 371 100	25
352 371 372 94 375 6	25
371 372 373 100	25
372 373 381 100	25
373 381 391 91 385 9	25
381 391 411 100	25
391 4118411 100	25
8345 245 345 100	25
245 345 341 100	25
345 341 351 100	25
351 3558355 100	25
8356 256 356 100	25
256 356 352 100	25
356 352 371 100	25
371 3758375 100	25
8376 276 376 100	25
276 376 372 100	25
376 372 373 100	25
8377 277 377 100	25
277 377 373 100	25
377 373 381 100	25
381 3858385 100	25
8395 295 395 100	25
295 395 391 100	25
395 391 411 100	25
Time Period 10	
MP30-34	
8300 3004760 6	50
8306 206 360 4	50
8307 207 489 8	50
MP34-42	
8345 2452159 9	50
8356 256 819 8	50
8376 276 400 5	50
8377 2771216 10	50
8395 295 430 9	50
MP30-42 OD Table	
300 301 6 300 340 11 300 351 3 300 371 5 300 381 6 300 411 69	74

302 340 13 302 351 2 302 371 5 302 381 6 302 411 74	74
303 340 14 303 351 2 303 371 5 303 381 6 303 411 73	74
341 351 8 341 371 6 341 381 7 341 411 79	74
352 371 8 352 381 8 352 411 84	74
372 381 12 372 411 88	74
373 381 12 373 411 88	74
391 411 100	74
0 8	170
MP30-34	210
8300 300 301 100	25
300 301 302 94 305 6	25
301 3058305 100	25
301 302 303 100	25
8306 206 306 100	25
206 306 302 100	25
302 303 340 100	25
8307 207 307 100	25
207 307 303 100	25
307 303 340 100	25
303 340 341 88 346 12	25
340 3468346 100	25
MP34-42	
340 341 351 100	25
341 351 352 95 355 5	25
351 352 371 100	25
352 371 372 94 375 6	25
371 372 373 100	25
372 373 381 100	25
373 381 391 91 385 9	25
381 391 411 100	25
391 4118411 100	25
8345 245 345 100	25
245 345 341 100	25
345 341 351 100	25
351 3558355 100	25
8356 256 356 100	25
256 356 352 100	25
356 352 371 100	25
371 3758375 100	25
8376 276 376 100	25
276 376 372 100	25
376 372 373 100	25
8377 277 377 100	25
277 377 373 100	25
377 373 381 100	25
381 3858385 100	25
8395 295 395 100	25
295 395 391 100	25
395 391 411 100	25
Time Period 11	
MP30-34	
8300 3004960 6	50
8306 206 360 4	50
8307 207 489 8	50
MP34-42	
8345 2452159 9	50
8356 256 819 8	50
8376 276 400 5	50
8377 2771216 10	50
8395 295 430 9	50

MP30-42 OD Table

300 301	6 300 340	11 300 351	3 300 371	5 300 381	6 300 411	69	74
302 340	13 302 351	2 302 371	5 302 381	6 302 411	74		74
303 340	14 303 351	2 303 371	5 303 381	6 303 411	73		74
341 351	8 341 371	6 341 381	7 341 411	79			74
352 371	8 352 381	8 352 411	84				74
372 381	12 372 411	88					74
373 381	12 373 411	88					74
391 411	100						74
							170
0	8						210
MP30-34							
8300	300 301	100					25
300	301 302	94 305	6				25
301	3058305	100					25
301	302 303	100					25
8306	206 306	100					25
206	306 302	100					25
302	303 340	100					25
8307	207 307	100					25
207	307 303	100					25
307	303 340	100					25
303	340 341	88 346	12				25
340	3468346	100					25
MP34-42							
340	341 351	100					25
341	351 352	95 355	5				25
351	352 371	100					25
352	371 372	94 375	6				25
371	372 373	100					25
372	373 381	100					25
373	381 391	91 385	9				25
381	391 411	100					25
391	4118411	100					25
8345	245 345	100					25
245	345 341	100					25
345	341 351	100					25
351	3558355	100					25
8356	256 356	100					25
256	356 352	100					25
356	352 371	100					25
371	3758375	100					25
8376	276 376	100					25
276	376 372	100					25
376	372 373	100					25
8377	277 377	100					25
277	377 373	100					25
377	373 381	100					25
381	3858385	100					25
8395	295 395	100					25
295	395 391	100					25
395	391 411	100					25
Time Period 12							
MP30-34							
8300	3005160	6					50
8306	206 360	4					50
8307	207 489	8					50
MP34-42							
8345	2452159	9					50
8356	256 819	8					50
8376	276 400	5					50
8377	2771216	10					50
8395	295 430	9					50

MP30-42 OD Table

300 301 6 300 340 11 300 351 3 300 371 5 300 381 6 300 411 69	74
302 340 13 302 351 2 302 371 5 302 381 6 302 411 74	74
303 340 14 303 351 2 303 371 5 303 381 6 303 411 73	74
341 351 8 341 371 6 341 381 7 341 411 79	74
352 371 8 352 381 8 352 411 84	74
372 381 12 372 411 88	74
373 381 12 373 411 88	74
391 411 100	74
	170
0 8	210
MP30-34	
8300 300 301 100	25
300 301 302 94 305 6	25
301 3058305 100	25
301 302 303 100	25
8306 206 306 100	25
206 306 302 100	25
302 303 340 100	25
8307 207 307 100	25
207 307 303 100	25
307 303 340 100	25
303 340 341 88 346 12	25
340 3468346 100	25
MP34-42	
340 341 351 100	25
341 351 352 95 355 5	25
351 352 371 100	25
352 371 372 94 375 6	25
371 372 373 100	25
372 373 381 100	25
373 381 391 91 385 9	25
381 391 411 100	25
391 4118411 100	25
8345 245 345 100	25
245 345 341 100	25
345 341 351 100	25
351 3558355 100	25
8356 256 356 100	25
256 356 352 100	25
356 352 371 100	25
371 3758375 100	25
8376 276 376 100	25
276 376 372 100	25
376 372 373 100	25
8377 277 377 100	25
277 377 373 100	25
377 373 381 100	25
381 3858385 100	25
8395 295 395 100	25
295 395 391 100	25
395 391 411 100	25
Time Period 13	
MP30-34	
8300 3005360 6	50
8306 206 360 4	50
8307 207 489 8	50
MP34-42	
8345 2452159 9	50
8356 256 819 8	50
8376 276 400 5	50
8377 2771216 10	50
8395 295 430 9	50

MP30-42 OD Table

300 301 6 300 340 11 300 351 3 300 371 5 300 381 6 300 411 69	74
302 340 13 302 351 2 302 371 5 302 381 6 302 411 74	74
303 340 14 303 351 2 303 371 5 303 381 6 303 411 73	74
341 351 8 341 371 6 341 381 7 341 411 79	74
352 371 8 352 381 8 352 411 84	74
372 381 12 372 411 88	74
373 381 12 373 411 88	74
391 411 100	74
0 8	170
	210
MP30-34	
8300 300 301 100	25
300 301 302 94 305 6	25
301 3058305 100	25
301 302 303 100	25
8306 206 306 100	25
206 306 302 100	25
302 303 340 100	25
8307 207 307 100	25
207 307 303 100	25
307 303 340 100	25
303 340 341 88 346 12	25
340 3468346 100	25
MP34-42	
340 341 351 100	25
341 351 352 95 355 5	25
351 352 371 100	25
352 371 372 94 375 6	25
371 372 373 100	25
372 373 381 100	25
373 381 391 91 385 9	25
381 391 411 100	25
391 4118411 100	25
8345 245 345 100	25
245 345 341 100	25
345 341 351 100	25
351 3558355 100	25
8356 256 356 100	25
256 356 352 100	25
356 352 371 100	25
371 3758375 100	25
8376 276 376 100	25
276 376 372 100	25
376 372 373 100	25
8377 277 377 100	25
277 377 373 100	25
377 373 381 100	25
381 3858385 100	25
8395 295 395 100	25
295 395 391 100	25
395 391 411 100	25
Time Period 14	
MP30-34	
8300 3005560 6	50
8306 206 360 4	50
8307 207 489 8	50
MP34-42	
8345 2452159 9	50
8356 256 819 8	50
8376 276 400 5	50
8377 2771216 10	50

8395 295 430 9	50
MP30-42 OD Table	
300 301 6 300 340 11 300 351 3 300 371 5 300 381 6 300 411 69	74
302 340 13 302 351 2 302 371 5 302 381 6 302 411 74	74
303 340 14 303 351 2 303 371 5 303 381 6 303 411 73	74
341 351 8 341 371 6 341 381 7 341 411 79	74
352 371 8 352 381 8 352 411 84	74
372 381 12 372 411 88	74
373 381 12 373 411 88	74
391 411 100	74
	170
0 8	210
MP30-34	
8300 300 301 100	25
300 301 302 94 305 6	25
301 3058305 100	25
301 302 303 100	25
8306 206 306 100	25
206 306 302 100	25
302 303 340 100	25
8307 207 307 100	25
207 307 303 100	25
307 303 340 100	25
303 340 341 88 346 12	25
340 3468346 100	25
MP34-42	
340 341 351 100	25
341 351 352 95 355 5	25
351 352 371 100	25
352 371 372 94 375 6	25
371 372 373 100	25
372 373 381 100	25
373 381 391 91 385 9	25
381 391 411 100	25
391 4118411 100	25
8345 245 345 100	25
245 345 341 100	25
345 341 351 100	25
351 3558355 100	25
8356 256 356 100	25
256 356 352 100	25
356 352 371 100	25
371 3758375 100	25
8376 276 376 100	25
276 376 372 100	25
376 372 373 100	25
8377 277 377 100	25
277 377 373 100	25
377 373 381 100	25
381 3858385 100	25
8395 295 395 100	25
295 395 391 100	25
395 391 411 100	25
Time Period 15	
MP30-34	
8300 3005760 6	50
8306 206 360 4	50
8307 207 489 8	50
MP34-42	
8345 2452159 9	50
8356 256 819 8	50
8376 276 400 5	50

8376 276 400	5	50
8377 2771216	10	50
8395 295 430	9	50
MP30-42 OD Table		
300 301 6 300 340 11 300 351 3 300 371 5 300 381 6 300 411 69		74
302 340 13 302 351 2 302 371 5 302 381 6 302 411 74		74
303 340 14 303 351 2 303 371 5 303 381 6 303 411 73		74
341 351 8 341 371 6 341 381 7 341 411 79		74
352 371 8 352 381 8 352 411 84		74
372 381 12 372 411 88		74
373 381 12 373 411 88		74
391 411 100		74
		170
		210
1		

FILE 2: MULTIPLE RAMPS METERING CONTROL CORSIM MODEL

EVALUATION OF THE POTENTIAL FOR USING RAMP METERING
IN THE ATMS OF THE I-80 SHOWCASE CORRIDOR

SPONSOR
NEW JERSEY DEPARTMENT OF TRANSPORTATION

A Sample Comment for Multiple Ramps Metering Control CORSIM Model
This data set introduces basic features of CORSIM and provides
comments of coding for the study site. This data set reflect
the real world case of I-80

```

8300--300--301-----302---303--340-----341--351-----352--
      \      /      /      \      /      \      /
      350    306  307    346    345    355    356
      \      /      /      \      /      \      /
      8305  206  207    8346  245    8355  256
      /      /      /      /      /      /
      8306  8307          8345          8356

--371-----372---373--381-----391--351--411--8411
  \      /      /      \      /      \      /
  375    376  377    385    395    355
  \      /      /      \      /      \      /
  8375  276  277    8385  295    8355
  /      /      /      /      /
  8376  8377          8395

```

Record Type 00 must be the first record types. These records are comment cards that include alphanumeric information that the user wants to print on the first page of the output report. To insert comment cards in the data set, use blank record types (i.e., Columns 78-80 are blanks).

Record Types 01 through 05 are called control records. These five records are required for each data set and entered only in the first time period.

Ramp Metering 03 25 01 Inst. of Trans., NJIT 1
by Noreen Zayas, Yuqing Ding, Jiangtao Luo and Xiaobo Liu

Record type 01 is the run identification card. It is used to indicate the use propose (e.g. Ramp Metering), date of run (3/25/01), name of the agency (e.g., Inst. of Trans., NJIT). Notice that 4 columns (45-48) are allocated for the year representation.

1 0 60 7981 10 0 0 0 8 000 7781 0721 2

Record type 02 is the run control card. The '1' in column 8 indicates that a simulation run will be performed. The '0' in column 12 indicates that off-line incident detection, point processing and MOE estimation are not desired in this run. '60' is the maximum number of minutes of fill time prior to simulation. Simulation starts

whether equilibrium is attained or not at the end of 60 minutes. Columns 22-29 (the '7981' in columns 26-29 ending with 1 is used to generate vehicle entry headway. The '10' in columns indicates fuel and emissions option for FRISIM. The '8' in column 52 specifies the model whose data appears after record type 02. The '8' denotes that the model is FRESIM. The '000' in columns 54-56 denotes the clock time (in military time) at the beginning of the simulation. Columns 61-68 ('7781), and 69-76 ('0721') provide the values for random number seeds.

180 180 180 180 180 180 180 180 180 180 180 180 180 180 180 180 180 180 180 180

3

Record type 03 gives the time period specifications. The '180' indicates the duration of the each time period. In this run there is 16 time period.

180

4

Record type 04 indicates the duration of the time step and the time interval per time period. The '60' is the duration of the time interval. The time step duration is specified in columns 12 to 16. Since in this run it is blank, the default value of 1 second is used. Notice that when both the NETSIM and FRESIM models are used this entry must be left blank. The '180' in columns 17-20 indicates the time interval duration of 180 seconds (3 minutes). Time interval duration controls the frequency by which cumulative simulation statistical results can be obtained.

9

5

Record type 05 is the reports and graphics card. This card can be used to generate cumulative output and intermediate output.

In this test case, the FRESIM sub-network is coded first. Although the order in which sub-networks are input does not affect the simulation run, all of the records for a sub-network must be input in numerical order.

MP30-34 Mainline

8300 300 301	0 3	1	19
300 301 302 58080	3 92 400	1 9	19
301 302 303 13200	3	1	19
302 303 340 10560	3 91 400	1	19
303 340 341149420	3 91 400 92 400	1 9	19
MP34-42			
340 341 351 53700	3	1	19
341 351 352 29300	3 91 1000101 800 92 400	1 9	19
351 352 371 14700	4	1	19
352 371 372102000	4 91 510 92 510	1 9	19
371 372 373 10500	4	1	19
372 373 381 11000	4 91 640	1	19
373 381 391 57700	4 91 650 92 650	1 9	19
381 391 411 43260	4	1	19
391 4118411 62800	4 91 935	1	19
MP30-34 Ramps			
301 3058305	8451 1	1	19
8306 206 306	1 1	1	19
206 306 302 7291	1	1	19
306 302 303 4001	1	9	19
8307 207 307	1 1	1	19
207 307 303 3871	1	1	19

307 303 340	4001 1	9	19
340 3468346	11921 1	1	19
MP34-42			
8345 245 345	1 2	1	19
245 345 341	12501 2	1	19
345 341 351	4001 2	10	19
351 3558355	6001 1	1	19
8356 256 356	1 1	1	19
256 356 352	3001 1	1	19
356 352 371	4001 1	9	19
371 3758375	8291 1	1	19
8376 276 376	1 1	1	19
276 376 372	4751 1	1	19
376 372 373	3301 1	9	19
8377 277 377	1 1	1	19
277 377 373	5501 1	1	19
377 373 381	3201 1	9	19
381 3858385	6531 1	1	19
8395 295 395	1 1	1	19
295 395 391	4551 1	1	19
395 391 411	401 1	9	19

Record type 19 is the link description card for the FRESIM model. One record type is required for each link. The entry and exit nodes are denoted by numbers between 8000 and 8999 (both inclusive). The upstream node number of the subject link is specified in columns 1-4 and the downstream node number is given in columns 5-8. The node that receives through traffic from the subject link is given in columns 9-12. Link lengths are indicated in columns 13-17. Link lengths are not specified for entry links. Column 20 indicates the number of through lanes in the link. Column 22 is the identification code for the first auxiliary lane. A '9' in that column represents the first auxiliary right lane. Column 23 indicates the lane type code for the specified auxiliary lane. A '1' specifies an acceleration lane, '2' specifies a deceleration lane, and a '3' specifies a full length auxiliary lane. Columns 24-28 indicate the length of the auxiliary lane. If another auxiliary lane exists, then the information is given in columns 29-44. Columns 45-46 denote the lane on the immediate downstream link that receives through traffic from lane 1 of the subject link represented in columns 1-8. Columns 47-48 denote the lane of the subject link that feeds lane 1 of the downstream off-ramp, if one exists. If there is no off-ramp it should be left blank.

MP30-34 Mainline

8300 300	65		20	
300 301 1	5000	65	5800	20
301 302	65			20
302 303	65			20
303 340	7500	65	14902	20

MP34-42 Mainline

340 341	7500	65		20
341 351		65	2920	20
351 352 2		65		20
352 371 1		65	5280	20
371 372-2	2000	65		20
372 373	2000	65		20
373 381	6000	65	5750	20
381 391	3500	65		20

341 351 352 95 355 5	25
351 352 371 100	25
352 371 372 94 375 6	25
371 372 373 100	25
372 373 381 100	25
373 381 391 91 385 9	25
381 391 411 100	25
391 411 8411 100	25
8345 245 345 100	25
245 345 341 100	25
345 341 351 100	25
351 355 8355 100	25
8356 256 356 100	25
256 356 352 100	25
356 352 371 100	25
371 375 8375 100	25
8376 276 376 100	25
276 376 372 100	25
376 372 373 100	25
8377 277 377 100	25
277 377 373 100	25
377 373 381 100	25
381 385 8385 100	25
8395 295 395 100	25
295 395 391 100	25
395 391 411 100	25

Record Type 25 specifies freeway turn movements. Columns 1-4 include the link's upstream node number, and columns 5-8 include the downstream node number. Columns 9-12 show the downstream node number that receives through traffic from the subject link. Columns 13-16 show the percentage of vehicles that make the through movement. For this example, 94% of the vehicles on freeway link (300,301) are going through. The remainder (6%) will exit to node 305, which leads to an off-ramp.

341 351 1 1 800	32
-----------------	----

Record Type 32 specifies the adding and/or dropping of freeway lanes. They must be specified wherever a through lane is added or dropped. Columns 1-4 include the link's upstream node number, and columns 5-8 include the downstream node number. A '1' in column 12 indicates a lane add (a '2' indicates a lane drop). The entry in column 14 is the identification number for the lane being added or dropped. Columns 17-21 specify the distance from the upstream node to the end of the lane drop or the beginning of the lane add. For link (341,351), lane 1 is being added, 800 feet from node 341.

Time Period 1	
306 1 0 55	37
307 1 0 47	37
345 1 0 97	
356 1 0 40	37
376 1 0 48	37
377 1 0 97	
395 1 0 45	37

Record Type 37 specifies freeway ramp metering control. One type of ramp metering control strategies is coded in this test case: pre-timed time (clock time).

372	381	12	372	411	88	74
373	381	12	373	411	88	74
391	411	100				74

Record Type 74s represent origin-destination. Columns 1-4 and 5-8 include the link's upstream and the downstream node number, respectively. All of these columns are described as follows:

Entry 1:
Column 1-4: origin node number

Entry 2:
Column 5-8: destination node number

Entry 3:
Column 11-12: percentage of vehicles that are entering through the origin node specified in Entry 1 and will travel to the destination node specified in Entry 2.

Entry 4-6:
Column 13-24: Same as Entry 1-3 but for another O/D exchange

Entry 7-9:
Column 25-36: Same as Entry 1-3 but for another O/D exchange

Entry 10-12:
Column 37-38: Same as Entry 1-3 but for another O/D exchange

Entry 13-15:
Column 49-60: Same as Entry 1-3 but for another O/D exchange

Entry 16-18:
Column 61-72: Same as Entry 1-3 but for another O/D exchange

170

Record Type 170 is the sub-network delimiter. It indicates, in this case, the end of the FRESIM sub-network data.

2	2	2
---	---	---

172

Record Type 172 represent environmental tables. The '2' in Columns 1-4 indicates that HC emission rate in the table is be modified. The '2' in Columns 5-8 indicates the vehicle performance index. The '2' in Columns 9-12 indicates the vehicle performance index 2 specified in Columns 5-8 had the same fuel or emission rate as another vehicle performance index.

MP30-42

8300			195
300	9016	7692	195
301	13549	9031	195
302	14753	9131	195
303	15900	9231	195
340	21427	10011	195
341	25430	9747	195
351	28353	10065	195
352	29805	10373	195
371	39915	11605	195
372	40880	11340	195
373	41614	10725	195

381	43528	6083	195
391	45754	3107	195
411	50392	671	195
8411			195
8305			195
305	13905	8621	195
8306	15173	8876	195
306	14572	8866	195
206	15050	8750	195
8307			195
207	15453	8804	195
307	15603	8974	195
346	21205	9230	195
8346			195
8345			195
245	24160	9255	195
345	25054	9680	195
355	28875	9851	195
8355			195
8356			195
256	29310	9878	195
356	29522	10090	195
375	40330	10887	195
8375			195
8376			195
276	40470	11048	195
376	40594	11294	195
8377			195
277	41042	10886	195
377	41391	10831	195
385	43172	5863	195
8385			195
8395			195
295	45259	3107	195
395	45714	3107	195

Record type 195, defines the node coordinates. Columns 1-4 denote the intersection node number. Columns 7-12 refer to the X coordinate and columns 15-20 indicate the Y coordinate.

300	301	2	196
303	340	1	196
340	341	2	196
371	372	1	196
372	373	1	196
373	381	1	196
381	391	2	196
391	411	1	196
301	305	2	196
306	302	1	196
206	306	1	196
307	303	1	196
207	307	1	196
340	346	1	196
345	341	1	196
245	345	1	196
351	355	1	196
376	372	1	196
276	376	1	196
377	373	1	196
277	377	1	196
381	385	1	196

377 373 381 100	25
381 3858385 100	25
8395 295 395 100	25
295 395 391 100	25
395 391 411 100	25
Time Period 3	
306 1 360 55	37
307 1 360 47	37
345 1 0 97	
356 1 360 40	37
376 1 360 48	37
377 1 0 97	
395 1 360 45	37
MP30-34	
8300 3003326 6	50
8306 206 360 4	50
8307 207 489 8	50
MP34-42	
8345 2452159 9	50
8356 256 819 8	50
8376 276 400 5	50
8377 2771216 10	50
8395 295 430 9	50
MP30-42 OD Table	
300 301 6 300 340 11 300 351 3 300 371 5 300 381 6 300 411 69	74
302 340 13 302 351 2 302 371 5 302 381 6 302 411 74	74
303 340 14 303 351 2 303 371 5 303 381 6 303 411 73	74
341 351 8 341 371 6 341 381 7 341 411 79	74
352 371 8 352 381 8 352 411 84	74
372 381 12 372 411 88	74
373 381 12 373 411 88	74
391 411 100	74
	170
0 8	210
MP30-34	
8300 300 301 100	25
300 301 302 94 305 6	25
301 3058305 100	25
301 302 303 100	25
8306 206 306 100	25
206 306 302 100	25
302 303 340 100	25
8307 207 307 100	25
207 307 303 100	25
307 303 340 100	25
303 340 341 88 346 12	25
340 3468346 100	25
MP34-42	
340 341 351 100	25
341 351 352 95 355 5	25
351 352 371 100	25
352 371 372 94 375 6	25
371 372 373 100	25
372 373 381 100	25
373 381 391 91 385 9	25
381 391 411 100	25
391 4118411 100	25
8345 245 345 100	25
245 345 341 100	25
345 341 351 100	25
351 3558355 100	25
8356 256 356 100	25

256 356 352 100	25
356 352 371 100	25
371 3758375 100	25
8376 276 376 100	25
276 376 372 100	25
376 372 373 100	25
8377 277 377 100	25
277 377 373 100	25
377 373 381 100	25
381 3858385 100	25
8395 295 395 100	25
295 395 391 100	25
395 391 411 100	25
Time Period 4	
306 1 540 54	37
307 1 540 47	37
345 1 0 97	
356 1 540 40	37
376 1 540 47	37
377 1 0 97	
395 1 540 44	37
MP30-34	
8300 3003560 6	50
8306 206 360 4	50
8307 207 489 8	50
MP34-42	
8345 2452159 9	50
8356 256 819 8	50
8376 276 400 5	50
8377 2771216 10	50
8395 295 430 9	50
MP30-42 OD Table	
300 301 6 300 340 11 300 351 3 300 371 5 300 381 6 300 411 69	74
302 340 13 302 351 2 302 371 5 302 381 6 302 411 74	74
303 340 14 303 351 2 303 371 5 303 381 6 303 411 73	74
341 351 8 341 371 6 341 381 7 341 411 79	74
352 371 8 352 381 8 352 411 84	74
372 381 12 372 411 88	74
373 381 12 373 411 88	74
391 411 100	74
0 8	170
	210
MP30-34	
8300 300 301 100	25
300 301 302 94 305 6	25
301 3058305 100	25
301 302 303 100	25
8306 206 306 100	25
206 306 302 100	25
302 303 340 100	25
8307 207 307 100	25
207 307 303 100	25
307 303 340 100	25
303 340 341 88 346 12	25
340 3468346 100	25
MP34-42	
340 341 351 100	25
341 351 352 95 355 5	25
351 352 371 100	25
352 371 372 94 375 6	25
371 372 373 100	25
372 373 381 100	25

373 381 391 91 385 9	25
381 391 411 100	25
391 4118411 100	25
8345 245 345 100	25
245 345 341 100	25
345 341 351 100	25
351 3558355 100	25
8356 256 356 100	25
256 356 352 100	25
356 352 371 100	25
371 3758375 100	25
8376 276 376 100	25
276 376 372 100	25
376 372 373 100	25
8377 277 377 100	25
277 377 373 100	25
377 373 381 100	25
381 3858385 100	25
8395 295 395 100	25
295 395 391 100	25
395 391 411 100	25
Time Period 5	
306 1 720 53	37
307 1 720 47	37
345 1 0 97	
356 1 720 40	37
376 1 720 46	37
377 1 0 97	
395 1 720 43	37
MP30-34	
8300 3003760 6	50
8306 206 360 4	50
8307 207 489 8	50
MP34-42	
8345 2452159 9	50
8356 256 819 8	50
8376 276 400 5	50
8377 2771216 10	50
8395 295 430 9	50
MP30-42 OD Table	
300 301 6 300 340 11 300 351 3 300 371 5 300 381 6 300 411 69	74
302 340 13 302 351 2 302 371 5 302 381 6 302 411 74	74
303 340 14 303 351 2 303 371 5 303 381 6 303 411 73	74
341 351 8 341 371 6 341 381 7 341 411 79	74
352 371 8 352 381 8 352 411 84	74
372 381 12 372 411 88	74
373 381 12 373 411 88	74
391 411 100	74
	170
0 8	210
MP30-34	
8300 300 301 100	25
300 301 302 94 305 6	25
301 3058305 100	25
301 302 303 100	25
8306 206 306 100	25
206 306 302 100	25
302 303 340 100	25
8307 207 307 100	25
207 307 303 100	25
307 303 340 100	25
303 340 341 88 346 12	25

340 3468346 100		25
MP34-42		
340 341 351 100		25
341 351 352 95 355 5		25
351 352 371 100		25
352 371 372 94 375 6		25
371 372 373 100		25
372 373 381 100		25
373 381 391 91 385 9		25
381 391 411 100		25
391 4118411 100		25
8345 245 345 100		25
245 345 341 100		25
345 341 351 100		25
351 3558355 100		25
8356 256 356 100		25
256 356 352 100		25
356 352 371 100		25
371 3758375 100		25
8376 276 376 100		25
276 376 372 100		25
376 372 373 100		25
8377 277 377 100		25
277 377 373 100		25
377 373 381 100		25
381 3858385 100		25
8395 295 395 100		25
295 395 391 100		25
395 391 411 100		25
Time Period 6		
306 1 900 52		37
307 1 900 46		37
345 1 0 97		
356 1 900 40		37
376 1 900 45		37
377 1 0 97		
395 1 900 42		37
MP30-34		
8300 3003960 6		50
8306 206 360 4		50
8307 207 489 8		50
MP34-42		
8345 2452159 9		50
8356 256 819 8		50
8376 276 400 5		50
8377 2771216 10		50
8395 295 430 9		50
MP30-42 OD Table		
300 301 6 300 340 11 300 351 3 300 371 5 300 381 6 300 411 69		74
302 340 13 302 351 2 302 371 5 302 381 6 302 411 74		74
303 340 14 303 351 2 303 371 5 303 381 6 303 411 73		74
341 351 8 341 371 6 341 381 7 341 411 79		74
352 371 8 352 381 8 352 411 84		74
372 381 12 372 411 88		74
373 381 12 373 411 88		74
391 411 100		74
		170
0 8		210
MP30-34		
8300 300 301 100		25
300 301 302 94 305 6		25
301 3058305 100		25

301 302 303 100	25
8306 206 306 100	25
206 306 302 100	25
302 303 340 100	25
8307 207 307 100	25
207 307 303 100	25
307 303 340 100	25
303 340 341 88 346 12	25
340 3468346 100	25
MP34-42	
340 341 351 100	25
341 351 352 95 355 5	25
351 352 371 100	25
352 371 372 94 375 6	25
371 372 373 100	25
372 373 381 100	25
373 381 391 91 385 9	25
381 391 411 100	25
391 4118411 100	25
8345 245 345 100	25
245 345 341 100	25
345 341 351 100	25
351 3558355 100	25
8356 256 356 100	25
256 356 352 100	25
356 352 371 100	25
371 3758375 100	25
8376 276 376 100	25
276 376 372 100	25
376 372 373 100	25
8377 277 377 100	25
277 377 373 100	25
377 373 381 100	25
381 3858385 100	25
8395 295 395 100	25
295 395 391 100	25
395 391 411 100	25
Time Period 7	
306 11080 51	37
307 11080 45	37
345 1 0 97	
356 11080 40	37
376 11080 44	37
377 1 0 97	
395 11080 41	37
MP30-34	
8300 3004160 6	50
8306 206 360 4	50
8307 207 489 8	50
MP34-42	
8345 2452159 9	50
8356 256 819 8	50
8376 276 400 5	50
8377 2771216 10	50
8395 295 430 9	50
MP30-42 OD Table	
300 301 6 300 340 11 300 351 3 300 371 5 300 381 6 300 411 69	74
302 340 13 302 351 2 302 371 5 302 381 6 302 411 74	74
303 340 14 303 351 2 303 371 5 303 381 6 303 411 73	74
341 351 8 341 371 6 341 381 7 341 411 79	74
352 371 8 352 381 8 352 411 84	74
372 381 12 372 411 88	74

373 381 12 373 411 88	74
391 411 100	74
	170
0 8	210
MP30-34	
8300 300 301 100	25
300 301 302 94 305 6	25
301 3058305 100	25
301 302 303 100	25
8306 206 306 100	25
206 306 302 100	25
302 303 340 100	25
8307 207 307 100	25
207 307 303 100	25
307 303 340 100	25
303 340 341 88 346 12	25
340 3468346 100	25
MP34-42	
340 341 351 100	25
341 351 352 95 355 5	25
351 352 371 100	25
352 371 372 94 375 6	25
371 372 373 100	25
372 373 381 100	25
373 381 391 91 385 9	25
381 391 411 100	25
391 4118411 100	25
8345 245 345 100	25
245 345 341 100	25
345 341 351 100	25
351 3558355 100	25
8356 256 356 100	25
256 356 352 100	25
356 352 371 100	25
371 3758375 100	25
8376 276 376 100	25
276 376 372 100	25
376 372 373 100	25
8377 277 377 100	25
277 377 373 100	25
377 373 381 100	25
381 3858385 100	25
8395 295 395 100	25
295 395 391 100	25
395 391 411 100	25
Time Period 8	
306 11260 50	37
307 11260 45	37
345 1 0 97	
356 11260 40	37
376 11260 44	37
377 1 0 97	
395 11260 41	37
MP30-34	
8300 3004360 6	50
8306 206 360 4	50
8307 207 489 8	50
MP34-42	
8345 2452159 9	50
8356 256 819 8	50
8376 276 400 5	50
8377 2771216 10	50
8395 295 430 9	50

MP30-42 OD Table

300 301 6 300 340	11 300 351	3 300 371	5 300 381	6 300 411	69	74
302 340 13 302 351	2 302 371	5 302 381	6 302 411	74		74
303 340 14 303 351	2 303 371	5 303 381	6 303 411	73		74
341 351 8 341 371	6 341 381	7 341 411	79			74
352 371 8 352 381	8 352 411	84				74
372 381 12 372 411	88					74
373 381 12 373 411	88					74
391 411 100						74
						170
0 8						210
MP30-34						
8300 300 301 100						25
300 301 302 94 305	6					25
301 3058305 100						25
301 302 303 100						25
8306 206 306 100						25
206 306 302 100						25
302 303 340 100						25
8307 207 307 100						25
207 307 303 100						25
307 303 340 100						25
303 340 341 88 346	12					25
340 3468346 100						25
MP34-42						
340 341 351 100						25
341 351 352 95 355	5					25
351 352 371 100						25
352 371 372 94 375	6					25
371 372 373 100						25
372 373 381 100						25
373 381 391 91 385	9					25
381 391 411 100						25
391 4118411 100						25
8345 245 345 100						25
245 345 341 100						25
345 341 351 100						25
351 3558355 100						25
8356 256 356 100						25
256 356 352 100						25
356 352 371 100						25
371 3758375 100						25
8376 276 376 100						25
276 376 372 100						25
376 372 373 100						25
8377 277 377 100						25
277 377 373 100						25
377 373 381 100						25
381 3858385 100						25
8395 295 395 100						25
295 395 391 100						25
395 391 411 100						25
Time Period 9						
306 11440 50						37
307 11440 45						37
345 1 0 97						
356 11440 40						37
376 11440 44						37
377 1 0 97						
395 11440 41						37
MP30-34						
8300 3004560 6						50

277 377 373 100	25
377 373 381 100	25
381 3858385 100	25
8395 295 395 100	25
295 395 391 100	25
395 391 411 100	25
Time Period 11	
306 11800 50	37
307 11800 48	37
345 1 0 97	
356 11800 40	37
376 11800 40	37
377 1 0 97	
395 11800 40	37
MP30-34	
8300 3004960 6	50
8306 206 360 4	50
8307 207 489 8	50
MP34-42	
8345 2452159 9	50
8356 256 819 8	50
8376 276 400 5	50
8377 2771216 10	50
8395 295 430 9	50
MP30-42 OD Table	
300 301 6 300 340 11 300 351 3 300 371 5 300 381 6 300 411 69	74
302 340 13 302 351 2 302 371 5 302 381 6 302 411 74	74
303 340 14 303 351 2 303 371 5 303 381 6 303 411 73	74
341 351 8 341 371 6 341 381 7 341 411 79	74
352 371 8 352 381 8 352 411 84	74
372 381 12 372 411 88	74
373 381 12 373 411 88	74
391 411 100	74
0 8	170
	210
MP30-34	
8300 300 301 100	25
300 301 302 94 305 6	25
301 3058305 100	25
301 302 303 100	25
8306 206 306 100	25
206 306 302 100	25
302 303 340 100	25
8307 207 307 100	25
207 307 303 100	25
307 303 340 100	25
303 340 341 88 346 12	25
340 3468346 100	25
MP34-42	
340 341 351 100	25
341 351 352 95 355 5	25
351 352 371 100	25
352 371 372 94 375 6	25
371 372 373 100	25
372 373 381 100	25
373 381 391 91 385 9	25
381 391 411 100	25
391 4118411 100	25
8345 245 345 100	25
245 345 341 100	25
345 341 351 100	25
351 3558355 100	25

8356 256 356 100	25
256 356 352 100	25
356 352 371 100	25
371 3758375 100	25
8376 276 376 100	25
276 376 372 100	25
376 372 373 100	25
8377 277 377 100	25
277 377 373 100	25
377 373 381 100	25
381 3858385 100	25
8395 295 395 100	25
295 395 391 100	25
395 391 411 100	25
Time Period 12	
306 11980 51	37
307 11980 49	37
345 1 0 97	
356 11980 40	37
376 11980 40	37
377 1 0 97	
395 11980 40	37
MP30-34	
8300 3005160 6	50
8306 206 360 4	50
8307 207 489 8	50
MP34-42	
8345 2452159 9	50
8356 256 819 8	50
8376 276 400 5	50
8377 2771216 10	50
8395 295 430 9	50
MP30-42 OD Table	
300 301 6 300 340 11 300 351 3 300 371 5 300 381 6 300 411 69	74
302 340 13 302 351 2 302 371 5 302 381 6 302 411 74	74
303 340 14 303 351 2 303 371 5 303 381 6 303 411 73	74
341 351 8 341 371 6 341 381 7 341 411 79	74
352 371 8 352 381 8 352 411 84	74
372 381 12 372 411 88	74
373 381 12 373 411 88	74
391 411 100	74
	170
0 8	210
MP30-34	
8300 300 301 100	25
300 301 302 94 305 6	25
301 3058305 100	25
301 302 303 100	25
8306 206 306 100	25
206 306 302 100	25
302 303 340 100	25
8307 207 307 100	25
207 307 303 100	25
307 303 340 100	25
303 340 341 88 346 12	25
340 3468346 100	25
MP34-42	
340 341 351 100	25
341 351 352 95 355 5	25
351 352 371 100	25
352 371 372 94 375 6	25
371 372 373 100	25

372 373 381 100	25
373 381 391 91 385 9	25
381 391 411 100	25
391 4118411 100	25
8345 245 345 100	25
245 345 341 100	25
345 341 351 100	25
351 3558355 100	25
8356 256 356 100	25
256 356 352 100	25
356 352 371 100	25
371 3758375 100	25
8376 276 376 100	25
276 376 372 100	25
376 372 373 100	25
8377 277 377 100	25
277 377 373 100	25
377 373 381 100	25
381 3858385 100	25
8395 295 395 100	25
295 395 391 100	25
395 391 411 100	25
Time Period 13	
306 12160 51	37
307 12160 49	37
345 1 0 97	
356 12160 40	37
376 12160 40	37
377 1 0 97	
395 12160 40	37
MP30-34	
8300 3005360 6	50
8306 206 360 4	50
8307 207 489 8	50
MP34-42	
8345 2452159 9	50
8356 256 819 8	50
8376 276 400 5	50
8377 2771216 10	50
8395 295 430 9	50
MP30-42 OD Table	
300 301 6 300 340 11 300 351 3 300 371 5 300 381 6 300 411 69	74
302 340 13 302 351 2 302 371 5 302 381 6 302 411 74	74
303 340 14 303 351 2 303 371 5 303 381 6 303 411 73	74
341 351 8 341 371 6 341 381 7 341 411 79	74
352 371 8 352 381 8 352 411 84	74
372 381 12 372 411 88	74
373 381 12 373 411 88	74
391 411 100	74
	170
0 8	210
MP30-34	
8300 300 301 100	25
300 301 302 94 305 6	25
301 3058305 100	25
301 302 303 100	25
8306 206 306 100	25
206 306 302 100	25
302 303 340 100	25
8307 207 307 100	25
207 307 303 100	25
307 303 340 100	25

303 340 341 88 346 12	25
340 3468346 100	25
MP34-42	
340 341 351 100	25
341 351 352 95 355 5	25
351 352 371 100	25
352 371 372 94 375 6	25
371 372 373 100	25
372 373 381 100	25
373 381 391 91 385 9	25
381 391 411 100	25
391 4118411 100	25
8345 245 345 100	25
245 345 341 100	25
345 341 351 100	25
351 3558355 100	25
8356 256 356 100	25
256 356 352 100	25
356 352 371 100	25
371 3758375 100	25
8376 276 376 100	25
276 376 372 100	25
376 372 373 100	25
8377 277 377 100	25
277 377 373 100	25
377 373 381 100	25
381 3858385 100	25
8395 295 395 100	25
295 395 391 100	25
395 391 411 100	25
Time Period 14	
306 12340 52	37
307 12340 50	37
345 1 0 97	
356 12340 40	37
376 12340 40	37
377 1 0 97	
395 12340 40	37
MP30-34	
8300 3005560 6	50
8306 206 360 4	50
8307 207 489 8	50
MP34-42	
8345 2452159 9	50
8356 256 819 8	50
8376 276 400 5	50
8377 2771216 10	50
8395 295 430 9	50
MP30-42 OD Table	
300 301 6 300 340 11 300 351 3 300 371 5 300 381 6 300 411 69	74
302 340 13 302 351 2 302 371 5 302 381 6 302 411 74	74
303 340 14 303 351 2 303 371 5 303 381 6 303 411 73	74
341 351 8 341 371 6 341 381 7 341 411 79	74
352 371 8 352 381 8 352 411 84	74
372 381 12 372 411 88	74
373 381 12 373 411 88	74
391 411 100	74
0 8	170
	210
MP30-34	
8300 300 301 100	25
300 301 302 94 305 6	25

301 3058305 100	25
301 302 303 100	25
8306 206 306 100	25
206 306 302 100	25
302 303 340 100	25
8307 207 307 100	25
207 307 303 100	25
307 303 340 100	25
303 340 341 88 346 12	25
340 3468346 100	25
MP34-42	
340 341 351 100	25
341 351 352 95 355 5	25
351 352 371 100	25
352 371 372 94 375 6	25
371 372 373 100	25
372 373 381 100	25
373 381 391 91 385 9	25
381 391 411 100	25
391 4118411 100	25
8345 245 345 100	25
245 345 341 100	25
345 341 351 100	25
351 3558355 100	25
8356 256 356 100	25
256 356 352 100	25
356 352 371 100	25
371 3758375 100	25
8376 276 376 100	25
276 376 372 100	25
376 372 373 100	25
8377 277 377 100	25
277 377 373 100	25
377 373 381 100	25
381 3858385 100	25
8395 295 395 100	25
295 395 391 100	25
395 391 411 100	25
Time Period 15	
306 12520 53	37
307 12520 51	37
345 1 0 97	
356 12520 43	37
376 12520 42	37
377 1 0 97	
395 12520 40	37
MP30-34	
8300 3005760 6	50
8306 206 360 4	50
8307 207 489 8	50
MP34-42	
8345 2452159 9	50
8356 256 819 8	50
8376 276 400 5	50
8377 2771216 10	50
8395 295 430 9	50
MP30-42 OD Table	
300 301 6 300 340 11 300 351 3 300 371 5 300 381 6 300 411 69	74
302 340 13 302 351 2 302 371 5 302 381 6 302 411 74	74
303 340 14 303 351 2 303 371 5 303 381 6 303 411 73	74
341 351 8 341 371 6 341 381 7 341 411 79	74
352 371 8 352 381 8 352 411 84	74

372 381 12 372 411 88	74
373 381 12 373 411 88	74
391 411 100	74
	170
0 8	210
MP30-34	
8300 300 301 100	25
300 301 302 94 305 6	25
301 3058305 100	25
301 302 303 100	25
8306 206 306 100	25
206 306 302 100	25
302 303 340 100	25
8307 207 307 100	25
207 307 303 100	25
307 303 340 100	25
303 340 341 88 346 12	25
340 3468346 100	25
MP34-42	
340 341 351 100	25
341 351 352 95 355 5	25
351 352 371 100	25
352 371 372 94 375 6	25
371 372 373 100	25
372 373 381 100	25
373 381 391 91 385 9	25
381 391 411 100	25
391 4118411 100	25
8345 245 345 100	25
245 345 341 100	25
345 341 351 100	25
351 3558355 100	25
8356 256 356 100	25
256 356 352 100	25
356 352 371 100	25
371 3758375 100	25
8376 276 376 100	25
276 376 372 100	25
376 372 373 100	25
8377 277 377 100	25
277 377 373 100	25
377 373 381 100	25
381 3858385 100	25
8395 295 395 100	25
295 395 391 100	25
395 391 411 100	25
Time Period 16	
306 12700 54	37
307 12700 52	37
345 1 0 97	
356 12700 44	37
376 12700 41	37
377 1 0 97	
395 12700 40	37
MP30-34	
8300 3005960 6	50
8306 206 360 4	50
8307 207 489 8	50
MP34-42	
8345 2452159 9	50
8356 256 819 8	50
8376 276 400 5	50
8377 2771216 10	50

8395 295 430 9

50

MP30-42 OD Table

300 301	6 300 340	11 300 351	3 300 371	5 300 381	6 300 411	69	74
302 340	13 302 351	2 302 371	5 302 381	6 302 411	74		74
303 340	14 303 351	2 303 371	5 303 381	6 303 411	73		74
341 351	8 341 371	6 341 381	7 341 411	79			74
352 371	8 352 381	8 352 411	84				74
372 381	12 372 411	88					74
373 381	12 373 411	88					74
391 411	100						74
							170
1							210

APPENDIX C

THEORY ANALYSIS

In this Appendix, queuing theory and the M/M/1 model are introduced, and the related derivations are presented. In addition, the theoretical characteristics and proofs associated with SPSA are presented.

C.1 Queuing Theory Application on Ramp Metering Control

The queuing process on metered ramp is assumed the following. Vehicles requiring service to pass through a metered ramp are generated over time by traffic demand on the ramp. These vehicles enter the queuing system and join a queue. At certain times, a vehicle of the queue for service by some rule known as queue discipline (e.g., first-come-first-serve). The required service is then performed for the vehicle with service time (e.g., metering headway) by the ramp meter, after which the vehicle leaves the queuing system.

One of elementary queuing models is the $M/M/1$ model which assumes that all arrival times are independently and identically distributed according to an exponential distribution, that all service times (lead to departure times) are independent and identically distributed according to another exponential distribution, and that the number of servers is 1. Suppose in a one-meter ramp control system, the mean arrival rate is m , while the mean metering rate is $R_i(k)$ to server vehicles on the ramp. When the maximum mean metering rate $R_i(k)$ exceeds the mean arrive rate m , a queuing system will eventually reach a steady-state condition. Based on queuing theory, for states of the queuing system n ($n = 0, 1, 2, \dots$), the steady-state probabilities P_n , the expected number of vehicles in the queuing system L , and the expected queue length (excludes vehicles being served) L_q can be expressed as the following (Hillier, et al., 1995).

$$P_n = C_n P_0, \quad \text{for } n = 0, 1, 2, \dots,$$

$$L = \sum_{n=0}^{\infty} n P_n,$$

$$L_q = \sum_{n=1}^{\infty} (n-1) P_n.$$

where, $C_n = \left(\frac{m}{R_i(k)} \right)^n = \tau^n$, for $n = 0, 1, 2, \dots$,

$$\begin{aligned} P_0 &= \left(\sum_{n=0}^{\infty} \tau^n \right)^{-1} \\ &= \left(\frac{1}{1-\tau} \right)^{-1} = 1-\tau. \end{aligned}$$

Thus, $P_n = (1-\tau)\tau^n$, for $n = 0, 1, 2, \dots$

$$\begin{aligned} L &= \sum_{n=0}^{\infty} n(1-\tau)P_n \\ &= (1-\tau)\tau \sum_{n=0}^{\infty} \frac{d}{d\tau}(\tau^n) \\ &= (1-\tau)\tau \frac{d}{d\tau} \left(\sum_{n=0}^{\infty} \tau^n \right) \\ &= (1-\tau)\tau \frac{d}{d\tau} \left(\frac{1}{1-\tau} \right) \\ &= \frac{\tau}{1-\tau} = \frac{m}{R_i(k) - m}. \end{aligned}$$

$$\begin{aligned} L_q &= \sum_{n=1}^{\infty} (n-1)P_n \\ &= L - (1 - P_0) \\ &= \frac{m^2}{R_i(k)(R_i(k) - m)} = \frac{\tau m}{R_i(k) - m}. \end{aligned} \tag{derivation for Equation 3.11}$$

Therefore, $R_i(k) = \left(\frac{L_q + \tau}{L_q} \right) m$. (derivation for Equation 3.12)

C.2 Theoretical Analysis for SPSA

This section presents the strong convergence of $\hat{\lambda}_h$ in SPSA. The proposition is proved based on the definitions, assumptions and lemma presented below.

C.2.1 Definition

At design levels $\hat{\lambda}_h \pm c_h \Delta_h$, let Equation 3.14 (i.e., $\mathbf{y}(\boldsymbol{\lambda}) = \mathbf{L}(\boldsymbol{\lambda}) + \text{noise}$) express as

$$\mathbf{y}(\boldsymbol{\lambda}) = \mathbf{L}(\hat{\lambda}_h + c_h \Delta_h) + \varepsilon_h^{(+)}$$

$$\mathbf{y}(\boldsymbol{\lambda}) = \mathbf{L}(\hat{\lambda}_h - c_h \Delta_h) + \varepsilon_h^{(-)}$$

where $\varepsilon_h^{(+)}$ or $\varepsilon_h^{(-)}$ represent measurement noise terms that satisfy

$$E(\varepsilon_h^{(+)} - \varepsilon_h^{(-)} | \Phi_h, \Delta_h) = 0 \quad \forall h,$$

$$\Phi_h \equiv \{ \hat{\lambda}_0, \hat{\lambda}_1, \hat{\lambda}_2, \dots, \hat{\lambda}_h \}.$$

Δ_h is independent of Φ_h and $E|\Delta_{hi}^{-1}|$ exists, which implies that $P(\Delta_{hi} = 0) = 0$.

$E(\hat{g}_h(\hat{\lambda}_h) | \hat{\lambda}_h) = E(\hat{g}_h(\hat{\lambda}_h) | \Phi_h)$ can be easily derived.

Defining the error term e_h as

$$e_h(\hat{\lambda}_h) = \hat{g}_h(\hat{\lambda}_h) - E(\hat{g}_h(\hat{\lambda}_h) | \hat{\lambda}_h),$$

Equation 3.18 (i.e., $\hat{\lambda}_{h+1} = \hat{\lambda}_h - \mathbf{a}_h \hat{g}_h(\hat{\lambda}_h)$) can be rewritten in the form of a generalized Robbins-Monro algorithm (Kushner, et al., 1978, Ljung, 1978, and Metivier, et al., 1984) as

$$\hat{\lambda}_{h+1} = \hat{\lambda}_h - \mathbf{a}_h [g_h(\hat{\lambda}_h) + b_h(\hat{\lambda}_h) + e_h(\hat{\lambda}_h)],$$

where $b_h(\hat{\lambda}_h)$ is the bias in $\hat{g}_h(\hat{\lambda}_h)$.

C.2.2 Lemma

Assume that α_0 , α_1 , and α_2 denote positive constants, and $\Omega = \{\omega\}$ denotes the sample space generating the sequence $\hat{\lambda}_1, \hat{\lambda}_2, \dots$. Consider all $h \geq H$ and $H \leq \infty$. Suppose that for h the $\{\Delta_{hi}\}$ ($i = 1, 2, \dots, p$) are mutually independent random variables and symmetrically distributed about 0 with $|\Delta_{hi}| \leq \alpha_0$ and $E|\Delta_{hi}^{-1}| \leq \alpha_1$. For almost all $\hat{\lambda}_h$ (at each $h \geq H$) suppose that $\forall \lambda$ in an open neighborhood of $\hat{\lambda}_h$ that is not a function of H or ω , $L^{(3)}(\lambda) \equiv \partial^3 L / \partial \lambda^T \partial \lambda^T \partial \lambda^T$ exists continuously with individual elements satisfying $E|L_{h_i i_i}^{(3)}(\lambda)| \leq \alpha_2$. Then for almost all $\omega \in \Omega$

$$\begin{aligned} b_h(\hat{\lambda}_h) &\equiv E(\hat{g}_h(\hat{\lambda}_h) - \hat{g}(\hat{\lambda}_h) | \hat{\lambda}_h) \\ & (= E(\hat{g}_h(\hat{\lambda}_h) - \hat{g}(\hat{\lambda}_h) | \Phi_h)) \\ & = O(c_h^2) \quad (c_h \rightarrow 0). \end{aligned}$$

This lemma gives conditions under which the bias $b_h(\hat{\lambda}_h)$ in $\hat{g}_h(\hat{\lambda}_h)$ goes to 0 as $h \rightarrow \infty$.

C.2.3 Assumptions

Five assumptions are discussed below.

Assumption 1: $\mathbf{a}_h, \mathbf{c}_h > 0 \forall h; \mathbf{a}_h \rightarrow 0, \mathbf{c}_h \rightarrow 0$ as $h \rightarrow \infty$;

$$\sum_{h=0}^{\infty} \mathbf{a}_h = \infty, \quad \sum_{h=0}^{\infty} \left(\frac{\mathbf{a}_h}{\mathbf{c}_h} \right)^2 < \infty.$$

Assumption 2: For some $\alpha_0, \alpha_1, \alpha_2 > 0$ and $\forall h, E\varepsilon_h^{(\pm)^2} \leq \alpha_0, EL(\hat{\lambda}_h \pm c_h \Delta_h)^2 \leq \alpha_1,$
and $E(\Delta_{hl}^{-2})^2 \leq \alpha_2$ ($l=1, 2, \dots, p$).

Assumption 3: $\|\hat{\lambda}_h\| < \infty \quad \forall h.$

Assumption 4: λ^* is an asymptotically stable solution of the differential equation
 $dx(t)/dt = -g(x).$

Assumption 5: Let $D(\lambda^*) = \{x_0 : \lim_{t \rightarrow \infty} x(t|x_0) = \lambda^*\}$ where $x(t|x_0)$ denotes the solution to the differential equation of Assumption 4 based on initial conditions x_0 (i.e., $D(\lambda^*)$ is the domain of attraction). There exists a compact $S \subseteq D(\lambda^*)$ such that $\hat{\lambda}_h \in S$ infinitely often for almost all sample points.

Assumption 1 and Assumption 2 are typical Stochastic Approximation (SA) conditions. Assumption 3 is not a restrictive condition and could be expected to hold in most application (Kushner, et al., 1978). Assumption 4 and Assumption 5 are motivated by considering a limiting form of the deterministic version of Equation 3.18, i.e., $\hat{\lambda}_{h+1} = \hat{\lambda}_h - \mathbf{a}_h \hat{g}_h(\hat{\lambda}_h)$ as $h \rightarrow \infty$.

C.2.4 Proposition

Let Assumptions 1 through 5 and the conditions of the lemma hold. Then as $h \rightarrow \infty$,

$$\hat{\lambda}_h \rightarrow \lambda^* \quad \text{for almost all } \omega \in \Omega. \quad (\text{B.1})$$

Proof:

Given Assumptions 1, 3, 4 and 5, it was known that Equation B.1 holds (Kushner, et al., 1978) if

- i) $\|b_h(\hat{\lambda}_h)\| < \infty \quad \forall h$ and $b_h(\hat{\lambda}_h) \rightarrow 0$ inequality
- ii) $\lim_{h \rightarrow \infty} P\left(\sup_{m \geq h} \left\| \sum_{i=h}^m a_i e_i(\hat{\lambda}_i) \right\| \geq \eta\right) = 0$ for any $\eta > 0$.

Now, i) follows immediately by the lemma and Assumption. Consider ii). Since $\{\sum_{i=h}^m a_i e_i\}_{m \geq h}$ is martingale sequence, an inequality (Doob, 1953, Kushner et al., 1978)

can be derived as

$$\begin{aligned} P\left(\sup_{m \geq h} \left\| \sum_{i=h}^m a_i e_i \right\| \geq \eta\right) &\leq \eta^{-2} E \left\| \sum_{i=h}^{\infty} a_i e_i \right\|^2 \\ &= \eta^{-2} \sum_{i=h}^{\infty} a_i E \|e_i\|^2 \end{aligned} \quad (\text{B.2})$$

where the equality follows by the fact that $E(e_i^T e_j) = E(e_i^T E(e_j | \hat{\lambda}_j)) = 0 \quad \forall i < j$.

Now, for any $l \in \{1, 2, \dots, p\}$,

$$\begin{aligned} E g_{hl}(\hat{\lambda}_h)^2 &\leq \frac{1}{4} E [L(\hat{\lambda}_h + c_h \Delta_h) - L(\hat{\lambda}_h - c_h \Delta_h) + \varepsilon_h^{(+)} - \varepsilon_h^{(-)}]^2 E \Delta_{hl}^{-2} \\ &\leq 2(\alpha_0 + \alpha_1) \alpha_2 c_h^{-2} \end{aligned} \quad (\text{using Assumption 2})$$

thus, $E \|e_h\|^2 \leq 2p(\alpha_0 + \alpha_1) \alpha_2 c_h^{-2}$. Then from Equation B.2 and Assumption 1, ii) has been shown, which completes the proof.

REFERENCES

1. Aerde, M. Van and Yagar, S. *Dynamic Integrated Freeway/Traffic Signal Networks: A Routing-Based Modeling Approach*. Transportation Research A, Vol. 22A, 1988, pp. 445-453.
2. Banks, J. H. *Flow Processes at a Freeway Bottleneck*. Transportation Research Record 1287, TRB, National Research Council, Washington, D. C., 1990, pp. 20-27.
3. Banks, J. H. *Effect of Response Limitations on Traffic-Responsive Ramp Metering*. Transportation Research Record 1394, TRB, National Research Council, Washington, D. C., 1991, pp. 16-25.
4. Bazaraa, M. S., Sherali, H. D. and Shetty, C. M. *Nonlinear Programming Theory and Algorithms*, John Wiley & Sons, Inc., New York, 1993.
5. Blumentritt, C. W., Pinnel, C. and McCasland, W. R. *Guidelines for Selection of Ramp Control Systems*. NCHRP Report 232, Transportation Research Board, May 1981.
6. California Department of Transportation (CALTRANS). *The Effects of Ramp Metering on City Streets*. 1979.
7. Chang, E., Messer, C. J. and Derr, B. R. *Off-line Freeway Traffic Control Strategies*. Conference Proceedings, 1989 Annual ITE Meeting in San Diego, California, September 1989.
8. Chang, G., Ho, P. K. and Wei, C. H. *A Dynamic System-Optimum Control Model for Commuting Traffic Corridors*. Transportation Research 1C, 1993, pp. 3-22.
9. Chang, G., Wu, J. and Lieu, H. *A Real-Time Incident-responsive system for Corridor Control: A Modeling Framework and Preliminary Results*. Presented at 73rd Annual Meeting of the Transportation Research Board, Washington, D.C., 1994.
10. Chang, G. and Wu, J. *Recursive Estimation of Time-Varying Origin-Destination Flows from Traffic Counts in Freeway Corridors*. Transportation Research 28B, 1994a, pp. 141-160.

11. Chang, G., Wu, J. and Cohen, S. L. *Integrated Real-Time Ramp Metering Model for Nonrecurrent Congestion: Framework and Preliminary Results*. Transportation Research Record 1446, TRB, National Research Council, Washington, D. C., 1994b, pp. 56-65.
12. Chen, C. I., Cruz, J. B. Jr. and Paquet, J. G. *Entrance Ramp Control for Travel-Rate Maximization in Expressways*. Transportation Research 8, 1974, pp. 503-508.
13. Chen, L. L., May, A. D. and Auslander, D. M. *Freeway Ramp Control Using Fuzzy Set Theory for Inexact Reasoning*. Transportation Research 24A, 1990, pp. 15-25.
14. Chien, S. and Chowdhury, S. *Freeway Capacity Analysis with Microscopic Simulation Models (CORSIM)*. Project Report - Phase II, Research and Development Division, Turner-Fairbank Highway Research Center, FHWA-USDOT, April 1998.
15. Chien, S. and Sigma, Xi. "Strategies for Traffic Control on Freeways". NJIT Chapter and IEEE, North Jersey Chapter, March 1998.
16. Davis, G. A. *Estimating Freeway Demand Patterns and Impact of Uncertainty on Ramp Controls*. Journal of Transportation Engineering, 1993, Vol. 119, No. 4, pp. 489-503.
17. Davis, G. A., Nihan, N. L., Hamed, M. M. and Jacobson, L. N. *Adaptive Forecasting of Freeway Traffic Congestion*. Transportation Research Board 1287, TRB, National Research Council, Washington, D. C., 1990, pp. 29-33.
18. Deepak, K. M., et al. *A Model and an Algorithm for the Dynamic Traffic Assignment Problems*. Transportation Science, Vol. 12, No. 3, August 1978, pp. 183-199.
19. Doob, J. L. *Stochastic Processes*. New York: Willey, 1953.
20. DOT. *Evaluation of Freeway High-Occupancy Vehicle Lanes and Ramp Metering*. DOT-OST078-050, 1980.
21. Drew, D. R. *Gap Acceptance Characteristics for Ramp-Freeway surveillance and Control*. Highway Research Board 157, TRB, National Research Council, Washington, D. C., 1967, pp. 108-143.

22. Federal Highway Administration. *Manual on Uniform Traffic Control Devices (MUTCD)*. 2001.
23. Federal Highway Administration (FHWA). *TRAF Users' Reference Guide*. Report No. FHWA-RD-92-103, Washington, D.C., 1992.
24. Federal Highway Administration (FHWA). *CORSIM User's Manual*. Contract No. DTFH61-92-Z-00074, Washington, D.C., 1996.
25. Federal Highway Administration. *Traffic Control System Handbook*. FHWA-SA-95-032, Feb. 1996.
26. Federal Highway Administration. *Freeway Management Handbook*. Report No. FHWA-SA-97-064, 1997.
27. Fitzsimmons, J. A. and Fitzsimmons, M. J. *Service Management: Operations, Strategy, and Information Technology*, Second Edition, 1997.
28. Garcia, Sandra A. *I-90 West Bound Ramp Meter Analysis Bellevue Way to Front Street*. Oct. 1998.
29. Garmen Associates. *Final Report: Interstate 80 Corridor Transportation Needs Assessment*. 1991.
30. Gartner, N. H. *OPAC: a Demand-Responsive Strategy for Traffic Signal Control*. Transportation Research Record 906, TRB, National Research Council, Washington, D. C., 1983, pp. 75-81.
31. Goldstein, N. B. and Kumar, K. S. P. *A Decentralized Control Strategy for Freeway Regulation*. Transportation Research 16B, 1982, pp. 279-290.
32. Hadj-Salem, H. and Papageorgiou, M. *Ramp Metering Impact on Urban Corridor Traffic, Field Results*. Transportation Research 29A, 1995, pp. 303-319.
33. Hall, F. L., Allen, B. L. and Gunter, M. A. *Empirical Analysis of Freeway Flow-Density Relationships*. Transportation Research 20A, 1986, pp. 197-210.
34. Hallenbeck, M. and Jacobson, L. N. *Description of the Seattle Integrated Arterial/Freeway Coordination System*. 70th Annual Transportation Research Board Meetings, 1991.

35. Hillier, F. S. and Lieberman, G. J. *Introduction to Operations Research (Sixth Edition)*. McGraw-Hill, Inc. 1995.
36. ITE. *A Toolbox for Alleviating Traffic Congestion*. Institute of Transportation Engineers, 1989.
37. Jacobson, E. L. and Landsman, J. *Case Studies of U. S. Freeway-to-Freeway Ramp and Mainline Metering and Suggested Policies for Washington State*. Transportation Research Record 1446, TRB, National Research Council, Washington, D. C., 1994, pp. 48-55.
38. Jacobson, L. N., Henry, K. C. and Mehyar, O. *Real-Time Metering Algorithm for Centralized Control*. Transportation Research Record 1232, TRB, National Research Council, Washington, D. C., 1989, pp. 17-26.
39. Kang, S. and Gillen, D. "Assessing the Benefits and Costs of Intelligent Transportation Systems: Ramp Meters", California PATH Research Report, UCB-ITS-PRR-99-19, July 1999, ISSN 1055-1425.
40. Kleinman, N. L., Hill, S. D. and Ilenda, V. A. *SPSA/ SIMMOD Optimization of Air Traffic Delay Cost*. Airport Modeling and Simulation. pp. 45-63.
41. Koka, M., Hourdakis, J. and Michalopoulos, P. G. *Computer Aided Testing and Evaluation of Adaptive Ramp Control Strategies*. The 79th Annual Meeting of the Transportation Research Board, Washington, D.C., Jan. 1994.
42. Kushner, H. J. and Clark, D. S. *Stochastic Approximation Methods for Constrained and Unconstrained systems*. New York: Springer-Verlag, 1978.
43. Lindley, J. A. *A Methodology for Quantifying Urban Freeway Congestion*. Transportation Research Record 1132, 1988, pp. 1-7.
44. Ljung, L. *Strong Convergence of a Stochastic Approximation Algorithm*. Ann. Stat., Vol. 6, pp. 680-696, 1978.
45. Lu, J. *Prediction of Traffic Flow by an Adaptive Prediction System*. Transportation Research Record 1287, TRB, National Research Council, Washington, D. C., 1990, pp. 54-61.
46. Masher, D. P., Ross, D. W., Wong, P. J., Tuan, P., Zeidler, H. M. and Petracek, S. *Guidelines for Design and Operation of Ramp Control Systems*. National

Cooperative Highway Research Program (NCHRP), Contract NCHRP, 1975, pp. 3-22.

47. May, A. D. *Traffic Flow Fundamentals*. Prentice Hall, Englewood Cliffs, N. J., 1990, pp. 238-245.
48. Mcdonnell, J. R., Fogel, D. B., Rindt, C. R., Recker, W. W. and Fogel, L. J. *Using Evolutionary Programming to Control Metering Rates on Freeway Ramps*. 1995.
49. Mcshane, W. R., Roess, R. P. and Prassas, E. S. *Traffic Engineering*. Second Edition. Published by Prentice-Hall, Inc., 1998.
50. Metivier, M. and Priouret, P. *Applications of a Kushner and Clark Lemma to General Classes of Stochastic Algorithms*. IEEE Trans. Informat. Theory, Vol. 30, pp. 140-151, 1984.
51. MN/DOT. *Freeway Operations Program Status Report*. Minnesota Department of Transportation, October. 1994.
52. NJDOT. Draft Report of “*ITS Strategic Business Plan*”. Traffic Operation Division, New Jersey Department of Transportation, Feb., 1998.
53. NJDOT. “*Road User Cost Manual*”. New Jersey Department of Transportation, June, 2001
54. Nsour, S. A., Cohen, S. L., Clark, J. E. and Santiago, A. J. *Investigation of the Impacts of Ramp Metering on Traffic Flow with and without Diversion*. Transportation Research Record 1365, TRB, National research Council, Washington, D. C., January 22-28, 1995.
55. Papageorgiou, M. *A New Approach to Time-of-Day Control Based on a Dynamic Freeway Traffic Model*. Transportation Research 14B, 1980, pp. 349-360.
56. Papageorgiou, M. *A Hierarchical Control System for Freeway Traffic*. Transportation Research 17B, 1983, pp. 251-261.
57. Papageorgiou, M., Blosseville. J. M. and Hadj-Salem, H. *Macroscopic Modeling of Traffic Flow on the Boulevard Peripherique in Paris*. Transportation Research 23B, 1989, pp. 29-47.

58. Papageorgiou, M., Blosseville. J. M. and Hadj-Salem, H. *Modeling and Real-Time Control of Traffic Flow on the Boulevard Peripherique in Paris: Part I: Modeling*. Transportation Research 24A, 1990, pp. 345-359.
59. Papageorgiou, M., Blosseville. J. M. and Hadj-Salem, H. *Modeling and Real-Time Control of Traffic Flow on the Boulevard Peripherique in Paris: Part II: Coordinated On-Ramp Metering*. Transportation Research 24A, 1990, pp. 361-370.
60. Papageorgiou, M., Hadj-Salem, H. and Blosseville. J. M. *ALINEA: a Local Feedback Control Law for On-Ramp Metering*. Transportation Research Record 1320, TRB, National Research Council, Washington, D. C., 1991, pp. 58-64.
61. Parsons Brinckerhoff Quade & Douglas, Inc. *I-80 HOV Lane Evaluation Study*. Report No. 97-004-7290, 1997.
62. Payne, H. J., Brown, D. and Cohen, S. L. *Improved Techniques for Freeway Surveillance*. Transportation Research Record 1112, TRB, National Research Council, Washington, D. C., 1987, pp. 52-60.
63. Piotrowicz, G. and Robinson J. *Ramp Metering Status in North America*. FHWA DOT-T-95-17, 1995.
64. Pooran, F. and Summer, R. (1996). *Coordinated Operation of Ramp Metering and Adjacent Traffic Signal Control Systems*. Publication No. FHWA-RD-95-130. U.S. Department of Transportation, Federal Highway Administration.
65. Prevedouros, R. D. and Wang, Y. *Simulation of a Large Freeway/Arterial Network with CORSIM, INTEGRATION and WATSim*. Preprints of Transportation Research Board Conference, Washington, D.C., 1998.
66. Rao, L. and Owen, L. "Validation of High-fidelity Traffic Simulation Models", The 79th Transportation Research Board, Paper No. 00896.
67. Salem, H. H., Blosseville, J. M. and Papageorgiou, M. *On Ramp Control: Coordinated Traffic-Responsive Strategies*. In Concise Encyclopedia of Traffic and Transportation Systems (M. Papageorgiou, ed.) Pergamon, London, 1991, pp. 289-294.
68. Shaw, L. and McShane, R. W. *Optimal Ramp Control for Incident Response*. Transportation Research 7, 1973, pp. 393-411.

69. Sheffi, Y. *Urban Transportation Networks*. Prentice-Hall, Inc., 1985.
70. Smith, B. L. and Demetsky, M. J. *Short-term Traffic Flow Prediction: Neural Network Approach*. TRB, Transportation Research Record 1453, 1995, pp. 98-104.
71. Spall, James C. *Multivariate Stochastic Approximation Using a Simultaneous Perturbation Gradient Approximation*. IEEE, 1992, pp. 332-341.
72. Spall, James C. *Implementation of the Simultaneous Perturbation Algorithm for Stochastic Optimization*. Submitted to American Statistician, Sep., 1995.
73. Spall, James C. *An Overview of the simultaneous Perturbation Method for Efficient Optimization*. Airport Modeling and Simulation, 1998, pp. 141-153.
74. State of California, Business, Transportation and Housing Agency, Department of Transportation, Division of Traffic Operations: *Ramp Meter Design Guidelines*. 1991.
75. Stephanedes, Y. J. and Chang, K. K. *Optimal Control of Freeway Corridors*. Journal of Transportation Engineering, 1993, Vol. 119, No. 4, pp. 504-515.
76. Stephanedes, Y. J., Kwon, E. and Chang, K. *Control Emulation Method for Evaluating and Improving Traffic-Responsive Ramp Metering Strategies*. Transportation Research Record 1360, TRB, National Research Council, Washington, D. C., 1991, pp. 42-45.
77. Stephanedes, Y. J., Kwon, E. and Michalopoulos, P. *On-Line Diversion Prediction for Dynamic Control and Vehicle Guidance in Freeway Corridors*. Transportation Research Record 1287, TRB, National Research Council, Washington, D. C., 1990, pp. 11-19.
78. Summer, R., et al. *A Freeway Management Handbook - Volume 1, 2, 3, 4*. DOT-FH-11-9706, Federal Highway Administration, May 1983.
79. Taylor, C., Meldrum, D. and Jacobson, L. *Fuzzy Ramp Metering: Design Overview and Simulation Results*. Preprints for Transportation Research Board Annual Meeting, 1998.

80. Taylor, C., and Meldrum, D. *Evaluation of a Fuzzy Logic Ramp Metering Algorithm: A Comparative Study Among Three Ramp Metering Algorithms Used in the Greater Seattle Area*. Draft Research Report, Research Project Agreement No. T9903, Task 84. Feb., 2000.
81. Taylor, C. and Meldrum, D. *Algorithm Design, User Interface, and Optimization Procedure for A Fuzzy Logic Ramp Metering Algorithm: A Training Manual for Freeway Operations Engineers*. Draft Technical Report, Research Project Agreement No. T9903, Task 84. Feb., 2000.
82. Ting, C. J. and Schonfeld, P. "Optimization Through Simulation of Waterway Transportation Investments", *Transportation Research Record* 1620, pp. 11-16.
83. U. S. DOT, Federal Highway Administration. "Coordinated Operation of Ramp Metering and Adjacent Traffic Signal Control Systems", Publication No. FHWA-RD-95-130, June 1996.
84. Van der Zijpp, N.J. and Lindveld, Ch. D. R., "Estimation of O-D Demand for Dynamic Assignment with Simultaneous Route and Departure Time Choice", The 80th Annual Meeting, TRB, 2001.
85. Venglar, S., Fambro, D. and Bauer, T. "Validation of Simulation Software for Modeling Light Rail Transit", The 74th Transportation Research Board, Paper No. 950491.
86. Wattleworth, J. A. *Peak-Period Analysis and Control of a Freeway System*. Highway Research Record 157, TRB, National Research Council, Washington, D. C., 1967, pp. 1-11.
87. Wattleworth, J. A. and Berry, D. S. *Peak-Period Control of a Freeway System – Some Theoretical Investigations*. Highway Research Board 89, TRB, National Research Council, Washington, D. C., 1965, pp. 1-25.
88. Wiener, R., Pignataro, L. J. and Yagoda, H. N. *A Discrete Markov Renewal Model of a Gap-Acceptance Entrance Ramp Controller for Expressways*. *Transportation Research* 4, 1970, pp. 151-161.
89. Wu, J. *Development and Evaluation of Real-time Ramp Metering Algorithms*. Final Report, University of Maryland, College Park & Federal Highway Administration, VA., 1993.

90. Yagar, S. *Metering Freeway Access*. Transportation Quarterly, 1989, Vol. 43, No. 2, pp. 215-224.
91. Yang, Q. *A Simulation Laboratory for Evaluation of Dynamic Traffic Management Systems*. Ph.D. Dissertation. Center for Transportation Studies, Massachusetts Institute of Technology, 1997.
92. Yuan, L. S. and Kreer, J. B. *Adjustment of Freeway Ramp Metering Rates to Balance Entrance Ramp Queues*. Transportation Research 5, 1971, pp. 127-133.
93. Zhang, Y., Owen, L. and Clark, J. “*Multiregime Approach for Microscopic Traffic Simulation*”, Transportation Research Record 1644, TRB, National Research Council, Washington, D.C., 1998, pp. 103-115.